ABSTRACT

SELECTIVE NEURAL STIMULATION BY LEVERAGING ELECTROPHYSIOLOGICAL DIVERSITY AND USING ALTERNATIVE STIMULUS WAVEFORMS

by
Bemin Ghobreal

Efforts on finding the principle mechanism for selective neural stimulation have concentrated on segregating the neurons based on their size and other geometric factors. However, neuronal subtypes found in different parts of the nervous system also differ in their electrophysiological properties. The primary objective of this study is to investigate the feasibility of selective activation of neurons by leveraging the diversity seen in passive and active membrane properties.

Using both a local membrane model and an axon model based on the CRRSS, the diversity of electrophysiological properties is simulated by varying four model parameters (membrane leakage-G_{leak} and capacitance-C_m, temperature coefficient-K_{temp}, and maximum sodium conductance-G_{Namax}) by ±25% around their default value. Temperature coefficient is used as a means to alter the opening rate of the sodium channel. Three different stimulus waveforms are implemented to test the effects of hyperpolarizing pre-pulsing (HPP) and depolarizing pre-pulsing (DPP) on selectivity in comparison to monophasic (Mono) waveform.

The default value of C_m is found to play a critical role in amplifying or attenuating the sensitivity of the chronaxie time (Chr) and rheobase (Rhe) to variations in all the membrane parameters. The HPP waveform is able to selectively activate neurons diversified in G_{leak} only. Maximum selectivity indices are obtained when passive parameters (C_m & G_{leak}) are allowed to vary. The

impact of dynamic parameter (K_{temp} and G_{Namax}) diversity increased slightly for the smallest value of C_m. In all cases, the HPP waveforms (with zero inter-phase gap) produce higher selectivity than the other two stimulus waveforms.

These results reveal a novel mechanism of selectivity based on electrophysiological diversity, and it is particularly pronounced with the hyperpolarizing pre-pulsing stimulation waveform. The proposed method of selectivity may lead to a paradigm-shifting approach if the electrophysiological diversity can also segregate neurons into functional subtypes, as evidence suggests in reports from numerous sites in the central nervous systems. This basic concept of selectivity should generalize to more complex neural models, though probably to different extents, that include a voltage-gated fast sodium channel and a leakage current, as in the CRRSS model.

Furthermore, this study expanded the investigation of neural selectivity to include stimulus waveform. Historically, rectangular stimulus pulse has been used in various neural stimulation application, however several limitations reside when using the tradition rectangular pulse to achieve selectivity. Hence, the study investigated using seven different non-rectangular waveforms as the stimulus pulse proceeded with hyperpolarizing pre-pulsing stimulus as a method to improve selectivity. The seven non-rectangular pulses are Charge-discharge curve (Chr-Dis), increasing and decreasing exponential (ExpInc and ExpDec) respectively, Gaussian (Gauss), KT^2, Linear (Lin), and sinewave (Sine). Results revealed that Kt^2 maximized selectivity, followed by Gauss, ExpInc, and ExpDec stimulus, when proceeded by hyperpolarizing pre-puls. Furthermore, results showed with higher diversity in neural cells, specifically in G_{Leak} & K_{temp} or G_{Leak} & G_{Namax} using Kt^2 allows higher stimulation selectivity between neural cells.

Additionally, to get more realistic results that represents the behavior of neural cell in the human body we expanded the investigation to include a compartmental axon mode. We used a 10 μm myelinated axon that incorporated the CRRSS local model at the nodes of Ranvier that had widths of 1 μm and an inter-nodal distance of 1 mm. A monopolar point electrode was placed 1 mm away from the axon and aligned with its central node. Using all eight stimulus waveforms the SD curves and SIs were found with the same passive and active parameter ranges tested in the local membrane model.

The Axon model further confirmed the results obtained from the local model revealing that diversification in the membrane parameters leads to selective neural stimulation. Both model results indicate that the most selective stimulus waveform changes depending on the membrane parameter combination that is allowed to vary, and no single stimulus waveform is the best for all combinations. These simulation results warrant further investigation of the concept of "selectivity based on electrophysiological diversity" using experimental data from real neurons.

**SELECTIVE NEURAL STIMULATION BY LEVERAGING
ELECTROPHYSIOLOGICAL DIVERSITY AND USING ALTERNATIVE
STIMULUS WAVEFORMS**

**by
Bemin Ghobreal**

**A Dissertation
Submitted to the Faculty of
New Jersey Institute of Technology
and Rutgers University Biomedical and Health Sciences – Newark
in Partial Fulfillment of the Requirements for the Degree of
Doctor of Philosophy in Biomedical Engineering**

Department of Biomedical Engineering

May 2021

.

APPROVAL PAGE

SELECTIVE NEURAL STIMULATION BY LEVERAGING ELECTROPHYSIOLOGICAL DIVERSITY AND USING ALTERNATIVE STIMULUS WAVEFORMS

Bemin Ghobreal

Dr. Mesut Sahin, Dissertation Advisor   Date
Professor of Biomedical Engineering, NJIT

Dr. Farzan Nadim, Dissertation Co-Advisor   Date
Professor of Biological Sciences, NJIT

Dr. Bryan Pfister, Committee Member   Date
Professor of Biomedical Engineering, NJIT

Dr. Sergei Adamovich, Committee Member   Date
Professor of Biomedical Engineering, NJIT

Dr. Viji Santhakumar, Committee Member   Date
Associate Professor of Pharmacology, Physiology, and Neuroscience, Rutgers

BIOGRAPHICAL SKETCH

Author: Bemin Ghobreal

Degree: Doctor of Philosophy

Date: May 2021

Undergraduate and Graduate Education:

- Doctor of Philosophy in Biomedical Engineering,
  New Jersey Institute of Technology, Newark, NJ, 2021

- Bachelor of Science in Biomedical Engineering,
  New Jersey Institute of Technology, Newark, NJ, 2012

- Bachelor of Science in Electrical Engineering,
  New Jersey Institute of Technology, Newark, NJ, 2012

Major: Biomedical Engineering & Electrical Engineering

Presentations and Publications:

Serrador, Jorge & Blatt, M. & Acosta, A. & Ghobreal, Bemin & Falvo, Michael. (2013). Blast exposure is associated with impaired cerebral blood flow regulation in US veterans. Cerebrovascular Diseases. 35. 36-36.

Serrador, Jorge & Blatt, M. & Acosta, A. & Ghobreal, Bemin & Falvo, Michael. (2013). Differences in Cerebral Autoregulation between Arterial Beds is Not Reflected in CO_2 Reactivity. Cerebrovascular Diseases. 35. 34-35.

Serrador, Jorge & Castro, Pedro & Rocha, Isabel & Blatt, M. & Ghobreal, Bemin & Sorond, Farzaneh & Azevedo, Elsa. (2013). Cerebral blood flow is reduced in the vascular territory of ischemic stroke in the first 24 hours. Cerebrovascular Diseases. 35. 36-36..

Castro, Pedro & Serrador, Jorge & Azevedo, Elsa & Rocha, Isabel & Blatt, M. & Ghobreal, Bemin & Sorond, Farzaneh. (2013). Ischemic stroke is associated with transiently impaired autoregulation. Cerebrovascular Diseases. 35. 25-25.

B. Ghobreal, E. H. Kim, P. R. Moinot and T. L. Alvarez, "Custom software for NJIT flexible visual stimulator," 2012 38th Annual Northeast Bioengineering Conference (NEBEC), 2012, pp. 49-50, doi: 10.1109/NEBC.2012.6206956.

B. Ghobreal, A. Giokas, F. Dort, A. Gandhi and R. Foulds, "Telemanipulation using Exact Dynamics iARM," 2012 38th Annual Northeast Bioengineering Conference (NEBEC), 2012, pp. 123-124, doi: 10.1109/NEBC.2012.6206993.

Praise the Lord, Praise the name of the lord.
Search me, O God and know my heart: try me, and know my thoughts.
See if there is any wicked way in me and lead me in the way everlasting.
To my beloved Parents, for their encouragement throughout my life,
Nabil Basta Ghobreal & Nadia Sabet Narouz.

ACKNOWLEDGMENT

First and foremost, I would like to sincerely thank my advisor, Dr. Mesut Sahin, on his continuous support, guidance, and encouragement. This work would not have been possible without his knowledge and mentorship. His expertise was invaluable in formulating the research topic and generating high-quality results. His insightful feedback pushed me to sharpen my thinking and brought my work to the highest quality level. His great commitment to the project inspired me to become the best version of myself.

Additionally, I would like to thank my Co-Advisor Dr. Farzan Nadim, who put a lot with my questions and offer a great insight and collaboration to guide me through that long path.

I would also like to thank Dr. Sergei Adamovich, Dr. Brian Pfister and Dr. Viji Santhkumar for serving on my dissertation committee and their valuable contributions to my research.

I would like to thank the NSF and NRC bridge to doctorate program for the partial financial support they provided me and special thanks to the Ronald E. McNair program director Dr. Angelo Perna and assistant director Zara Williams.

Above all, I am forever indebted to my parents, my uncle, my sister and my brother for praying and believing in me, encouraging and supporting me.

Always thankful for my soul mate, my love and future wife who always has been with me through the tough times.

TABLE OF CONTENTS

TABLE OF CONTENTS
(Continued)

LIST OF TABLES

LIST OF FIGURES

CHAPTER 1

INTRODUCTION

Neural diseases are one of the leading causes of disabilities in the world. According to the United Nation World Health Organization's (WHO) report, about 1 billion people, nearly one in sixth of the world's population, suffer from neurological disorders like Alzheimer's disease (AD), Parkinson's disease, stroke, multiple sclerosis and epilepsy [4], causing roughly 6.8 million people to die every year [4]. In 2006, the U.S. National Institute for Neurological Disorders and Stroke (NINDS) estimated about 50,000 new cases of Parkinson's disease are diagnosed in the U.S. every year [5]. Therefore, finding a treatment for neural disorders has been the research focus for decades.

Electrical neural stimulation techniques have been used for decades showing a great impact on patients' health. It remains one of the most critical brain disorder treatments known to be effective at low cost [6, 7]. Various clinical approaches, as oral medication and surgical procedure, may accomplish similar therapeutic results, nevertheless neural electrical stimulation has higher spatiotemporal precision compared to oral medication combined with low cost and reversibility that is not present in surgical procedures [7]. Currently, it is a widely used treatment for several brain diseases and has proved to be an effective tool for patients who suffer from neurological and neuropsychiatric disorders [8].

Yet, neural electrical stimulation has several limitations and challenges that needed to be addressed. One of the most critical challenges, which we are addressing in this study, is neural stimulation selectivity [6, 7, 9]. Several

applications require the ability to selectively activate or inhibit a targeted population or neurons without activating neighboring neurons. Neural stimulation selectivity is a measure of the efficiency of the stimulus. Current electrical stimulation techniques stimulate a large area of the tissue, causing a nonlinear response [10], high rate of damaged tissue close to the stimulation electrode, loss of power and decrease in the stimulation efficiency [6, 7]. High power consumption increases the number of replacement surgeries for implanted pulse generators, since it reduces the battery lifetime [7, 10]. It is also important to acknowledge that, as a result the mechanism of action for neural electrical stimulation is still not well comprehended in addition to how neural network dynamics relate to single-cell dynamics remains poorly understood [7, 10]. Therefore, there is a high demand to develop more precise neural stimulation technique with the ability to target a specific group of neurons.

1.1 Selectivity

Neural electrical stimulation is an effective therapy for the majority of neural dysfunctions, however, there remains a clear clinical need to improve the technology [7, 8] to increase stimulation selectivity. Selectivity of a stimulus is the ability to stimulate a specific group of neurons without targeting other neurons within the same range. Improving neural stimulation selectivity increases the efficiency of the therapeutic effect and reduces the magnitude of the side effects [10]. Selectivity could be determined based on several neural cell properties, geometry properties, and stimulation properties, however, the two most studied

types of selectivity are diameter selectivity and spatial selectivity. Diameter selectivity indicates the capability to stimulate a specific population of neurons that have a common diameter, while simultaneously not including other neighboring populations [1, 10]. Spatial selectivity is the ability to excite or inhibit a specific group of neurons located from a specific distance from the stimulation electrode. For instance targeting neurons farther away from the stimulation electrode without targeting the neuron close to the electrode [1].

1.2 Selectivity Via Current-Diameter Relationship

Several studies showed the possibility of selectively stimulating a group of neurons or nerve fibers that have the same diameter size. In 1991 Fang and Mortimer conducted a study to investigate the possibility of targeting fibers based on their diameter, using quasitrapezoidal current pulses [11]. The study demonstrated that at lower current levels, the larger alpha motor axons could be blocked more than smaller alpha motor axons [11].

In another study, DONALD R. MCNEAL plotted the relationship between Activation threshold current and fiber diameter as shown Figure 1.1. [12]. The study concluded that between (2<d< 25 µm) the activation threshold current increases as fiber diameter decreased, at larger diameters (d> 15 µm) the threshold inversely proportional to the square root of the fiber diameter, and at smaller diameters (d<2 µum) the activation threshold has an inverse square relationship with fiber diameter [12].

Moreover, Mortimer and Creasey were able to influence the action potential, on small diameter motor fibers serving the bladder, without affecting larger diameter motor fibers [1]. In another application, Kristen E I. and Deurloo, Jan investigated the influence of subthreshold of depolarizing prepulses on threshold-diameter relationship, concluding that smaller fibers have a lower threshold current than the larger fibers up to a certain distance from stimulation electrode [13].

In 2014, Kurt Qing and Mathew P. Ward proposed a novel technique to change the current diameter recruitment order. Using a Brust Modulated rectangular waveform they showed selective activation between A (larger diameter) and C (small diameter) fibers. They compared between the traditional rectangular pulse and the burst modulated pulse. The burst modulated waveform is created by replacing each pulse with a burst of narrow pulses "pulsons". Each pulson burst has a defined pulse width (pWx), amplitude (ampx), interpulson interval (Iplx) and number of pulses (Nop) [14]. The results suggested that waveform with short PW or pWx more likely to be more selective to larger diameters than shorter fibers [14].
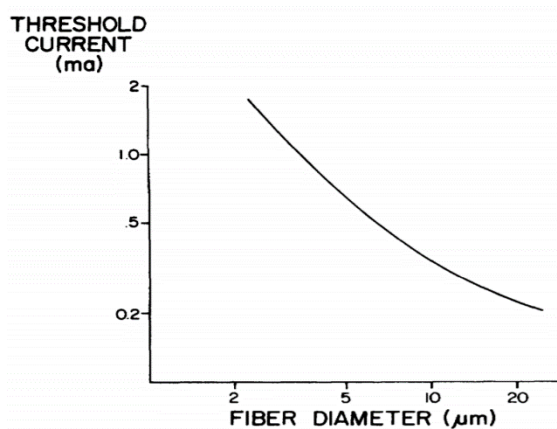
Figure 1.1 Threshold current as a function of fiber diameter. Current-Diameter relationship.

1.3 Stimulation Waveform

Published data has shown that stimulation parameters play a critical role in increasing stimulation selectivity. Several parameters were investigated, including but are not limited to, stimulation waveform [15], electrode polarity [16, 17], electrode distance from the target (electrode location), and waveform pulse width [18]. A study lead by Sahin, Mesut, investigated the effect of various non-rectangular waveforms on the stimulation efficiency, demonstrating that optimum pulse width changes as a function of the stimulus waveform, the study also showed that linearly and exponentntially decreasing and Gaussian waveforms are the most efficient pulse shapes, because the chronaxie time was longer compared to traditional rectangular pulse. The study showed that non-rectangular pulse shapes can move the chronaxie time to longer pulse duration.

Lately, non-rectangular waveforms have been gaining more interest as a unique stimulus pulse that could perform better than the traditional rectangle pulse and improve neural stimulation. Previous research demonstrated the benefits of non-rectangular waveform as a mean to decrease energy consumption. For instance, the exponentially rising waveform was shown to be the optimal stimulus to decrease energy consumptions [19, 20]. Moreover, Exponentially increasing, Gaussian and Sinusoidal stimulus pulses reduced energy requirements depending on the stimulation pulse width (PW) [15]. Additionally, in 2010 a study by Grill using a genetic algorithm concluded that a waveform similar to Gaussian was optimal for peripheral nerve stimulation [21].

The type of stimulus waveform has been always tied to stimulation selectively, several studies tried to improve selectivity by manipulating the stimulus pulse parameters. As we discussed previously, in majority of cases the biphasic pulse is used to reach higher selectivity by introducing the cathodic pulse first then followed by the anodic pulse. Other studies investigated adding a small intermediate gap between the two phases. A study was done in 2014, concluded that using the anodic pulse immediately after the short cathodic phase immediately may abolish the activation of targeted fibers [22]. Moreover, they recommended adding a 100 μsec gap between the two phases to decrease the charge required for activating nerve fibers [22, 23]. However, they reported that adding the 100usec gap reduced the selectivity index (SI). Likewise, in a previous paper of this series, we demonstrated that add a 200 μsec [22] gap between the two stimulus phases negates the effect using HPP – no inter-gap on selectivity Index.

Although, all previous studies revealed that the advantage of the non-rectangular pulse out weights the advantages of the rectangular pulse, yet more studies are required to better understand the specific details for the optimal stimulus pulse. Hence, we are extending the previous work and focusing on using non-rectangular waveform as a mean to improve electrical stimulation selectivity.

1.4 Selectivity Via Current-Distance Relationship

Spatial selectivity requires that the stimulation electrode sets in a close distance to the targeted population of neurons [1, 24]. However, Deurloo, Jan. performed a modeling study presenting that in order to stimulate distant fibers without stimulating close fibers, one should use subthreshold depolarizing repulses [13], which is confirmed by Grill and Mortimer Figure 1.2. [3]. A recent study conducted by Lehto, L.J. and his team investigated the effect of implanted electrode orientation on the neural stimulation selectivity. The results showed that maximum selectivity achieved when axons are parallel to the electric field orientation [8]. Additionally, type of electrode influence the recruitment characteristics of the stimulus, data showed that monopolar electrodes have higher selectivity compared to ring electrodes [25].

Several other studies tried improving spatial selectivity by manipulating multipolar electrode configuration, and some other tried to reverse the recruitment order using prepulsed stimulus. Yet, a study by Melissa Dali and Olivier Rossel [26], combined both methods together to guarantee both spatial selectivity while reversing the diameter recruitment order using the CRRSS model. Using three different multipolar configurations in addition to pre-pulses stimulus they achieved both spatial selectivity while reversing the diameter current relation [26]. The first configuration was a single 300 μsec pulse duration with TT electrode configuration (TT: One cathode at 90° and two anodes at 0° and 180°). The second configuration was Four pre-pulses with TT electrode configuration, finally the third configuration (Conf 3) used four pre-pulses in addition to the activation pulse with LTR electrode

configuration (LTR: cathodes at 0°, 90°, 180°, 270°) Figure 1.3 [26]. The previous three configurations were used on four different fiber diameters 5µm, 10µm, 15µm, 20µm. The pre-pulse parameters were set to reduce the activation of both 15µm and 20µm diameter fibers. From the study results, the first configuration activated the closer and larger diameter fibers first, the 2nd configuration reversed the current distance relationship yet, still recruited the larger diameter before the smaller ones. Finally, the third configuration which was designed to inactivate 15µm and 20µm fibers over the whole nerve, activated the 10µm diameter fiber in addition to reversing the current distance relationship, Figure 1.4 [26].
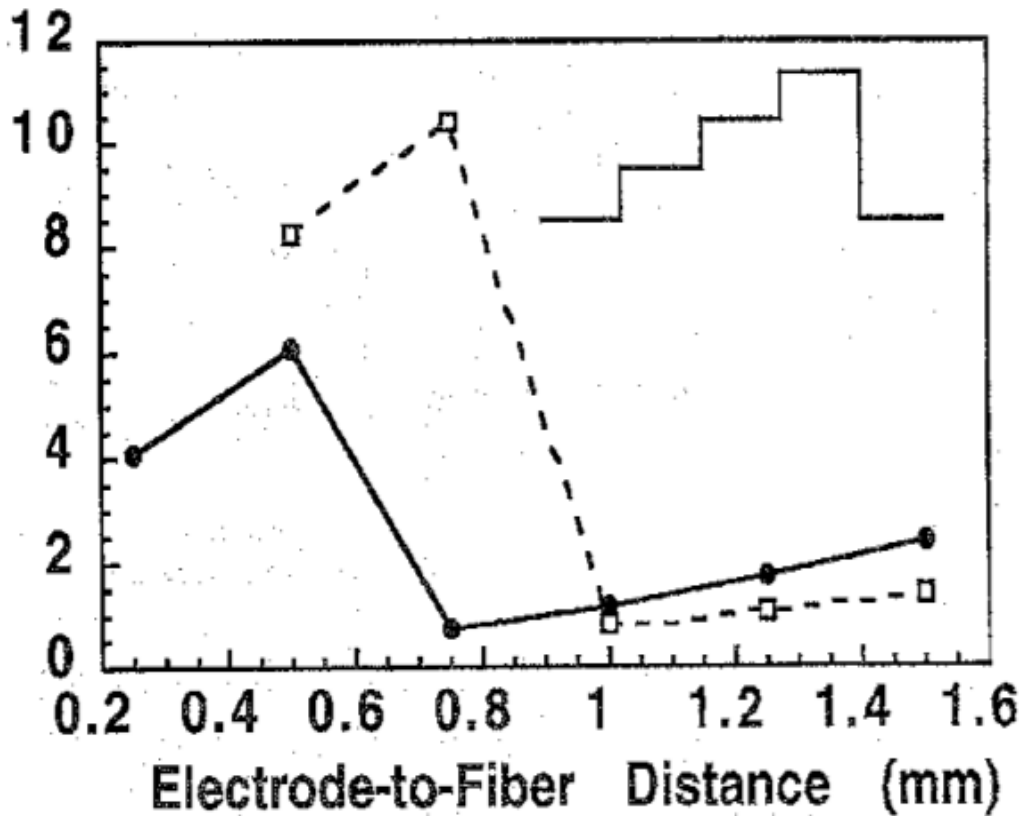
Figure 1.2 The inversion of the current distance relationship, using a pre-pulsed stimulus waveform. Smaller activation threshold at distant fibers. [3]
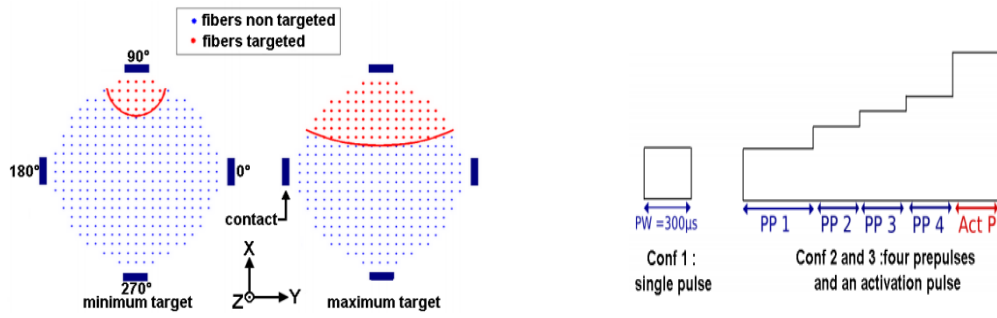
Figure 1.3 Pulse Waveform. Conf 1: single pulse. Conf 2 and 3: 4 pre-pulses, pp1 to pp4 followed by the activation pulse.
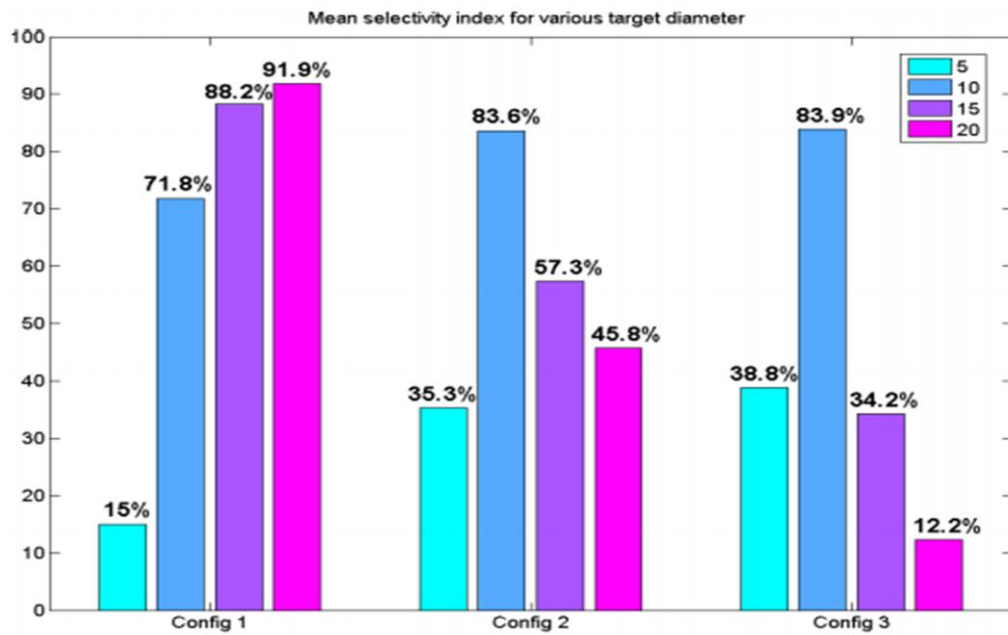
Figure 1.4 Mean selectivity index for each configuration and various target size SI is the optimal fibers with 10μm diameter.

1.5 Neural Model

1.5.1 Hodgkin-Huxley Model (H-H)

One of the early developed neural models is the Hodgkin-Huxley (H-H) model which is based on experimental data collected with squid giant axon. H-H model successfully explain the behavior of the dynamic membrane parameters via serious of mathematical equations [27]. They also developed an electrical circuit model that mimics the behavior of the neural cell as seen in Figure 1.5. If the ion concentration and temperature is known then the total membrane current I as a function of time and voltage can be calculated using the following equation [27]:

$$I = C_m \frac{dV}{dt} + \bar{g}_k n^4 (V - E_k) + \bar{g}_{Na} m^3 h\ (V - V_{Na}) + \bar{g}_l (V - V_l) \qquad (1.1)$$

$$\alpha_n = \frac{0.01\ (V + 10)}{exp^{\frac{V+10}{10}} - 1} \qquad (1.2)$$

$$\beta_n = 0.125\ exp^{\frac{V}{80}} \qquad (1.3)$$

$$\alpha_m = \frac{0.1\ (V + 25)}{exp^{\frac{V+25}{25}} - 1} \qquad (1.4)$$

$$\beta_m = 4\ exp^{\frac{V}{18}} \qquad (1.5)$$

$$\alpha_h = 0.07\ exp^{\frac{V}{20}} \qquad (1.6)$$

$$\beta_h = \frac{1}{exp^{\frac{V+30}{10}} + 1} \qquad (1.7)$$

1.5.2 CRRSS Model

In 1987. Sweeney et al. published the first model based on one of the mammalian nerves, which uses data of Chiu et al. [15, 28, 29]. The model based of a voltage -clamp study was carried out on a single rabbit myelinated nerve fibers and it was fitted to the Hodgkin-Huxley (H-H) model. Data then altered to set the model temperature to 37° [29] [15] and the leakage conductance was adjusted to give action potential conduction velocity of 57 m/s (ref). The Chiu-Ritchie-Rogart-Stagg-Sweeney (CRRSS) model has only voltage-gated sodium channel and a leakage current, and no potassium current, which fits well with the purpose of this study since there are almost no potassium currents in mammalian nodes of Ranvier. Hence, the CRRSS model was used in the simulation for both the local and the axon models. The Electrical circuit of the model shown in Figure 1.6 and the following mathematical equation are the representation of the model and they were used in the simulation [15, 29]. The change in Membrane potential is given by

$$\frac{dV}{dt} = \frac{i_{st} - i_{Na} - i_L}{C_m} \tag{1.8}$$

$i_{st} \rightarrow is\ the\ stimulation\ current$

$i_{Na} \rightarrow is\ the\ current\ densitiy\ of\ sodium\ cannel\ (\mu A\ Cm^{-2})$

$i_L \rightarrow is\ the\ current\ densitiy\ of\ Leakage\ cannel\ (\mu A\ Cm^{-2})$

$$i_{Na} = \bar{g}_{Na} m^2 h(V - E_{Na}) \tag{1.9}$$

$$i_L = \bar{g}_L(V - E_L) \tag{1.10}$$

Where m is the gating variable, which are gives as

$$m(t) = m_0 - [(m_0 - m_\infty)(1 - e^{\frac{-t}{T_m}})] \tag{1.11}$$

$$m_\infty = \frac{\alpha_m}{\alpha_m + \beta_m} \tag{1.12}$$

$$\alpha_m = k\frac{126 + 0.363\,V}{1 + e^{-\frac{V+49}{5.3}}} \tag{1.13}$$

$$\beta_m = k\frac{\alpha_m}{e^{\frac{V+56.2}{4.17}}} \tag{1.14}$$

$$T_m = \frac{1}{\alpha_m + \beta_m} \tag{1.15}$$

Then the equations for h, α_h and β_h are

$$h(t) = h_0 - [(h_0 - h_\infty)(1 - e^{\frac{-t}{T_h}})] \tag{1.16}$$

$$h_\infty = \frac{\alpha_h}{\alpha_h + \beta_h} \tag{1.17}$$

$$\beta_h = k\frac{15.6}{1 + e^{-\frac{V+56}{10}}} \tag{1.18}$$

$$\alpha_h = k\frac{\beta_h}{e^{\frac{V+74.5}{5}}} \tag{1.19}$$

$$T_h = \frac{1}{\alpha_h + \beta_h} \tag{1.20}$$

1.5.3 Inferior Olive Model

Another well-known neural model is the inferior olive model which was developed by *Torben-Nielsen, B., I. Segev, and Y. Yarom*. Inferior Olive (IO) Is the major source input to the cerebellum, and it is a part of the medulla oblongata. It is formed from a gray folded layer opened in the middle by a hilum, where the olivocerebellar

fibers pass through. It is the only source of the climbing fibers to the Purkinje cells in the cerebellum and it projects to both the cortex and the deeper nuclei of the cerebellum [30]. Its function is not well known, however it is thought that it is responsible for learning and timing of movements, for example it transmits error signals during eye-blink conditioning or adaptation of the vestibulo-ocular reflex. Additionally, it carries motor command signals beating on the rhythm of the oscillating and synchronous firing of ensembles of olivary neurons [30, 31]. The used IO model contains only a leak current and a low threshold (T-Type) Ca2+ current and there is no Sodium channel like the CRRSS model. The dynamics of the model are described by :

$$\frac{dV}{dt} = -1 \frac{1}{Cm} (I_L + I_{Ca}) \tag{1.21}$$

$$I_L = g_L (V - E_1) \tag{1.22}$$

$$I_{Ca} = g^-_{Ca} m^3_\infty h (V - E_{Ca}) \tag{1.23}$$

$$m^3_\infty = \left[1 + exp^{\left(\frac{-61-V}{4.2}\right)} \right]^{-3} \tag{1.24}$$

$$\frac{dh}{dt} = \frac{h_\infty(V) - h}{t_h(V)} \tag{1.25}$$

$$h_\infty = \left[1 + exp^{\left(\frac{V+85.5}{8.6}\right)} \right]^{-1} \tag{1.26}$$

$$t_h(V) = 40 + 30 \left[exp^{\left(\frac{V+84}{8.3}\right)} \right]^{-1} exp^{\left(\frac{V+160}{30}\right)} \tag{1.27}$$

In which the dynamic membrane parameters in this model are, the maximum conductance of calcium channels (g_{Ca}), the maximum conductance of leakage channel (g_L), and the gating coefficients are (m & h).
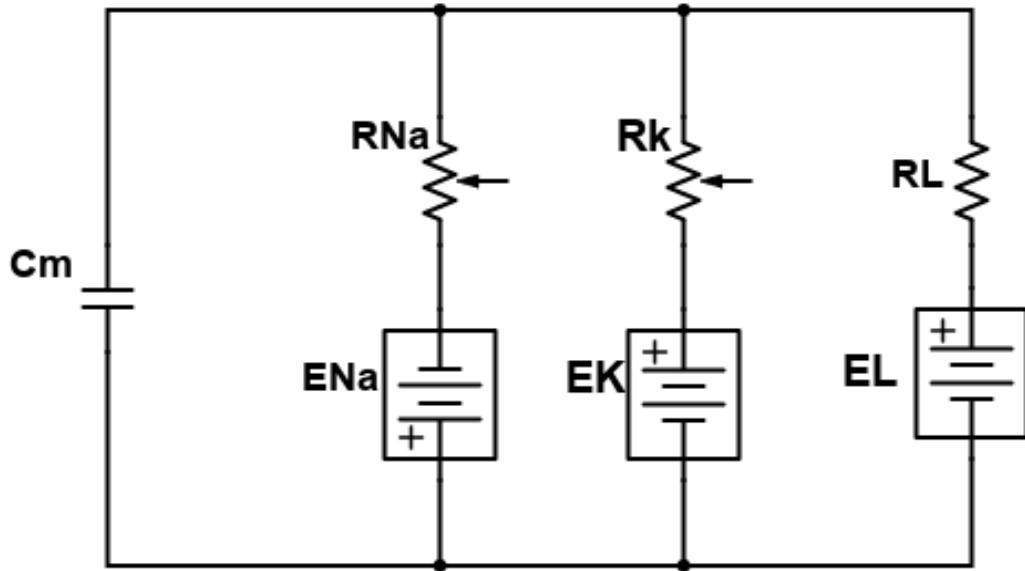
Figure. 1.5 Electrical circuit representing H-H model membrane parameters which are GNa, Gl, Gk, and Cm.
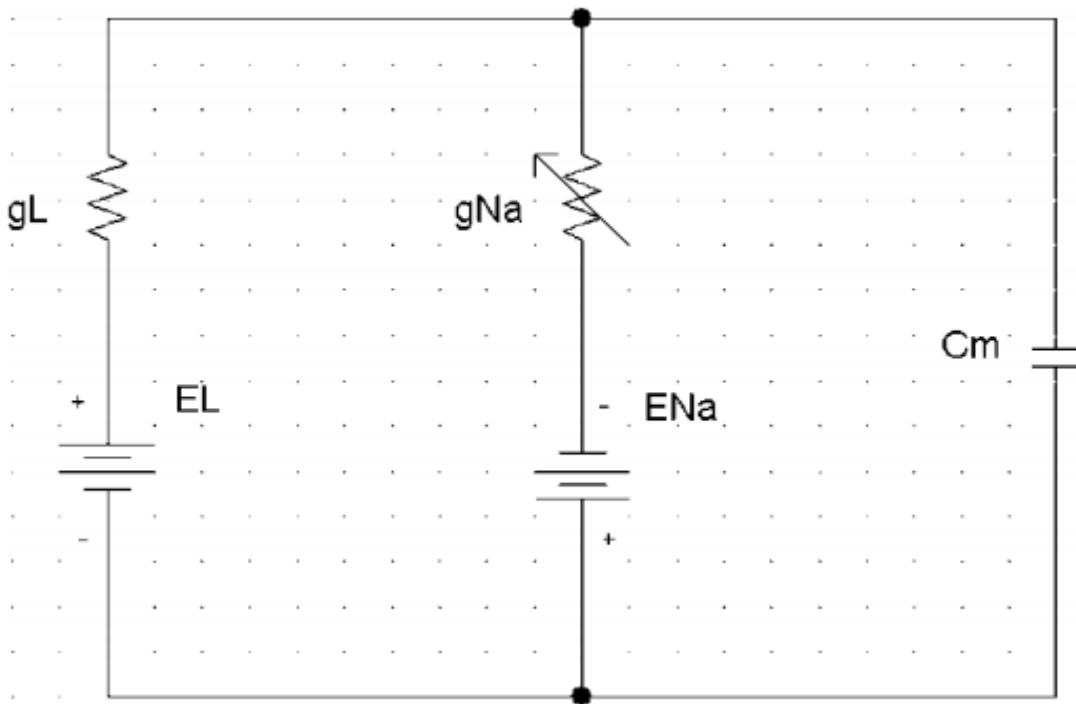
Figure. 1.6 The CRRSS Local model is represented as an electrical circuit. The circuit showing both Leakage channel (gL) and sodium channel (gNa).

1.6 Dynamic Membrane Parameters

Although there have been several studies focused on improving electrical stimulation selectivity, however, there is little attention paid to membrane parameters as a method to increase stimulation selectivity, even though it plays a critical role in determining cell activation threshold and in generating membrane action potential. Dynamic membrane properties were first explained in 1952 by Hodgkin and Huxley (H-H) [27] when they successfully modeled the giant axon of the squid. They revealed that both sodium conductance (G_{na}) and potassium conductance (G_k) are functions of time and membrane potential, while the rest of parameters are constant [32].

The original H-H model had three types of channels, sodium gated channel, leakage channels and potassium channels [27, 32]; in the purpose of this study, we will focus on the first two channels type Sodium channel and leak channel. Sodium channels are permeable to Na+ and the conductance depends on the voltage across the membrane [27] and it plays a vital role in generating action potential. The maximum conductance of the sodium channels (**G_{Namax}**) is a function in the variable m & h gates, where m is the activation gating variable and h is the inactivation gating variable. In the H-H model, the assumption was, that the model contains three m gates and one H gate, therefore $G_{na} = m^3*h*$ **G_{Namax}** [27]; however, in the Chiu-Ritchie-Rogart-Stagg-Sweeney (CRRSS) model, sodium channels have two m gates, therefore the conductance is modeled as, $G_{na} = G_{namax}* m^2 * h$, since it is a mammalian nerve fiber, as shown in Figure 1.7. [1, 2]. The values of m and h range from 0 to 1, causing the G_{na} to vary between 0 and

G_{namax} [1]. Hence, changes in the value of G_{namax} change the range for the sodium gate conductance causing a change in cell activation threshold.

Another two parameters of interest are α & β, which are the opening and closing rates for sodium channel gates. Alpha (α) is the number of time per second the gate will open, while beta (β) is the number of time per second that a gate will close [27, 32]. An increase in alpha increases the rate of opening for the gates causing higher probabilities to ions to flow in, conversely increasing beta will cause a higher closing rate lowering the probabilities for ions to flow through, causing a change in activation threshold. Therefore, we expect that membrane properties affect the activation threshold, and influence stimulation selectivity. Both Alpha and Beta can be altered simultaneously by changing the temperature coefficient of the model (**K_{temp}**) Equation 0.1.

$$\alpha = K_{temp}\ \frac{126 + 0.363 * V}{1 + e^{-(\frac{V+49}{5.3})}} \tag{1.28}$$

$$\beta\ =\ K_{temp}\ \frac{\alpha}{e^{(\frac{V+56.2}{4.17})}} \tag{1.29}$$
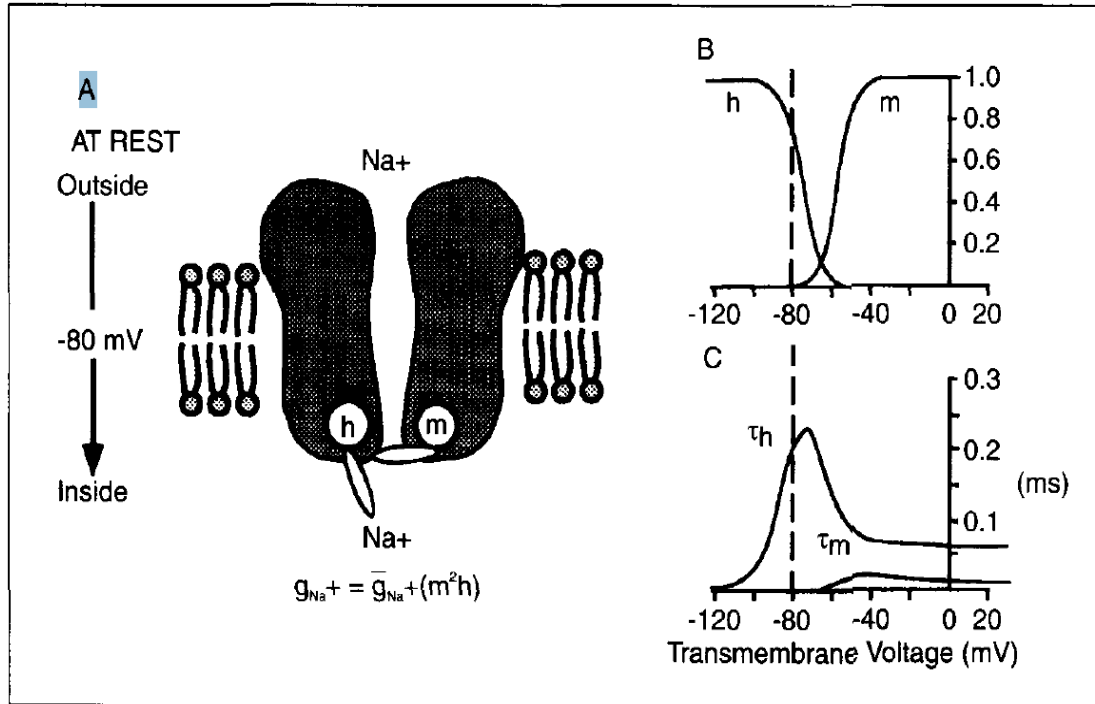
Figure 1.7 Voltage gated sodium channel at rest. A) sodium channel pore opening is modeled by the activation variable m, while the inactivation gate is modeled by the inactivation variable, h. The conductance of the channel depends on the value of both gating variables. (B) the steady-state values of m and has a function of transmembrane voltage. (C) The steady state values of the time constant of the activation variables, τm, and the inactivation variable, τh, as a function of membrane voltage [1, 2].

1.7   Passive Membrane Parameters

The Passive membrane parameters are leak conductance (G_{leak}) and membrane capacitance (C_m). Leakage channels has a low conductance G_{leak} and it is mainly responsible for resting membrane potential (33). Leak current is calculate based on the value of G_{leak}.

$$I_L = \overline{G_L}(V - E_L)$$

Membrane capacitance is a fundamental parameter in modelling the electrophysiological properties of neurons [33, 34] . The specific membrane capacitance is determined by the thickness of the membrane, its lipid constituents of the cell and influenced by its protein content [33]. Cm is a crucial functional role in signal propagation, it is directly related to the membrane time constant

$$T_m = R_m * C_m$$

where Rm is membrane resistance and Cm is membrane Capacitance. The direct relation between CM and tm plays an important role on influencing the chronaxie time of the Strength Duration curves.

1.8 CRRSS Action Potential

The CRRSS model contains sodium channel and leakage channel, the sodium channel is responsible for generating an action potential. Sodium channel has three m gates and one h gates which are activation and inactivation gates, respectively. When neural cell is in the resting state the membrane potential stays around -80 mV. Once electrical pulse begins to excite the cell membrane, m gates (activation gates) start to open, and h gates start to close Figure (1.8). The opening of the m gate causes a graduate increase in the sodium Ions Na^+ to enter the cell membrane changing the voltage gradient and depolarizing the cell membrane. Once the cell membrane voltage crosses the threshold value which is around -55mV, all m gates are open, and all h gates are closed hence an influx of the sodium ions Na^+ rush into the cell membrane. The influx of Na^+ ions cause the cell membrane to further depolarize generating a large spike in the membrane potential reaching the action potential peak, Figure (1.8). In the depolarization state, m gates are fully opened, and h gates are fully closed and sodium conductance G_{Na} at the maximum value. The sodium channel starts self-inactive by opening the h gate and closing m gates; hence cell membrane enters the repolarization state bringing the cell membrane potential back to resting potential, Figure (1.8).

There is no refractory period in the AP generated in the CRRSS model because there is no potassium channel. The H-H model has a potassium channel, which mainly is slower than sodium channel. The slow opening of the potassium channel causes longer repolarization stage and slower discharge of the positive

ions. Additionally, it drives the cell to hyperpolarization state before going back to

resting membrane potential.
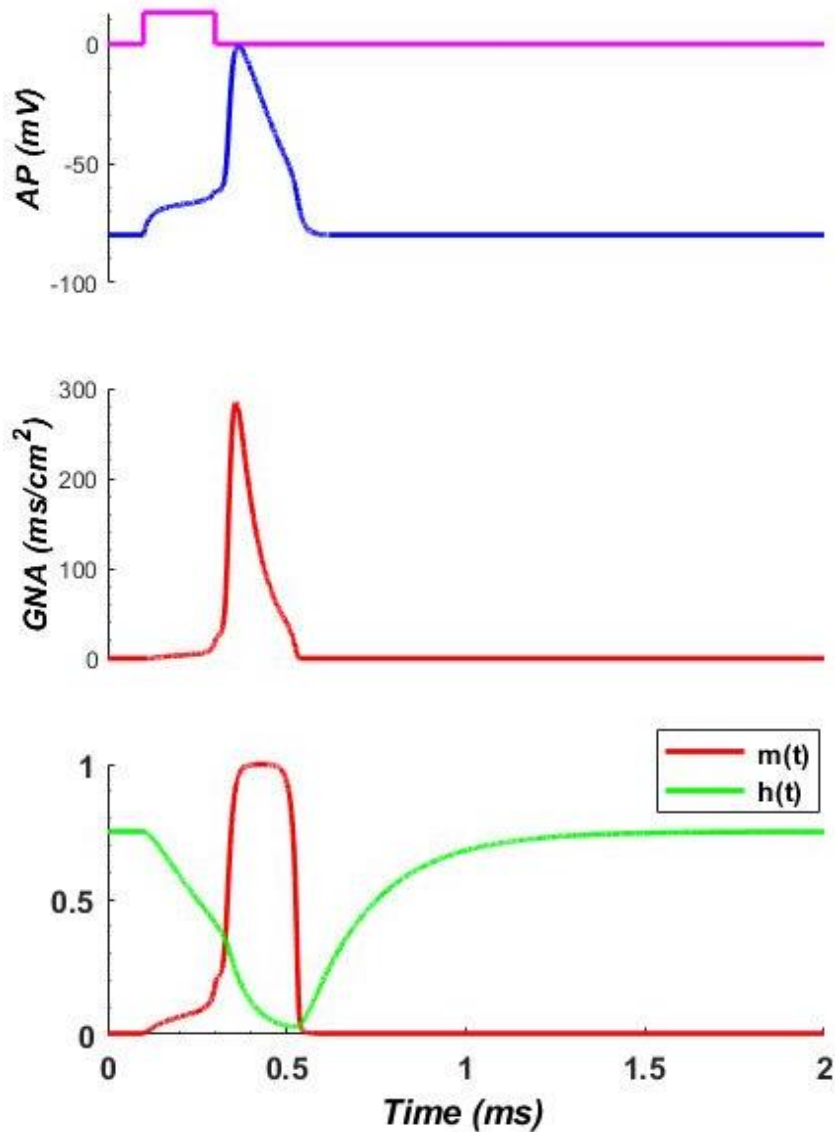
Figure 1.8 CRRSS Action Potential is generated when a rectangular pulse stimulates the nerve cell. Sodium conductance follows the action potential curve shape. Both m and h gate are showing, m gate is open during the peak of AP and h gate is close.

1.9   Strength-Duration Curve

Is a well-defined method that is used to quantify stimulation selectivity. Strength-duration (SD) curve has been used in several studies as a measure to stimulation selectivity [1, 35]. The two-dimensional curve, plots the stimulus strength as a function of pulse width (PW), as shown in Figure 1.8 [35]. Selectivity of stimulation is represented with a crossing between two curves on the SD curve. For instance on Figure 1.8. [35], shows an intersection between neuron B4 & B21, and a stimulus strength of 15 µA at PW 250 µs can activate B4 without activating B21, also a stimulus with amplitude of 5 uA at Pw = 2000 µs can activate B21 without activating B4 or any of the other neurons. The same measures can be used with neurons B25& B19. Accordingly, we can design a custom stimulus waveform that can be selective to neuron B4, but not to B21, B19 or B25.
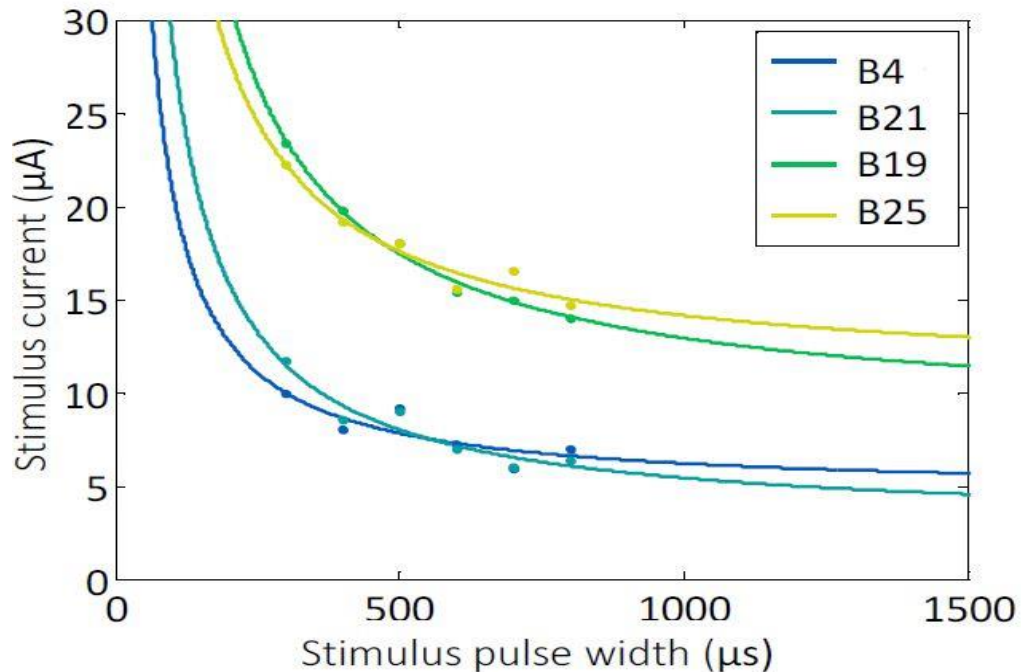
Figure 1.9 The strength–duration activation curves are plotted for four different neurons. Crossing found between B25 &B19, B4&B21.

CHAPTER 2

SELECTIVE NEURAL STIMULATION BASED
ON ELECTROPHYSIOLOGICAL DIVERSITY

2.1 Objective / Background and Significance

Stimulation of neurons by way of delivering small electric currents has led to treatment of numerous neurological disorders and injuries in the central and peripheral nervous system. One of the primary limitations of electrical nerve stimulation is the lack of specificity [6, 7]. In general, larger axons and somas have lower activation thresholds and are activated before the smaller ones, the opposite of the natural order of recruitment for motor neurons by volition. Also, due to fast decline of the electric field strength by distance from the stimulating electrode, the nearby neurons or axons are activated before the distant ones (current-distance relation). Both of these phenomena often emerge as major limitations in selectively activating neuronal subtypes defined by their electrophysiological properties or function rather than their size or distance from the electrode.

Earlier efforts considered placing a depolarizing pre-pulse before the stimulating phase (pre-pulsing) [3, 13], in order to reduce the excitability of the nearby and large axons to reverse the recruitment order defined by either the size principle or current-distance relation. Introducing a short time gap between the two phases of the charge-balanced biphasic waveform removes the effect of the first phase on the excitation threshold [36]. Shorter pulse widths [37], biphasic waveforms as opposed to monophasic ones [37], and hyperpolarizing pre-pulses [38]; none of these reverses the recruitment order, but they allow a better control of muscle force by increasing the margin between the stimulus thresholds dictated

by fiber size or distance. Overall, the techniques proposed for selective activation usually make the assumption that the neurons share the same electrophysiological properties but only differ in their size and morphology [39], and sometimes the types of ionic channels and their density in different neuronal compartments.

No study so far has tried to leverage the intrinsic variations in membrane properties that occur naturally between different neural subtypes as a means to achieve selective activation. Diversity in passive and dynamic membrane properties of neurons clearly exists as evidenced in many parts of the central nervous system (CNS). For instance, four different pyramidal neuron subtypes were found in layer V of the rat medial prefrontal cortex [40], classified based on their morphology and membrane resistance. Different neurons had significantly different membrane time constants and rheobase currents. It is difficult to study the threshold currents and chronaxie times independent of the cell size. However, the range of distribution in the action potential rise times and the sub-threshold time constants between the pyramidal cells of different layers as well as within layer V clearly indicates a great deal of diversity in electrophysiological properties [40, 41].

Another well-known case of diversity is found in the motoneuron (MN) pools of the spinal cord. The MNs in the ventral horn present electrophysiological diversity in the cellular subtypes where each MN pool reflects the characteristics of the muscle fiber types that it controls [42, 43]. A MN pool is defined as a compact anatomical group of MNs sharing similar intrinsic characteristics and connecting to

a single type of extrafusal fibers in the skeletal muscle; mainly slow-twitch fatigue-resistant, fast-twitch fatigue-resistant, or fast-twitch fatigable types [44].

A third example can be found in Purkinje Cells (PCs) of the cerebellar cortex that have been studied extensively for their membrane dynamics. De Schutter and Bower developed a comprehensive model of the cerebellar PCs based on ten different types of voltage-gated membrane channels and matched the Hodgkin-Huxley type model parameters to the voltage clamp data [45-47]. The diversity in the Na+ channel parameters was documented as the source of differentiation in the PC spiking patterns.

Diversification of intrinsic membrane parameters is not random, but it is systematic and linked to function as seen in these examples. With more attention to intrinsic diversity, future studies will probably find more evidence associating the electrophysiological diversity to some form of functional specialization in other parts of the CNS as well. Such reports of experimental data are scarce perhaps due to methodological difficulties.

"Selectivity based on diversity" of electrophysiological membrane properties can lead to functionally selective stimulation, and thus improve therapeutic effects and reduce the magnitude of side effects [10]. The list of applications includes many forms of deep brain stimulation, applications dealing with spinal cord stimulation, and various forms of sensory prostheses. The degree of selectivity will depend on how well the cells can be segregated into functionally distinct units as defined by their membrane properties.

In this chapter, we examined vertical and horizontal translations, introduced by variations in each membrane parameter, of the strength-duration curves using a local membrane model. The sensitivity of chronaxie time and rheobase to each of the membrane parameters was investigated individually and in pairs. We demonstrated that significant levels of selectivity can be achieved as the strength-duration curves begin to cross as a result of these translations. Rectangular stimulation waveforms with hyperpolarizing and depolarizing pre-pulses were tested to investigate if the design of the stimulus waveform can further improve this form of selectivity.

2.2 Methods

2.2.1 Neuron Model

In order to avoid geometry specific effects and maximize the potential for the results to generalize to many neuronal types in the CNS, a basic local membrane model with only one voltage-gated fast sodium channel was used in this study. The Chiu-Ritchie-Rogart-Stagg-Sweeney (CRRSS) model [2, 29, 48], based on myelinated rabbit nerve node data, was utilized as the local membrane model. The CRRSS model is built on gating mechanism similar to the Hodgkin-Huxley (H-H) model [27] and it was altered using a Q_{10} value to bring the model to 37°C and the leakage conductance (G_{leak}) was adjusted to give the action potential conduction velocity of 57 m/s by Sweeney *et al.* [29]. The original H-H model has two voltage-gated currents, sodium and potassium, and a leakage current [27, 32]. The CRRSS model contains only the voltage-gated sodium and the leakage current,

since there are almost no potassium currents in mammalian nodes of Ranvier [2, 48, 49].

2.2.2 Sensitivity Analysis

For sensitivity analysis, we varied both the passive and active membrane parameters by ±25% around their default value, first individually and then in pairs. The ±25% change in membrane parameters is representative of the natural diversity, for instance, observed in the reported values of the cell input resistance and the action potential rise times from the cortical pyramidal neurons [40, 41, 50]. These variations in input resistance and action potential rise time were simulated by changing the membrane leakage conductance (G_{leak}) and the temperature coefficient of the model (K_{temp}), respectively. The other two parameters were the membrane capacitance (C_m) and the maximum sodium conductance (G_{Namax}). We hypothesized that if the passive membrane properties impose a much shorter time constant than the active sodium kinetics, the dynamic parameters that control the latter (K_{temp} and G_{Namax}) would start making a stronger influence on the chronaxie time. To test this hypothesis, we set the default value of C_m ($C_{m\text{-}def}$) to three different numbers, 0.5, 2, and 4 $\mu F/cm^2$ to adjust the passive time constant.

2.2.3 Rectangular Stimulus Waveforms

Three different variations of the rectangular waveform were defined for the (intracellular) stimulation current; a monophasic-anodic pulse (Mono), a biphasic waveform where the (cathodic) hyperpolarizing pre-pulse (HPP) precedes the anodic phase, and an anodic pulse with (anodic) depolarizing pre-pulse (DPP),

(Figure 2.1). The hyperpolarizing pre-pulse was identical to the anodic phase in amplitude and duration to make the waveform charge-balanced. The DPP pre-pulse amplitude was set to 95% of the excitation threshold [38] at each pulse width independently. In order to determine the shortest duration for the depolarizing pulse, we investigated the effect of DPP duration on the selectivity index (SI) (Supplemental Figure A.1) and observed that selectivity index increased with DPP duration and reached 85% of its maximum effect at DPP duration of 1ms when two membrane parameters are varied simultaneously. So, we decided to use 1ms of fixed DPP duration in selectivity analysis. We also investigated the effect of adding a 200 µs gap between the two phases in the HPP waveform, as it is commonly used in neural stimulation applications [38].

2.2.4 Strength-Duration Curve

The pulse-width (PW) of the primary stimulating (anodic) phase was varied from 0.01 to 1 ms, in order to compute the strength-duration (SD) curve for each neuron designed with a unique set of membrane parameters. The strength-duration (SD) curve is defined by threshold level PW and pulse amplitude pairs that result in an action potential. The action potential threshold for each stimulation was determined by a quick search algorithm until the step size was smaller than 0.01 $\mu A/cm^2$. An action potential was decided to occur if the m-gate variable exceeded the 0.98 threshold. The rheobase (Rhe) and chronaxie time (Chr) were determined by fitting the Lapicque equation [51] to the simulated SD curve.

2.2.5 Selectivity Index (SI)

Selectivity here is defined as the ability to stimulate a neuron in exclusion of others that differ in their membrane properties under the exact same stimulus waveform. Different neurons can be activated selectively by carefully choosing the stimulus parameters only if the strength-duration (SD) curves of those neurons cross. The neuron with the red strength-duration (SD) curve in Figure 2.2, for instance, can be activated selectively before the black one with appropriate selection of stimulus parameters on the right side of the crossing point. For selective stimulation of the neuron with black SD curve, another intensity-PW pair has to be chosen on the left side of the crossing point between the two SD curves. Thus, maximization of the separation between the SD curves implies maximization of the intensity range on both sides of the SD curve that can be utilized for selectivity.

The passive ($\mathbf{C_m}$ and $\mathbf{G_{leak}}$) and active ($\mathbf{G_{Namax}}$ and $\mathbf{K_{temp}}$) membrane parameters were varied individually by ± 25% (Table 2.1), and produced three different neurons with the minimum, maximum and default value of each parameter. All possible parameter combinations were tested in pairs to produce nine different neurons and strength-duration (SD) curves were plotted for each. The MATLAB (MathWorks) algorithm found the crossing points between each SD curve pair and calculated a selectivity index (SI). The selectivity index was calculated at the PW where the ratio of the amplitude difference between the SD curves divided by the amplitude of the higher SD curve is maximum. The maximum SI was found on each side of the crossing point ($SI1 = A1/(A1 + B1)$ and $SI2 = A2/(A2 + B2)$ as shown in Figure 2.2) and the smaller of the two was taken as a

conservative value for the final SI for that particular neuron pair. Note that the SI

measure here will be somewhat dependent on the minimum and maximum PWs

tested because in most cases the largest SI value occurs at the extreme ends of

the PW range. Other measures, such as the SD crossing angle, were considered

but the ratiometric measure defined here was chosen as the best representative

metric for selectivity.
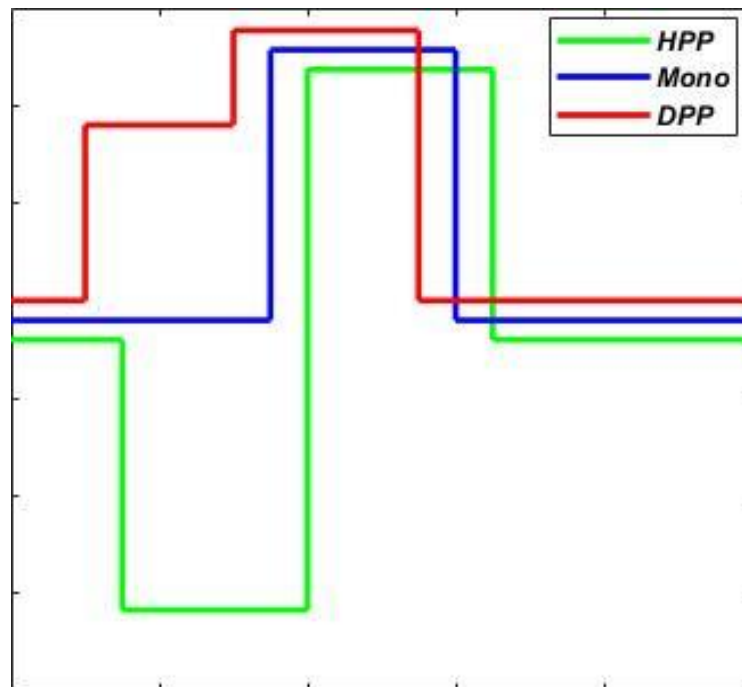
Figure 2.1 Stimulus waveforms: Mono-phasic (Mono), Mono with hyperpolarizing pre-pulse (HPP), and Mono with depolarizing pre-pulse (DPP). Waveforms are shifted to show overlapping parts clearly.
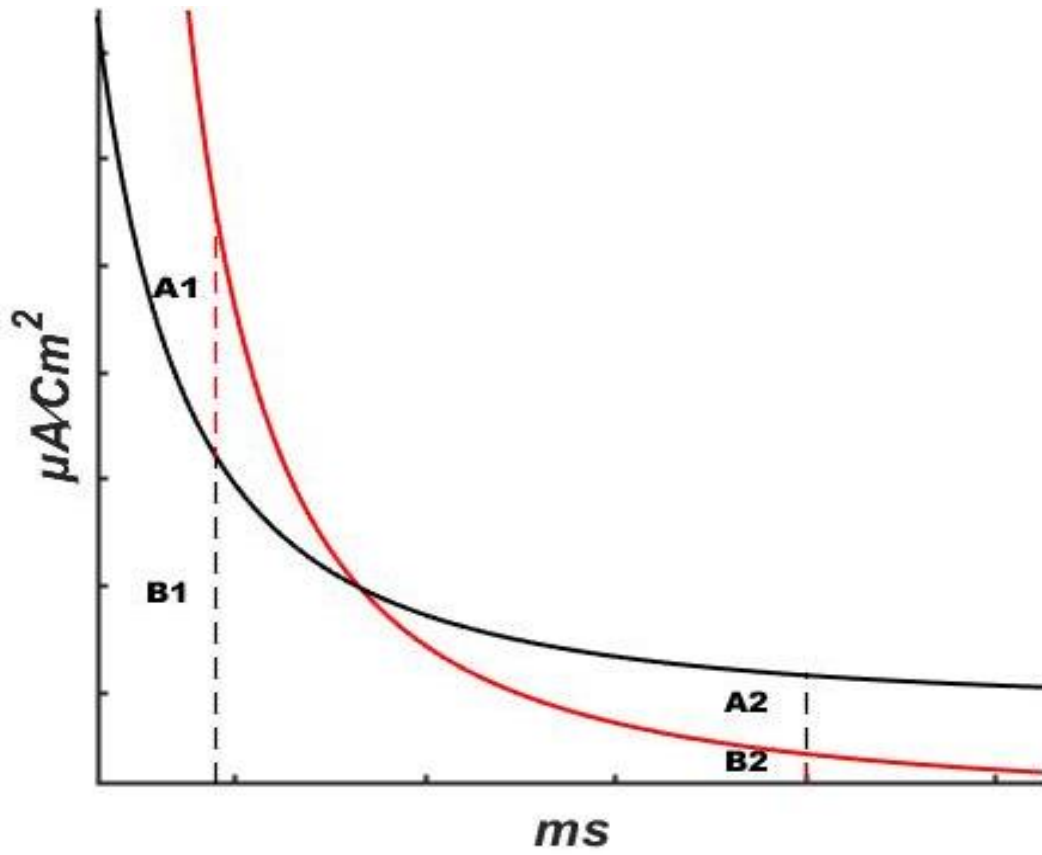
Figure 2.2 Definition of Selectivity Index based on crossing of strength-duration curves.

(a)

(b)
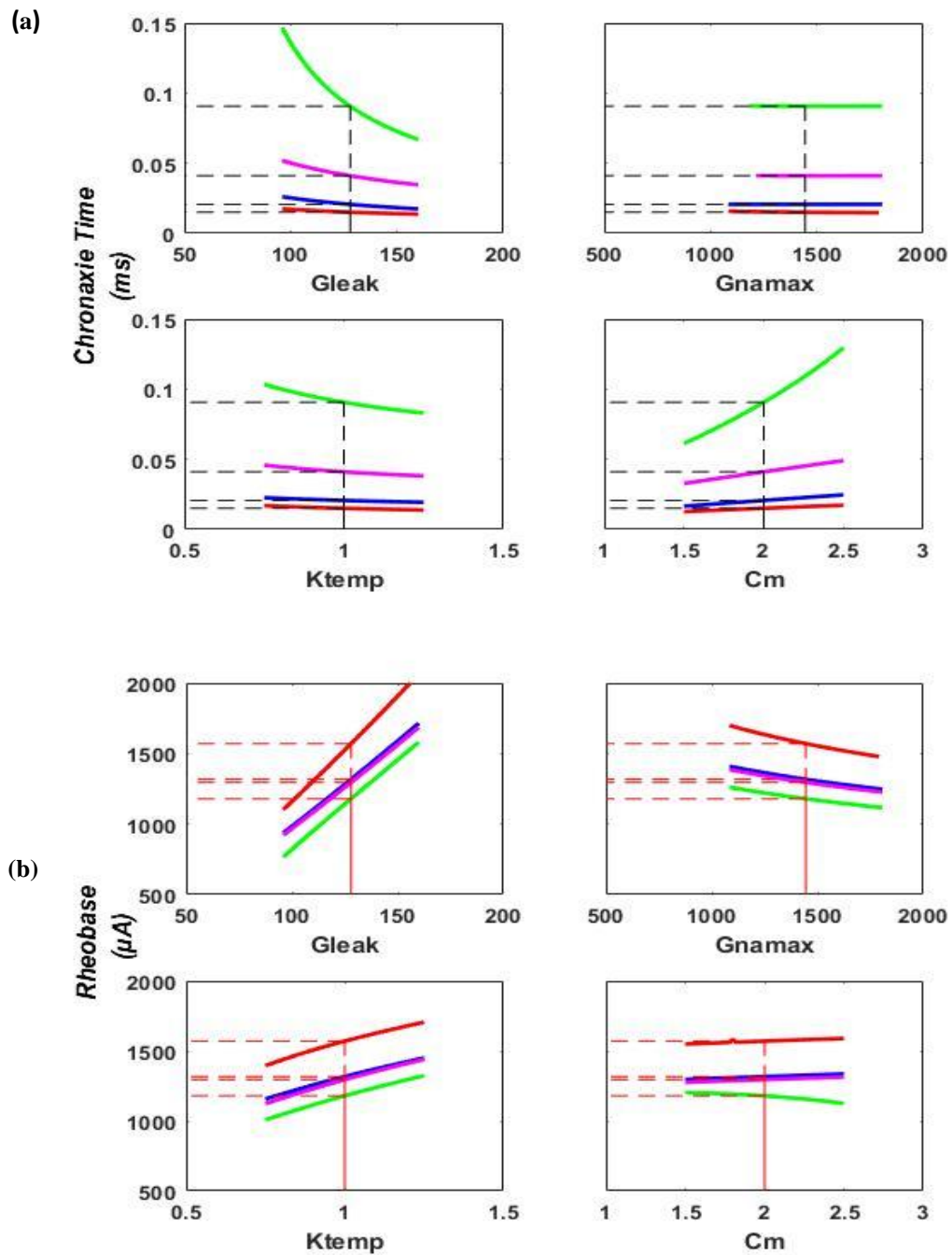
Figure 2.3 Sensitivity analysis of (a) chronaxie time (b) rheobase, repeated for three different stimulus waveforms shown in Figure 2.1 Mono in blue, DPP in Red, and HPP in Green, in addition to HPP with 200 µsec inter-phase gap in Purple. Default value of C_m is 2 µF/cm^2. (a) Chronaxie time increases with C_m while G_{leak} and K_{temp} have opposite effects for all three stimulation waveforms. (b) Rheobase increases with G_{leak}, K_{temp}, and C_m (except for HPP), and decreases with G_{Namax}.

31

2.3 Results

2.3.1 Sensitivity to Individual Membrane Parameters

strength-duration (SD) curves will cross if one moves with respect to the other as the membrane parameters are varied. The horizontal and vertical translations of the SD curve can be captured by examining the chronaxie time (Chr) and the rheobase (Rhe). Any membrane parameter (by itself or in combination with others) that alters these two characteristics in such a way that the SD curve moves along the left-tilted diagonal (\), as opposed to moving along the other diagonal (/), can potentially make the SD curve cross with others and lead to selectivity. Thus, we first performed a sensitivity analysis for Chr and Rhe to the four membrane parameters individually (Figure 2.3 (a) & (b)). Interestingly, increases in both G_{Leak} and K_{temp} decreased Chr and increased Rhe, thus shifted the SD curve to the left and up on the chart. C_m primarily increased Chr and had small effect on Rhe. Increasing G_{Namax} caused a significant reduction in Rhe with virtually no change in Chr. This analysis suggested that G_{leak} and K_{temp} are most likely to produce a crossing in the SD curves, followed by C_m and G_{Namax} combination if they are varied together.

In order to further expand the sensitivity analysis, we set the default value of C_m (C_{m-def}) to two other values, 0.5 and 4 $\mu F/cm^2$, besides the original value of 2 $\mu F/cm^2$ (Figure 2.4). The rationale was to investigate the effects of the other membrane parameters on the strength-duration (SD) curve when the passive time constant of the membrane was substantially lower or higher than those dictated by sodium dynamics. The rise time of the action potential (from 10% to 90% of the

peak) with a very small C_{m-def} in the model (0.1 µF/cm^2) was measured as 12.8 µs. The passive time constant for the same C_m, measured with a small amplitude long hyperpolarization pulse, was less than a microsecond, suggesting that the measured action potential rise time was primarily determined by the sodium channel kinetics for this small value of C_{m-def}. The passive time constant for $C_m = 2$ µF/cm^2 was around 16 µs, which was comparable to the rise time dictated by the sodium kinetics, and ~32 µs for $C_m = 4$ µF/cm^2.

Changing C_{m-def}, first and foremost, altered the sensitivity of Chr to perturbations of C_m around C_{m-def} (Figure 2.4 bottom right). Reducing C_{m-def} to 0.5 µF/cm^2 decreased the slope of the Chr vs. G_{leak} plot and increased the slopes of Chr vs. K_{temp} and G_{Namax} plots. In summary, reducing C_{m-def} reduced the effect of G_{leak} and increased the effects of C_m, K_{temp}, and G_{Namax} on Chr. On the other hand, Increasing the C_{m-def} to 4 µF/cm^2 had an opposite effect on the slopes of these plots, but to a much lesser extent (black lines). Moreover, varying C_{m-def} had no significant effect on the slopes of the plots for Rhe vs. other membrane parameters (Supplemental Figure A.2). This is understandable because Rhe is calculated for a long PW where C_m is completely charged, and the capacitive current is zero before the end of the stimulus.

Table 2.1 The three different values used for each membrane parameter to represent diversity.

Parameter	*Max*	*Default*	*Min*
K_{temp}	1.25	1	0.75
G_{leak} (mS/cm^2)	160	128	96
G_{Namax} (mS/cm^2)	1806	1445	1084
C_m $(\mu F/cm^2)$	0.625	0.5	0.375
	2.5	2	1.5
	5	4	3

Note: The min and max are ±25% deviations from the default. Three different default values of C_m are tested.
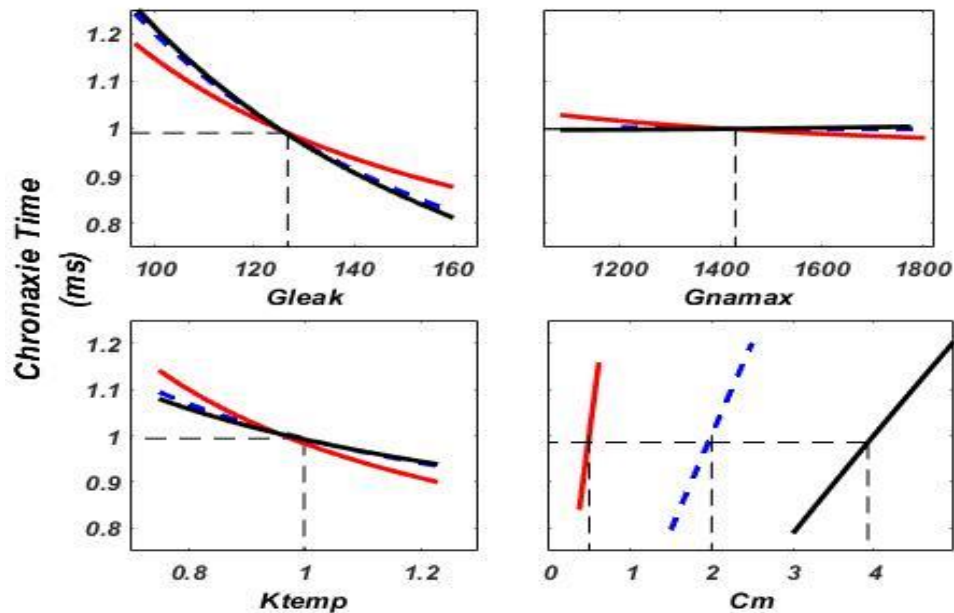
Figure 2.4 Sensitivity of chronaxie time, normalized to the default value, to the membrane parameters (**G_{leak}, G_{namax}, K_{temp}, and C_m**) as they are altered by ±25% from the default value and evaluated at intermediate values. The analysis is repeated for three different default values of **C_m; C_{m-def}**=0.5 µF/cm2 (***Red***), **C_{m-def}** =2 µF/cm2 (***Blue-Dash***), and **C_{m-def}** =4 µF/cm2 (***Black).*** Black dash lines show the default values.
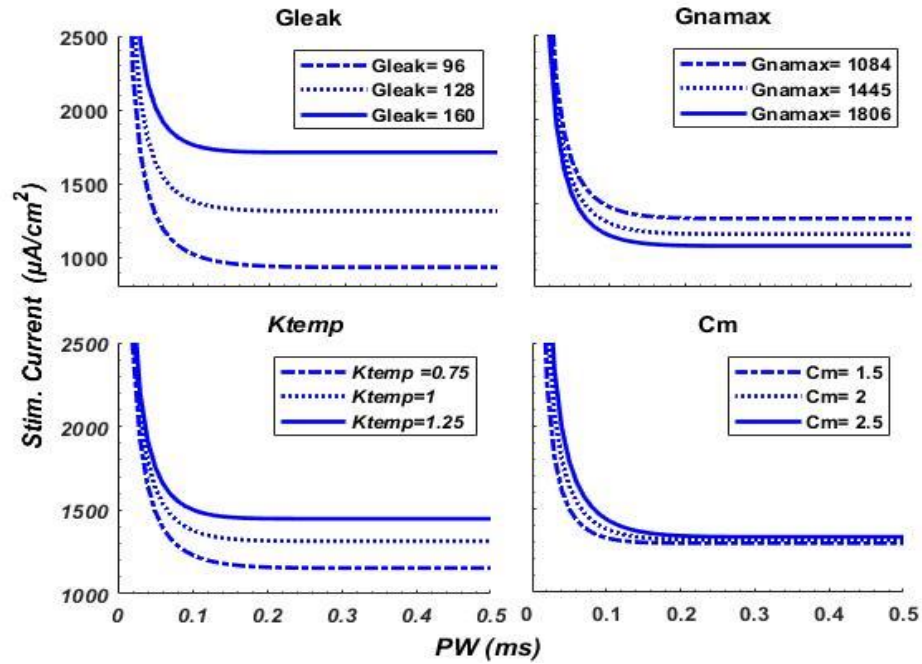
Figure 2.5 The effects of the four model parameters on the strength-duration curve as they are altered individually by ±25%. None of the perturbations produces SD curve crossings. Mono stimulus waveform is used. . **C**$_{m-def}$ = 2 μF/cm^2 .
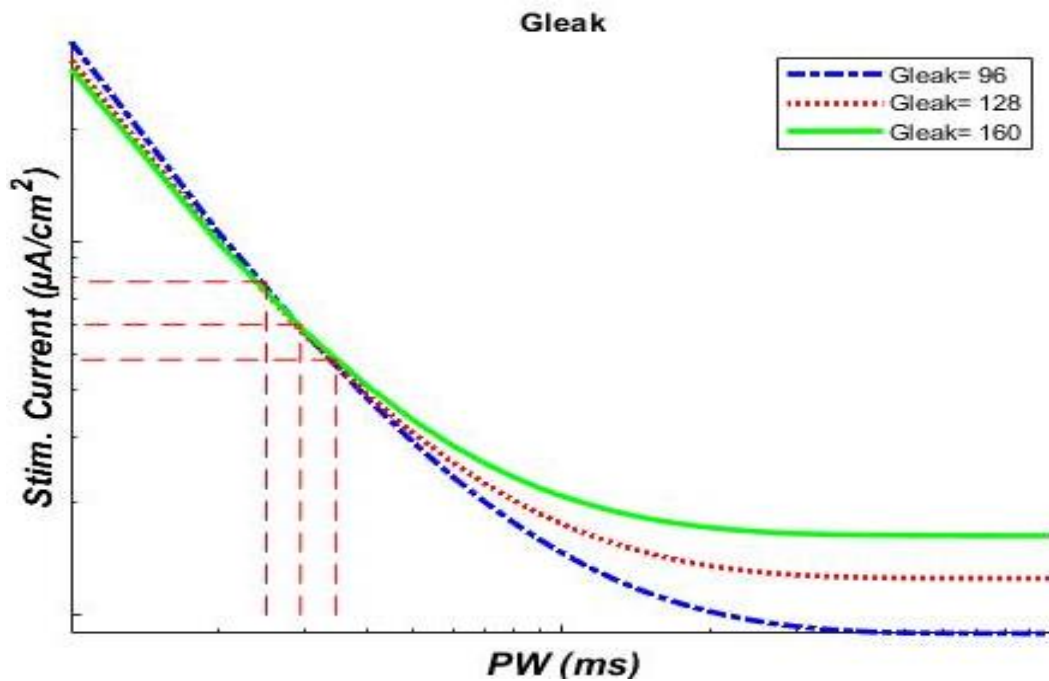
Figure 2.6 Varying **G**$_{leak}$ and using hyperpolarization pulse (HPP) causes crossing between SD Curves.
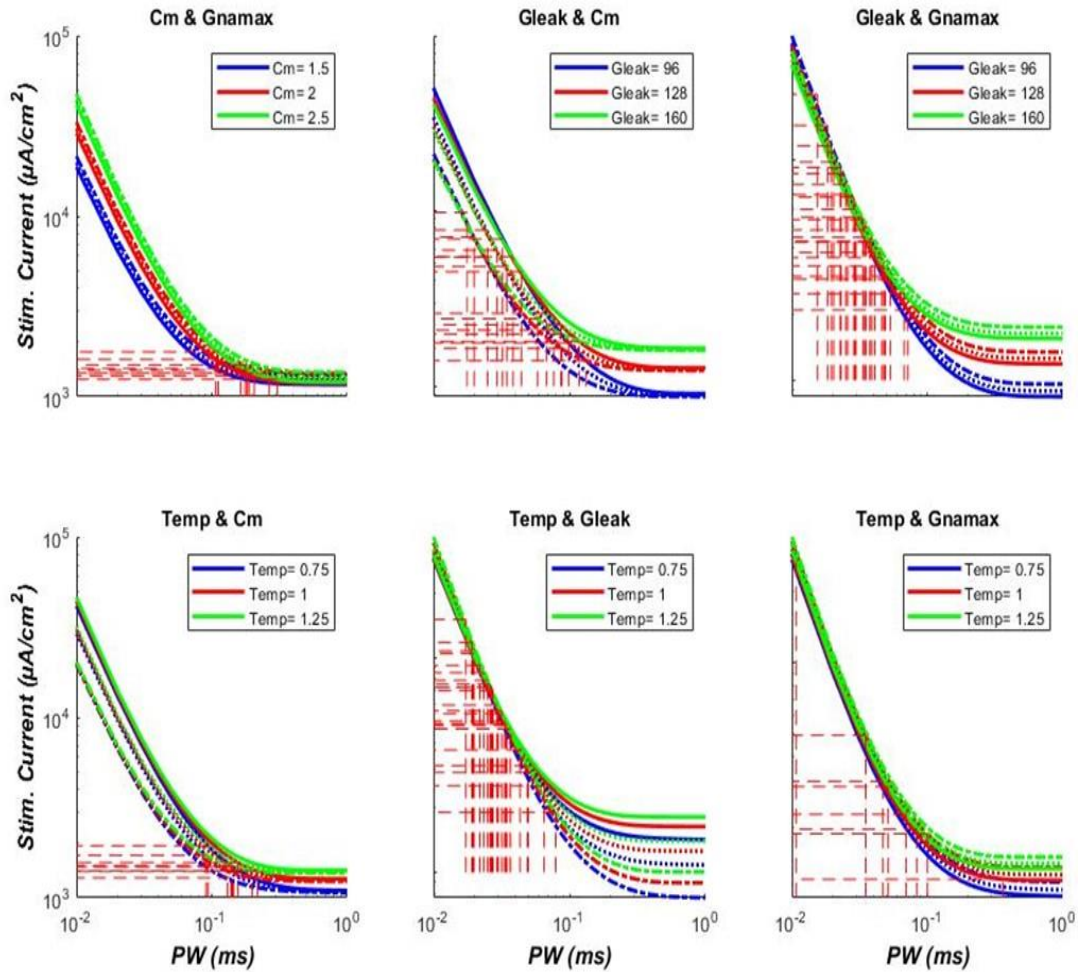
Figure 2.7 Two of the four membrane parameters are altered simultaneously in each case by the same amount as in Fig.4, using HPP waveform. Different colors in each subplot indicate different values for the first parameter shown on top. Second parameter is not color coded for clarity. Red dash lines mark the points of SD crossings, some of which fall outside the figure window.
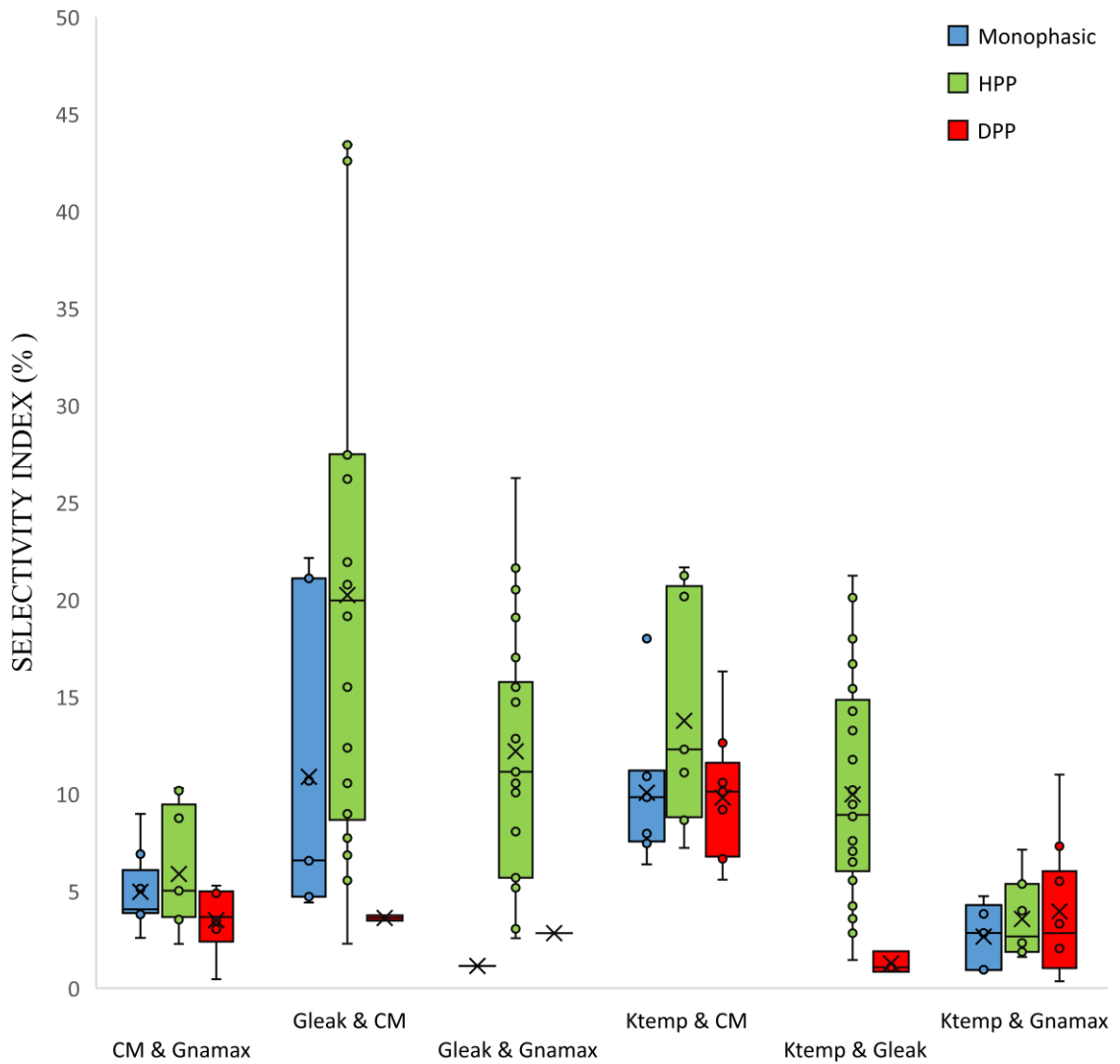
Figure 2.8A Comparison of SI values with **Mono (Blue)**, **HPP (Green),** and **DPP (Red)** stimulus waveforms and for each parameter combination. *Default Cm=2μF⁄cm²* **.** Each dot in the plot represents an SD crossing. **C_m & G_{leak}** combination produces the largest SI values with Mono and HPP stimulus waveforms. The plot highlights the mean value at the cross mark, the median at the line mark which divides the box into the 2nd and 3rd Quartiles and the max & min value at the top and bottom whiskers, respectively.
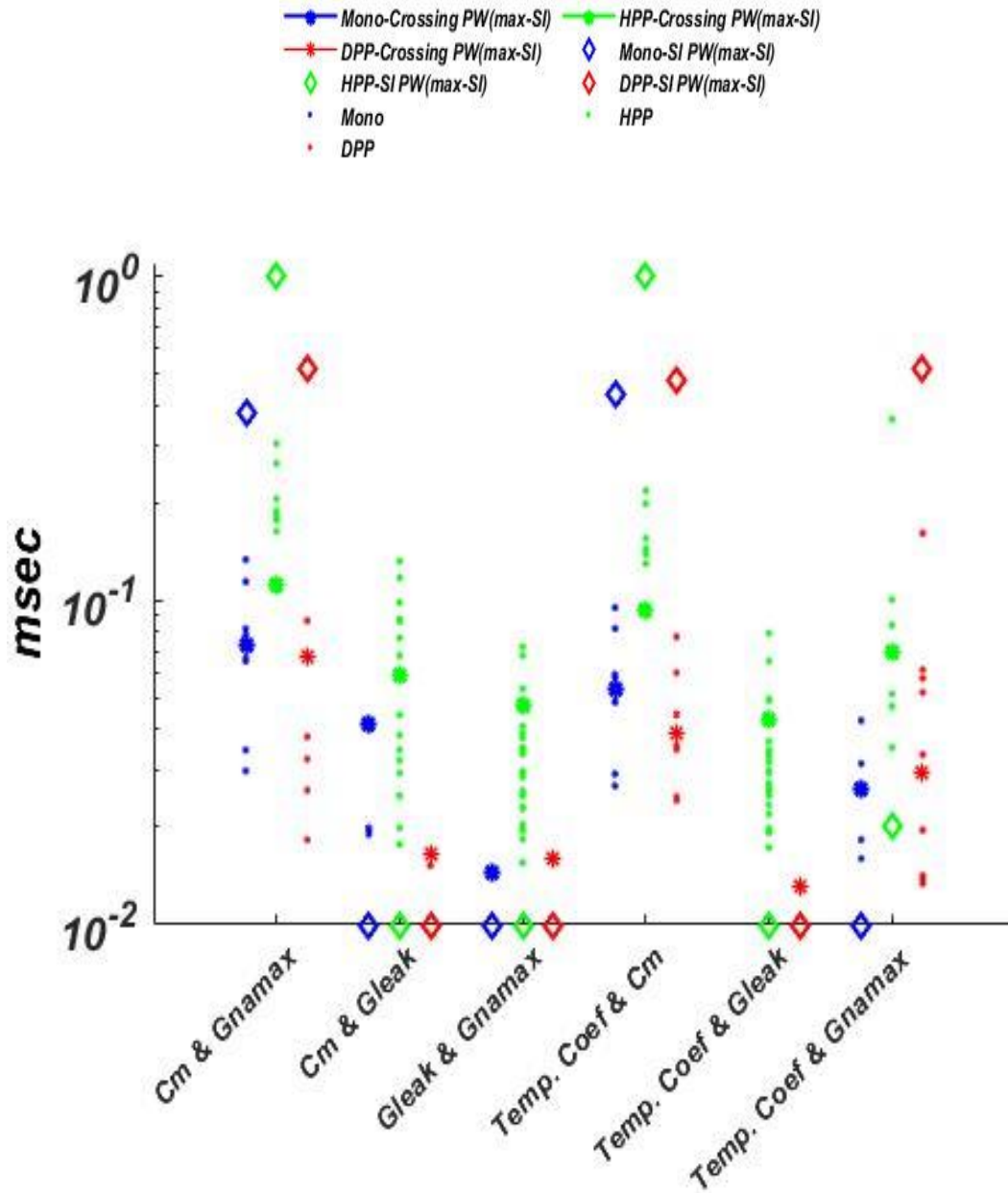
Figure 2.8B Shows the crossing PW at the maximum selectivity index ratio for each parameter marked with "*" . Crossing PW is the point where both SD curves cross together. Diamond shape points "♦" are marking the PW where SI ration is maxima. Rectangular "▲" and "X" markers representing the two SI ratio at the left and right of the crossing point receptively, showing only for maximum SI. Dots '•' marks all other crossing PW points. Mono in blue, HPP in Green DPP in Red

2.3.2   Selectivity with Single Parameter Variation

The strength-duration (SD) curves are shown in Figure 2.5 as the four membrane parameters are altered individually by ±25% and using the traditional monophasic rectangular current pulse (Mono) for stimulation. Each parameter was tested for two extreme and the default values (Table 2.1). As mentioned, the G_{leak} and K_{temp} shifted the SD curves most, although not enough to make them cross. When we added a hyperpolarizing pre-pulse (HPP) to the stimulus waveform, more radical shifts in the SD curve were observed leading to crossing for G_{leak} variations (Figure 2.6 & Supplemental Figure A.3), as predicted by the sensitivity analysis in Figure 2.3. However, the SD crossings were at the lower end of the PW range and the crossing angles were small.

Next, we included a depolarizing pre-pulse (DPP) to the Mono waveform (Figure 2.1). The SD curves with DPP and single parameter diversity did not yield to SD crossings (Supplemental Data, Figure A.4).

Finally, a short time interval of 200 µs between the two phases of the HPP waveform was inserted, giving a waveform commonly used in neural stimulation applications [38]. The effect of having a gap in the HPP waveform on the SD curve was to negate the effects produced by single parameter alterations in all cases (Supplemental Figure A.5).

2.3.3   Selectivity with Dual Parameter Variation

In order to maximize selectivity index (SI), two of the membrane parameters were altered in pairs for all three-stimulus waveform tested. Since each parameter was set to three different values; min, max, and default, the combinations produced

nine different SD curves and a maximum of 36 possible crossings between them. This time, multiple strength-duration (SD) curves crossed for different parameter combinations (Figure 2.7). Although most of the crossings occurred at the extreme pulse widths, there were many crossings in the middle of the PW range as well.

The selectivity index (SI), as defined in Methods, was computed for each one of these SD curve crossings to quantify and compare the selectivity obtained for each stimulus waveform (Figure 2.8A). As expected, HPP (with no gap) stimulus had much higher selectivity values across all combinations compared to Mono and DPP waveforms. The largest selectivity index (SI) values were produced by diversifying G_{Leak} & C_m combination followed by G_{Leak} & G_{Namax} , K_{temp} & C_m and K_{temp} & G_{Leak}, respectively. Contrarily, the DPP waveform produced smaller SI values especially when G_{Leak} is one of the parameters varied. Interestingly, DPP did better than other waveforms only with the K_{temp} & G_{Namax} combination, the dynamic membrane parameters. K_{temp} & C_m combination stood out among those SI where DPP is the stimulus waveform.

For the SI values reported in Figure 2.8A, the PWs at which SD crossings occur and where the SIs are measured are depicted in Figure 2.8B. The crossing PWs are pushed to longer PWs by inclusion of the hyperpolarizing pre-pulse (HPP vs. Mono and DPP) for almost all membrane parameter combinations. The PWs where the maximum SI values occur are usually at the ends of the PW range tested (0.01ms and 1ms). Nonetheless, one can use PWs longer than 0.01ms by sacrificing some selectivity. The longer PWs are preferable for the design of

implantable stimulators where the current intensities are lower and electronic efficiencies are higher.

Then, the selectivity analysis was repeated for three different default values of C_m ($C_{m\text{-def}}$ = 0.5, 2, and 4 $\mu F/cm^2$), and for each default value, all membrane parameters, including C_m, were perturbed ±25% from their default value. As anticipated from sensitivity analysis (Figure 2.4), for $C_{m\text{-def}}$ = 0.5 $\mu F/cm^2$, the effect of G_{leak} was reduced. Thus, the SI for all parameter combinations that included G_{leak} was significantly lower (Figure 2.9), compared to the cases for $C_{m\text{-def}}$ = 2 $\mu F/cm^2$. Although increasing $C_{m\text{-def}}$ from 2 to 4 $\mu F/cm^2$ did not produce appreciable changes in Chr (Figure 2.4), it produced significant differences in selectivity (Figure 2.9). The dynamic membrane parameter combination, K_{temp} & G_{Namax}, generated the smallest selectivity for $C_{m\text{-def}}$ = 4 $\mu F/cm^2$.

2.4 Discussion

2.4.1 Sensitivity to Individual Membrane Parameters

In this study, we investigated a potential mechanism of selective neural stimulation that leverages diversity in passive and active membrane parameters, which we refer to as diversity-based selectivity. The motivation for the current study comes from the correlation reported in literature that links the intrinsic variations in the passive and active membrane parameters to neuronal subtypes that serve different functions in the CNS, as mentioned in the Introduction. This correlation suggests that diversity-based selectivity may lead to functional selectivity, the ultimate objective in all previous efforts on selective neural stimulation.

The spatial selectivity in real neural tissue depends on many geometric factors, including the size and shape of the cell soma, the axon, and other neuronal compartments, and their orientation in the electric field. A 3D model would provide more realistic results, but a local membrane model was selected here to avoid geometry specific effects and maximize the potential for the results to generalize to many neuron types in the CNS. Nonetheless, maximizing the stimulation selectivity based on diversity of membrane parameters can also provide spatial and size selectivity if neurons with distinct membrane parameters also differ in size and localization, which are often linked to function. This step would require 3D neuron models to study if the predicted selectivity values can reverse the current-distance relation and/or the large-to-small recruitment order. The ultimate levels of selectivity will be proportional to the degree by which the neurons can be separated by their membrane properties. Such a separation will have to be verified with electrophysiological experiments in neural tissue, and the selectivity figures would most likely be different in different parts of the CNS.

2.4.2 Mechanisms of Selectivity

2.4.2.1 Temperature Coefficient Effect

Altering the temperature coefficient of the model is equivalent to scaling both α and β coefficients that determine the opening and closing rates of the membrane channels in the model [2, 27, 52]. This scalar, expressed as a function of Q10 coefficient, is typically used to set the temperature of the model to values other than the temperature at which the experimental data were collected. Increasing temperature makes the model faster and shifts the SD curve to the left, (in the -X

direction), resulting in smaller chronaxie times (Figure 2.3-a)   [53, 54]. Furthermore, the initial values of the rate coefficients also affect the stimulus threshold. Particularly increasing α, the channel opening rate, makes the neuronal membrane more permeable to Na+ ions, which in turn increases the activation threshold (Supplemental Figure A.5) and moves the SD curve upward (in the +Y direction); Ktemp in Figure 2.3 (b) & Figure 2.5). Note that this result is in contrast with the temperature effect seen in another report with Frankenhaeuser-Huxley model [55], where, unlike the CRRSS model, a potassium current that has a negative Nernst potential below the resting membrane voltage, is included. Thus, the net effect of the temperature increase on rheobase could be in opposite directions in these two models. However, the effect on chronaxie, which is due sodium kinetics, should be same.

2.4.2.2 Effect of G_{leak}

Conductivity of the leakage channel is relatively low compared to the maximum conductivity of the sodium channel (GNamax), but it significantly influences two other parameters, the cell input resistance (Ri) and the resting membrane voltage. Because G_{leak} is a parallel current pathway, it directly contributes to the input conductance, the inverse of input resistance, and determines the passive time constant of the membrane together with C_m. Thus, an increase in Gleak reduces the differential depolarization in the transmembrane voltage as a response to the same stimulus current pulse. This increases the stimulus thresholds and moves the strength-duration (SD) curve in the (+Y) direction (Figure 2.3-b and Figure 2.5 bottom left). On the other hand, the passive time constant of the cell also

determines how fast the transmembrane potential will move towards the activation threshold at sub-threshold voltages before the voltage-gated currents become significant. A larger G_{leak} results in a shorter time constant, and thus a shorter chronaxie time (Figure 2.3 (a)). Similar trends in G_{leak} effects on the strength-duration SD curve were observed by Bostock based on myelinated axon model by Goldman and Albus [56]. In sum, a reduction in the input resistance due to a G_{leak} increase moves the strength-duration SD curve up (+Y) and to the left (-X), hence potentially making the SD curves cross even without needing any other parameter to be modified (Supplemental Figure A.2 - Top right).

2.4.2.3 Effect of Capacitance

C_m determines the passive time constant of the cell and directly affects the chronaxie time, but does not influence the rheobase or the resting cell potential, as also confirmed by the Bostock study [57] . We repeated the analysis for three different default values of C_m (C_{m-def}) in order to see how the sensitivites to other membrane parameters change for different values of the passive membrane time constant. No significant change was observed in the rheobase plots for ±25% variation of C_m around any of the $C_{m\text{-}def}$ values. However, switching $C_{m\text{-}def}$ to lower and higher values (0.5 and 4 µF/cm^2) influenced the sensitivity of Chr to all the other membrane parameters as well as to C_m itself. Decreasing C_{m-def} reduced the effect of G_{Leak}, but amplified the effects of K_{temp}, C_m, and G_{Namax} on Chr. This confirms our hypothesis that a smaller passive time constant allows the temporal dynamics, imposed by sodium channels, to dominate the activation time. Consequently, it reduces the effect of G_{leak}, the other passive membrane

parameter. Conversely, it increases the effects of the dynamic parameters, K_{temp} and G_{Namax}. The sensitivity of Chr to C_m itself seems to become larger for the smaller value of C_{m-def} because of the increase in slope (Figure 2.4), but in fact the total change in Chr is less for the smaller C_{m-def} (0.5 µF/cm^2). The opposite trends should occur with the larger value of C_{m-def} (4 µF/cm^2). Indeed, they do but only to a lesser extent because at 2 µF/cm^2 the passive time constant (16 µs) is already quite dominant and increaseing it further provides only marginal effects. However, those small changes in Chr and Rhe result in substantial improvements in the SI values in the final plots when G_{Leak} is one of the parameters allowed to vary (compare plots for C_{m-def} = 2 and 4 µF/cm^2 in G_{Leak} & G_{Namax} and K_{temp} & G_{Leak} in Figure 1.8).

2.4.2.4 *Effect of G_{Namax}*

G_{Namax} defines the maximum conductance of the sodium channel [58, 59]. While at first sight, this may not seem directly related to the activation threshold, the small percent of change that G_{Namax} introduces to the sodium current at the onset of sodium channel activation seems to be significant enough to make the SD curve move downward (in the -Y direction), by decreasing Rhe (Figure 2.3 (b)). Similarly, the Bostock study reported a 10% decrease in rheobase when G_{Namax} was doubled and 10% increase when G_{Namax} was reduced by 50% [57]. Nonetheless, G_{Namax} effect on Chr was insignificant for C_{m-def}=2 µF/cm^2 (Figure 2.3(a)) and very small for C_{m-def}=0.5 µF/cm^2 (Figure 2.4). This is comparable to results of the Bostock study where doubling the G_{Namax} reduced the chronaxie time only by 3% [57].

2.4.2.5 Dual Parameter Effects

When two membrane parameters are allowed to vary, the individual effects begin to add and make the SD curves move by larger amounts, thereby leading to higher selectivity. For instance, G_{Leak} & C_m combination produces the largest number of crossings at mid-values of the PW with large angles, yielding the highest selectivity index (SI) values. Supporting evidence exists in literature that these variations in individual membrane parameters occur in the CNS neurons [44, 60-62]. However, it is not clear if we can realistically assume that two or more parameters can simultaneously differ by significant amounts in groups of CNS neurons that sub-serve different functions. Literature reporting on such comprehensive set of measurements on neuronal properties is scarce.

2.4.2.6 Rectangular Stimulus Waveform

A study by Grill et al. [38] investigated the effect of depolarizing pre-pulsing (DPP) on the current-distance relationship and showed that it increases the activation threshold of fibers close to the electrode more than the fibers further away, whereas the HPP produces the opposite effect. In this study, HPP moves Rhe in (-Y) direction causing more strength-duration (SD) crossings and increases the SI, whereas DPP moves it in the (+Y) direction sending the SD curve away from the crossing region and reduces selectivity, as shown with larger Rhe in Figure 2.3 (b). This is interesting to note since DPP was proposed to reverse the current-distance relation by activating the distant (and smaller) fibers before the closer (and larger) ones [3], and HPP did not provide any selectivity. Contrarily, our results show that

HPP waveform in fact provides larger selectivity values than DPP. This suggests that the selectivity mechanism reported here is only possible if diversity of electrophysiological parameters is introduced to the model. In addition, our results showed that adding a 200 µsec gap between the phases in the HPP waveform eliminated the effect of hyperpolarizing pre-pulse, which confirms the earlier reports on the effects of pre-pulsing [36, 38].

2.4.2.7   Reversing the size or distance rule

We can find out how much spatial or fiber size selectivity the computed diversity-based SI values correspond to using some simple calculations. Let us assume that the proposed electrophysiological diversity exists among the axonal fibers of the same caliber at a few nodes of Ranvier nearest to the stimulation electrode. An activation function was formulated by Rattay [25, 63] for a myelinated fiber in an infinite homogeneous medium at a certain distance from a monopolar electrode. After all terms that do not depend on the fiber diameter, including the nodal lengths, are eliminated in the function, it can be shown that the second difference of the voltage along the axon is what determines if the stimulus current can generate an action potential:

$$V_{e,n-1} - 2V_{e,n} + V_{e,n+1} \qquad\qquad (2.1)$$

where n is the index for the node of Ranvier. Thus, the activation function is different for different fiber sizes only because the inter-nodal distance increases

almost proportionally with the fiber dimeter. As the activation function is evaluated for a 10 µm fiber located at 1.0 mm and 1.25 mm from the stimulation electrode, we find a 40% difference in the threshold (Supplement Figure A.6). This implies that the SI values reported in this paper (Figure 2.8 (A)) can reverse the stimulation order for these two fibers in favor of the distant one. The 0.25 mm separation between these two fibers is a practically useful level of spatial selectivity for many neural stimulation applications. Note that the threshold difference would be larger for fiber pairs closer to the electrode with the same inter-fiber separation.

A similar analysis can be conducted for fibers of different caliber but at the same distance from the electrode (Supplemental Figure A.7). As we compare a 10 µm and 20 µm axons both at 1 mm from the electrode, we find that the threshold difference is 47%, which is also comparable to the best SI values reported here. This implies that the fiber size order can be reversed in favor of the smaller fiber by the selectivity gained by electrophysiological diversity together with the HPP waveform.
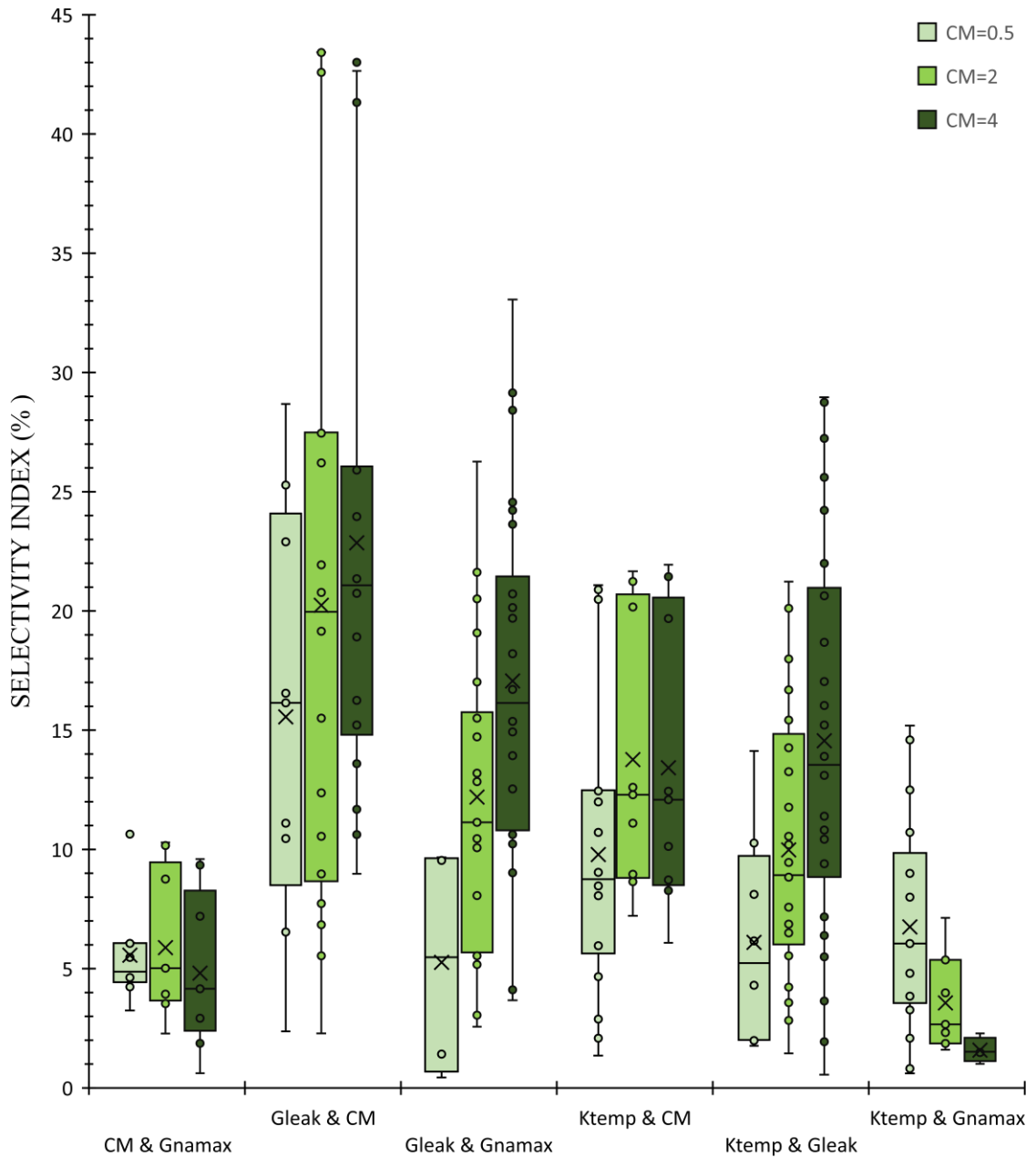
Figure 2.9 Comparison between three CRRSS model variations produced by setting the default value of C_m to 0.5µF$/cm^2$, 2 µF$/cm^2$, and 4 µF$/cm^2$, represented in different shades of green. HPP is the stimulus waveform. The smaller value of Cm provides superior SI values only with Temp & G_{Namax} combination, both of which are dynamic membrane parameters. With all other parameter pairs where at least one of the parameters is a passive membrane parameter, the larger C_m values (2 and 4 µf/cm2) produce higher SI values.

CHAPTER 3

DIVERSITY-BASED NEURAL SELECTIVITY USING ALTERATIVE STIMULUS WAVEFORMS

3.1 Background and Significance

Stimulation of neurons by way of delivering small electric currents has led to treatment of numerous neurological disorders and injuries in the central and peripheral nervous system. One of the primary limitations of electrical nerve stimulation is the lack of specificity [6, 7]. The techniques proposed for selective activation make the assumption that the neurons or axons share the same membrane properties but only differ in their size, morphology [39], or location in the electric field.

No study so far has tried to select an optimal stimulus waveform that would match the neuronal membrane properties of neuronal subtypes as a means to achieve selective activation. Diversity in passive and dynamic membrane properties of neurons clearly exists as evidenced in many parts of the central nervous system (CNS). For instance, four different pyramidal neuron subtypes were found in layer V of the rat medial prefrontal cortex [40], classified based on their morphology and membrane resistance. Different neurons had significantly different membrane time constants and rheobase currents. The range of distribution in the action potential rise times and the sub-threshold time constants between the pyramidal cells of different layers as well as within layer V clearly indicates a great deal of diversity in electrophysiological properties [40, 41].

Diversification of intrinsic membrane parameters is not random, but it is systematic and linked to function. With more attention to intrinsic diversity, future studies will probably find more evidence associating the electrophysiological diversity to some form of functional specialization in other parts of the CNS as well. Such reports of experimental data are scarce perhaps due to methodological difficulties.

Selective activation of neurons by levering their differences in the electrophysiological membrane properties can lead to functional selective stimulation, and thus improve therapeutic effects and reduce the magnitude of side effects [10].

Historically, rectangular waveform has been widely used for neural stimulation in most therapeutic applications. Offiner (1964) determined that an exponentially increasing stimulus can minimize the power required for stimulation, hence it reduces the neural damage caused by the generated heat [64]. In our lab, we investigated seven different non-rectangular waveforms for minimization of the stimulus energy, and showed that a linear ramp, exponential decrease (ExpDec), and Gaussian (Gauss) waveforms were most efficient [15]. They required the smallest electrode surface area to generate the strongest stimulation effect. Inspired by this original finding, several other reports looked at efficiency of non-rectangular waveforms. Kajimoto et al (2004), Fishler (2000), and Jezernike & Morarii (2005) all agreed that an exponentially increasing (ExpInc) waveform is the most energy optimal waveform for current stimulation [20, 65, 66].

A study by Grill et al investigated the effect of stimulus waveform on stimulus selectivity. The study compared between the traditional rectangular pulse and the depolarization pre-pulses (DPP), the study showed that DPP inverses the slope of the current-distance relationship allowing the stimulation on fibers further away from the electrode at lower current than for closer ones[38].

In the first chapter, we showed that selectivity could be achieved using the rectangular stimulus waveform preceded by a hyperpolarizing pulse (HPP) in a population of neurons with varying passive and active membrane parameters. In this chapter, we further investigate this topic by introducing non-rectangular waveforms for the main stimulation phase of the stimulus. The results suggest that non-rectangular waveform can significantly increase the level of selectivity when combined with hyperpolarization pre pulse (HPP).

3.2 Methods

3.2.1 Neuron Model

The methodology used is similar to the method use in the first chapter . Briefly, the Chiu-Ritchie-Rogart-Stagg-Sweeney (CRRSS) model [2, 29, 48], based on myelinated rabbit nerve node experimental data and modified for body temperature, is utilized as a local membrane model in this study. The CRRSS model contains only the voltage-gated sodium and the leakage current, since there are almost no potassium currents in mammalian nodes of Ranvier [2, 48, 49]. The data produced using a basic model, like the CRRSS, may generalize across many

neuronal subtypes since most excitable neurons have voltage-gated sodium channels and leakage.

3.2.2 Sensitivity Analysis:
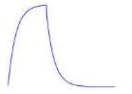
As in chapter one, we varied all the membrane parameters by ±25% around their default value, first individually and then in pairs, to simulate the diversity and its effect on strength duration (SD) curve. The ±25% change in membrane parameters is taken as a representative value for the natural diversity reported for some of these parameters, such as the cell input resistance and the action potential rise times [40, 41, 50]. Unfortunately, there are no reported studies that looked into the diversity of all or most electrophysiological parameters in a specific neuronal subtype for us to adopt here. In the previous chapter, depolarizing and hyperpolarizing pre-pulsing options with rectangular stimulus waveform were tested for selectivity. In this chapter, we introduced eight different stimulus waveforms [15, 19], with and without the hyperpolarization pre-pulse (HPP) [38], which was critical to maximize the selectivity. We hypothesized that using non-rectangular stimulus waveforms may shift the SD curves in a way to achieve higher levels of selectivity than the classical rectangular waveform in the presence of electrophysiological diversity.

3.2.3 Stimulus Waveforms

Eight stimulus waveforms tested were (Table 1); Charge-discharge curve (Chr-Dis), increasing and decreasing exponential (ExpInc and ExpDec) respectively, Gaussian (Gauss), KT^2, Linear (Lin), sinewave (Sine), and rectangular (Rect) as

defined and tested previously for minimization of stimulation energy [15]. All stimulus waveforms were applied either as a monophasic-anodic pulse (Mono) or a biphasic waveform where a rectangular hyperpolarizing pre-pulse (HPP), cathodic, preceded the anodic phase (Table 3.1). The hyperpolarizing pre-pulse had the same duration as the stimulus pulse and identical area to the anodic phase to make the waveform charge-balanced.

Table 3.1 Eight monophasic stimulus waveforms tested.

1		Chr-Dis	$K \left[1 - e^{-\frac{10t}{\tau}} \quad\quad 1 - e^{-\frac{10(\tau-t)}{\tau}}\right]$
2		ExpDec	$K(e^{-\frac{5(\tau-t)}{\tau}})$
3		ExpInc	$K(e^{-\frac{5t}{\tau}})$
4		Gauss	$\dfrac{K}{(\tau/5)\sqrt{2\pi}} e^{-\left(\frac{t-\frac{\tau}{2}}{\sqrt{2}\frac{\tau}{5}}\right)^2}$
5		Kt²	Kt^2
6		Lin	Kt
7		Sine	$K\sin(\dfrac{\pi t}{\tau})$
8		Rect	$K[u(t) - u(t-\tau)]$

3.2.4 *Strength-Duration Curve (SD)*

The SD curve shows the threshold values for the pulse width (PW) and pulse amplitude that result in an action potential. The PW of the primary stimulating (anodic) phase was varied from 0.01 to 5 ms in order to compute the strength-duration (SD) curve for each neuron designed with a unique set of membrane parameters. The threshold amplitude at each PW was determined by an adaptive search algorithm that finds the smallest step size that allows cell activation. An action potential was decided to occur if the m-gate variable exceeded the 0.98 threshold. The rheobase current (Rhe) and chronaxie time (Chr) were determined by following the general accepted definitions from SD curve, i.e. the Chr is the pulse width at which the threshold is twice the Rhe. The idea of fitting the Lapicque-Weiss [51] or Lapicque-Blair [67, 68] equations to the simulated SD curve for estimation of Rhe and Chr was abandoned because of poor curve fittings for the non-rectangular waveforms.

3.2.5 Selectivity Index (SI)

Selectivity here is defined as the ability to stimulate a group of neurons in exclusion of others that differ in their membrane properties under the same stimulus waveform. The passive (C_m and G_{leak}) and active (G_{Namax} and K_{temp}) membrane parameters were varied individually by ± 25%, and produced three different neurons with the minimum, maximum and default value of each parameter. Then, parameters were varied in pairs to produce nine different neurons (3x3). Crossing between SD curves implied selectivity. The MATLAB (MathWorks Inc., MA) algorithm found the crossing points between SD curve pairs and calculated a

selectivity index (SI). The selectivity index was calculated by dividing the largest amplitude difference between the SD curves on each side of the crossing point by the amplitude of the higher SD curve at that pulse width, e.g. $SI1 = A1/(A1 + B1)$ and $SI2 = A2/(A2 + B2)$. The smaller of SI1 and SI2 was taken as a conservative value for the final SI for that particular neuron pair.
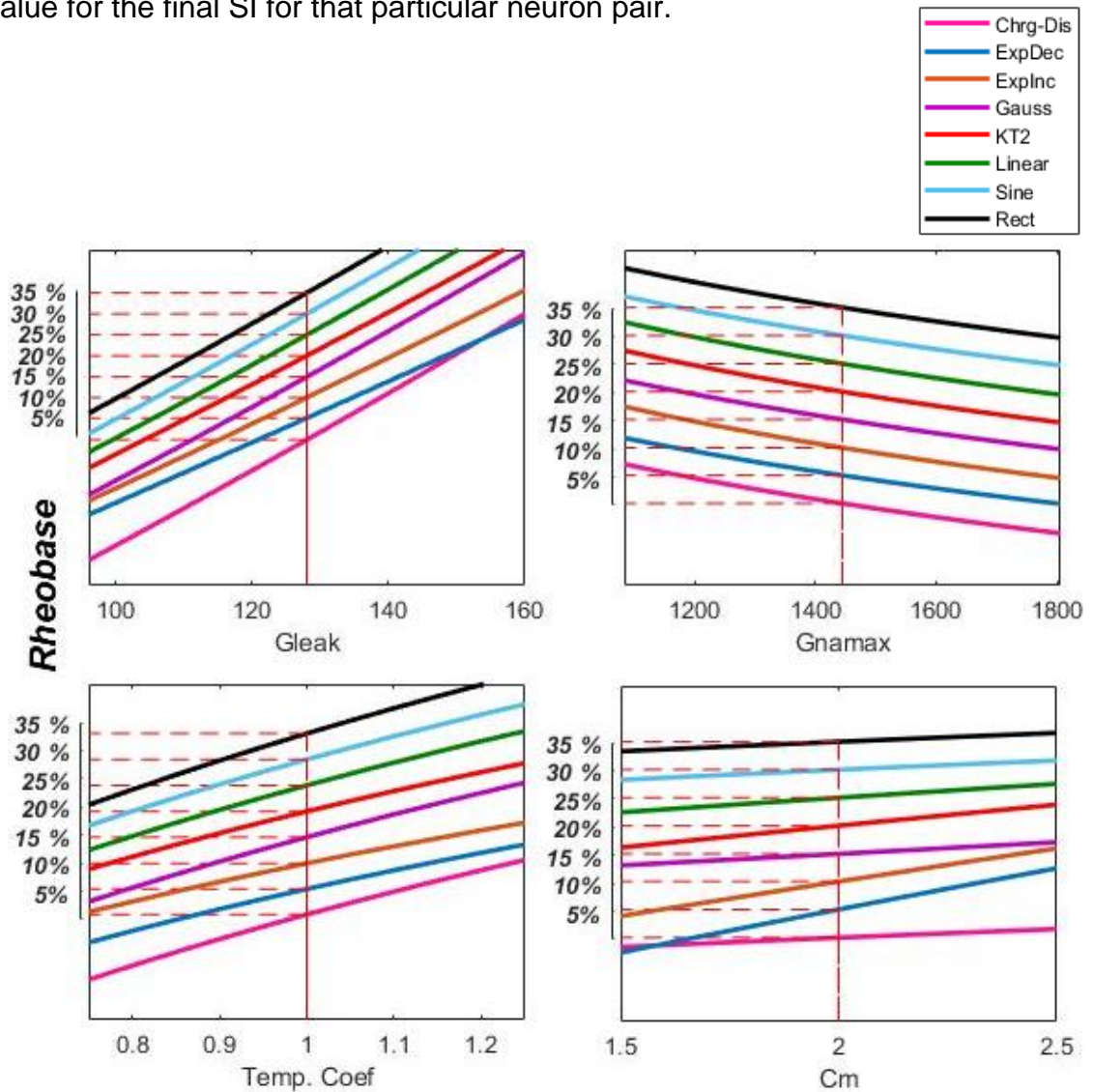
Figure 3.1A Sensitivity analysis showing the Rheobase data, each line represents the behavior of stimulus waveform. Eight stimulus waveforms are used with a hyperpolarization pulse (HPP) included.
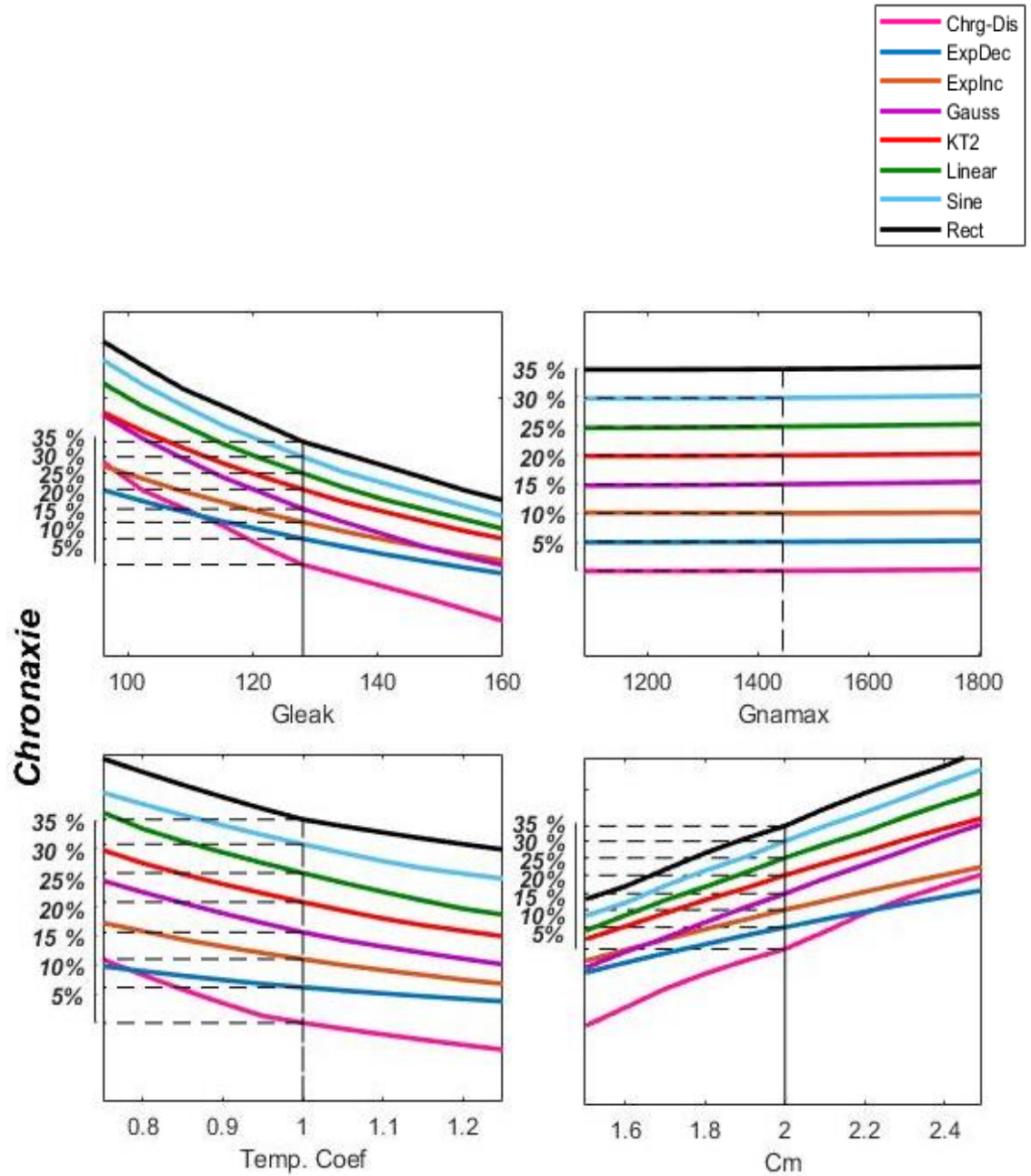
Figure 3.1B Sensitivity analysis showing the Chronaxie data, each line represents the behavior of stimulus waveform. Eight stimulus waveforms are used with a hyperpolarization pulse (HPP) included.

3.3 Results

3.3.1 Sensitivity to Individual Membrane Parameters

SD curve's horizontal and vertical translations as the membrane parameters are varied can be captured by examining the Chr and the Rhe. Any stimulus waveform that alters these two characteristics in such a way to make the SD curves cross can lead to selectivity. Thus, we first performed a sensitivity analysis for Chr and Rhe to the four membrane parameters individually while each one of the eight different stimulus waveforms is being used for stimulation (Figure 3.1).

Interestingly, the choice of the stimulus waveform played a critical role in augmenting the diversity effects of membrane parameters on the SD curve. However, this was true only when the HPP was included in the waveform. Without the HPP (i.e., Mono), the SD sensitivity plots for various membrane parameters did not deviate more than a few percent from that of the Rect (Supplementary Figure B.1). When HPP included, the parameter diversity introduced larger percent changes in Rhe with the non-rectangular waveforms than with the Rect (smaller slopes in Figure 3.1 A). The most prominent baseline translations were observed with ExpDec and ExpInc. Moreover, ExpDec, ExpInc, and Kt^2 had smaller slopes in the Chr plots (Figure 3.1 B), i.e. stronger dependence on the membrane parameter compared to that of Rect. An increase in the Chr slope tends to spread the SD crossing points towards the center of the PW range. The Chr slope for Sine and Gauss were almost identical, small percent of change, to that of the Rect for all four parameters (Table 3.2). Consistently, rheobase analysis revealed that

ExpDec, ExpInc, and Kt^2 slope had a decrease, shown by (-) sign, in the slope when varying $\mathbf{G_{Leak}}$ and $\mathbf{K_{temp}}$. When Varying $\mathbf{C_m}$ all eight waveform had equal or greater slope, specially ExpDec and ExpInc have a high percent change compared to Rect, specially for Rhe. Additionally, for all four parameters the Chr and Rhe slope for Sine was almost identical to that of Rect. The effects of all eight stimulus waveforms were negligible on both Chr and Rhe when $\mathbf{G_{Namax}}$ was diversified.

Table 3.2. Percent of change in Chronaxie and Rheobase slopes for HPP stimulus waveforms compared to Rect waveform

	$\mathbf{G_{Leak}}$	$\mathbf{G_{Namax}}$	$\mathbf{K_{temp}}$	$\mathbf{C_m}$
Percent Change in Chr %				
Chrg-Dis	-1.43	0.00	-3.60	1.09
ExpDec	-47.14	0.00	-61.60	-45.10
ExpInc	-40.00	0.00	-33.03	-37.31
Gauss	-4.29	0.00	-7.58	-3.69
Kt^2	-20.00	0.00	-5.24	-18.72
Linear	-8.57	0.00	11.54	-7.26
Sine	-1.43	0.00	-3.53	-1.32
Rect	0.00	0.00	0.00	0.00
Percent Change in Rheobase %				
Chrg-Dis	0.00	0.00	-8.94	-1.82
ExpDec	-20.65	0.00	-25.51	357.75
ExpInc	-14.13	0.00	-32.09	267.78
Gauss	-2.17	0.00	-9.52	26.44
Kt^2	-6.52	0.00	-19.33	132.83
Linear	-2.17	0.00	-9.44	54.71
Sine	-1.09	0.00	-7.72	5.47
Rect	0.00	0.00	0.00	0.00

Note: Change in slope were calculated using the following equation 100*(Sw-SRect)/SRect). Sw is the slope for non-rectangular waveform, and SRect is the slope for rectangular waveform.

ExpInc and ExpDec waveforms stand out for having a higher change in slope than others in terms of sensitivity of both Chr and Rhe to changes in G_{Leak} and Cm. Chr and Rhe sensitivities to K_{temp} diversity are the highest with ExpDec waveform only (Chr and Rhe slopes are -0.12 and 0.38, respectively, compared to that of Rect: -0.31 and 0.508) with a 61.6 % change in Chr and 25.5 % change in Rhe. Furthermore, for G_{namax} diversity, Rhe had a slope of 0.0002 for ExpDec while Chr slope was near zero for all other waveforms (Supplement Table B.2). Although, Rhe slopes with KT^2 were in the same range as with other waveforms, KT^2 imporved the effect of the parameters to make the SD curves cross and lead to selectivity more so than other stimulus waveforms.

3.3.2 Selectivity with Single Parameter Variation

Varying a single parameter did not results in SD curve crossings except in the case of G_{Leak}. In the first chapter we showed that using hyperpolarization pre-pulse with the Rect stimulus waveform in combination with G_{Leak} diversity led to selectivity. In this paper, we investigated the effect of non-rectangular stimulus waveform. The results are similar for all non-rectangular stimulus waveforms with HPP and all introduced crossings when G_{Leak} is varied. Only ExpInc produced crossings when K_{temp} is varied as well (Supplementary. Figure B.5).

3.3.3 Selectivity with Dual Parameter Variation

The selectivity index (SI) was calculated as defined earlier at the PW where the ratio of the amplitude difference between the SD curves divided by the amplitude of the higher SD curve is maximum. The maximum SI was found on each side of

the crossing point ($SI1=A1/(A1+B1)$) and $SI2=A2/(A2+B2$ in and the smaller of the two was taken as the conservative value for the final SI for that particular neuron pair. In order to maximize the SI two of the membrane parameters were altered in pairs. Since each parameter in the pair was set to three different values; min, max, and default, the combinations produced 9 different SD curves (i.e. neurons) and a maximum of 36 possible crossings between the SD curves. This time, multiple SD curves crossed for all parameter combinations (Supplementary. Figures. B.2, B.3, and B.4). Each stimulus pulse was tested as a monophasic waveform (Mono, not shown) and with hyperpolarization pre-pulse (HPP) added. All crossings occurred at PWs shorter than the chronaxie times of the SD pairs.

To take a closer look at how the calculated SI value was dependent on the PW at which it is calculated, the SI was plotted as a function of PW for three of the six parameter pairs and for two of the waveforms (Lin and Rect) as examples in Figure 3.2. The SI values are zero at the points of SD crossings. Most SDs cross only once but others cross at two different PWs. The SI takes its maximum values mostly at the extreme ends of the PW range. However, there are cases where the maximum occurs in the mid-PW values especially when there are two crossings in the SD pair (see top right panel in Figure 3.2). In those case, three SI values; one to the left of the first crossing, one between the two crossings, and a third one to the right of the second crossing were calculated at the PWs that maximized the SI value, and that the second from the largest value was taken as the final SI measurement. The PWs where the final SI values are taken are shown in Figure 3.4 for all membrane parameter pairs and different stimulus waveforms (with HPP).

The PWs for SI measurements distributed across the entire range for most waveforms, except for DecExp and IncExp where they were taken either at the smallest (10μs) or largest PW (5ms) in most cases. These plots show that for these two stimulus waveforms, the SI value was monotonously increasing as the PW moved from that of the crossing point. For all other waveforms, the SI had local peaks.

The max SIs computed from multiple SDs obtained by diversifying each membrane parameter pair are plotted in Figure 3.5 for all stimulus waveforms. When G_{Leak} is one of the diversified parameters (G_{Leak} & C_m, G_{Leak} & G_{Namax}, and G_{Leak} & K_{temp}) the biphasic waveforms (with HPP) produced much higher selectivity values compared to that of Mono with all stimulus waveforms. (compare blue, purple and green bars in Figure. 3.5A and 5B). For all remaining three pairs (K_{temp} & G_{Namax}, C_m & G_{Namax}, and K_{temp} & C_m), the difference was less and not necessary in favor of the biphasic waveform. Diversifying G_{Leak} & G_{Namax}, and G_{Leak} & K_{temp} introduced a large increase in the SI for all non-rectangular stimulus waveforms compared to that of Rect but only when HPP included (purple and green bars in Figure 3.5 B). In fact, G_{Leak} & K_{temp} diversity did not even result in any SD crossings (zero selectivity) with Mono (purple bars in Figure 3.5 A). Furthermore, Kt^2 stood out as the most selective waveform followed by ExpInc, Lin and Gauss (Figure 3.5 B). Interestingly, in case of Mono, the SI was the largest with all waveforms when C_m was one of the parameters (blue, black, and red bars in Figure 3.7A). Thus, G_{Leak} & C_m combination was the best both for Mono and biphasic waveforms (blue bars in Figures 3.7 A and 3.7 B).
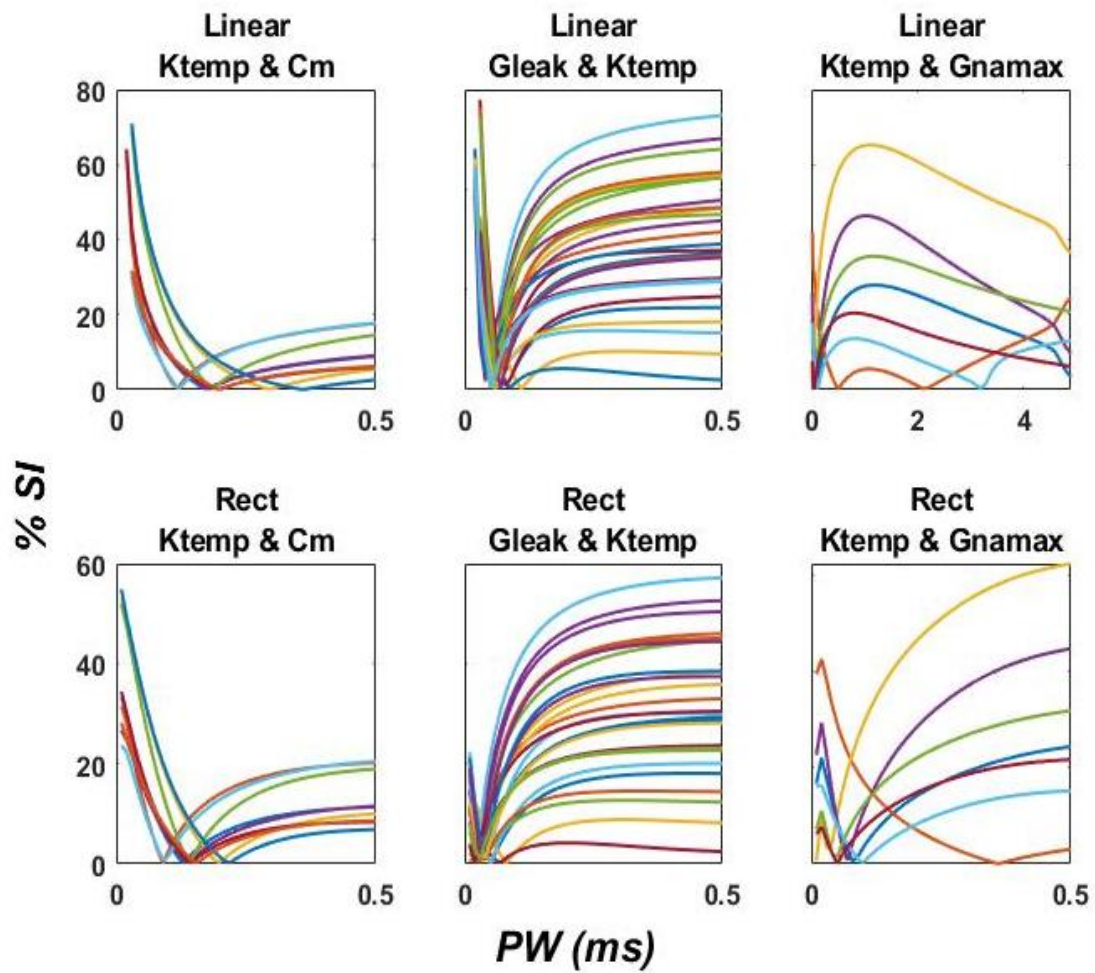
Figure 3.2 Percentage of all possible Selectivity Index ratio (%SI) is plotted in the y-axis in relation to the PW(ms) in x-axis. The top three plots are for the linear stimulus waveform and the bottom three plots when using a rectangular waveform. Only three combinations are shown, KTEMP & CM, KTEMP & GLEAK and KTEMP & GNAMAX.
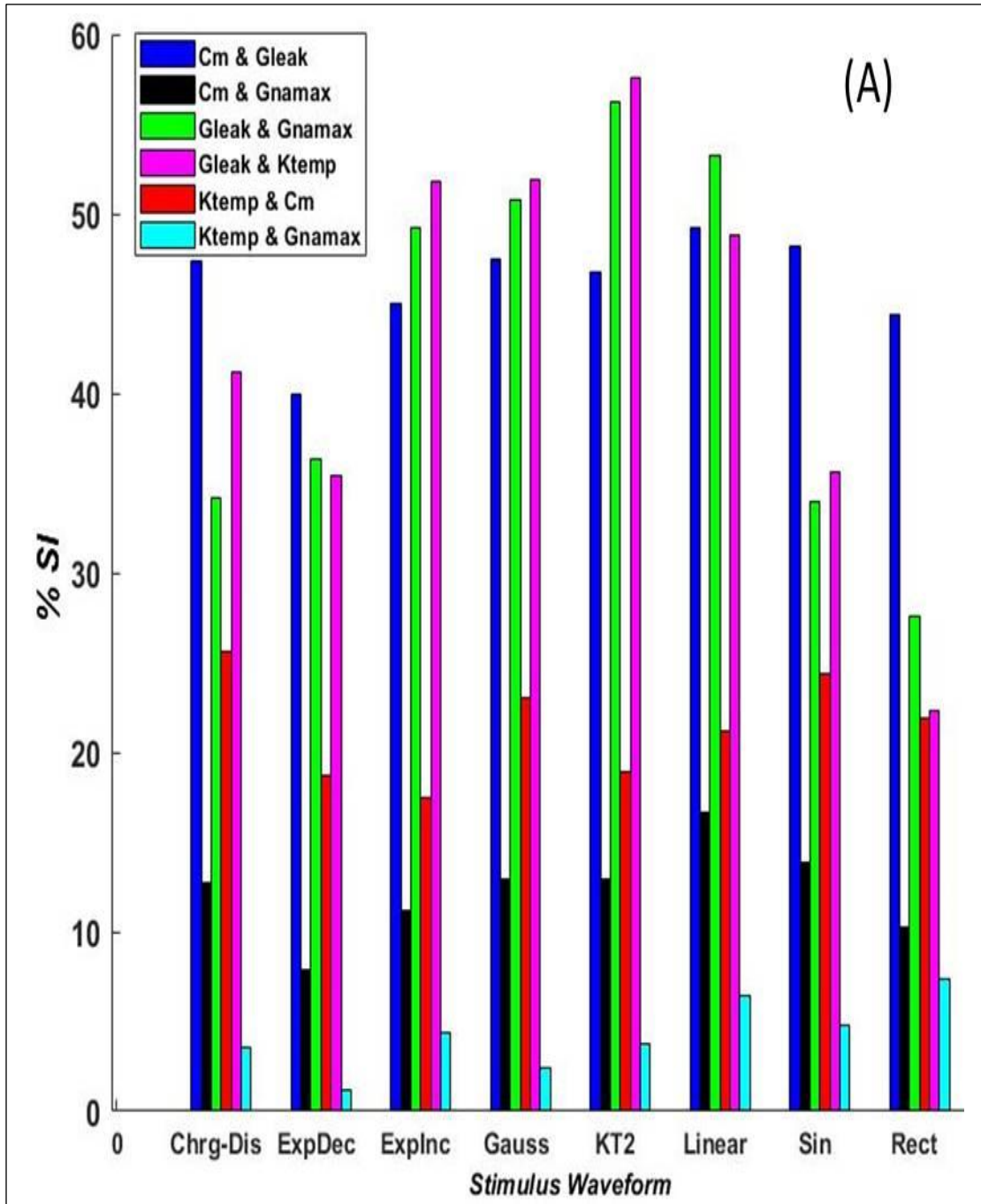
Figure 3.3 The Selectivity Index ratio is plotted in percentage (%SI). The graph is color coded to differentiate between different parameters companions. Bars are grouped by stimulus Type. A) For stimulus with hyperpolarization pre-pulse. B) For Using Monophasic stimulus pulse.
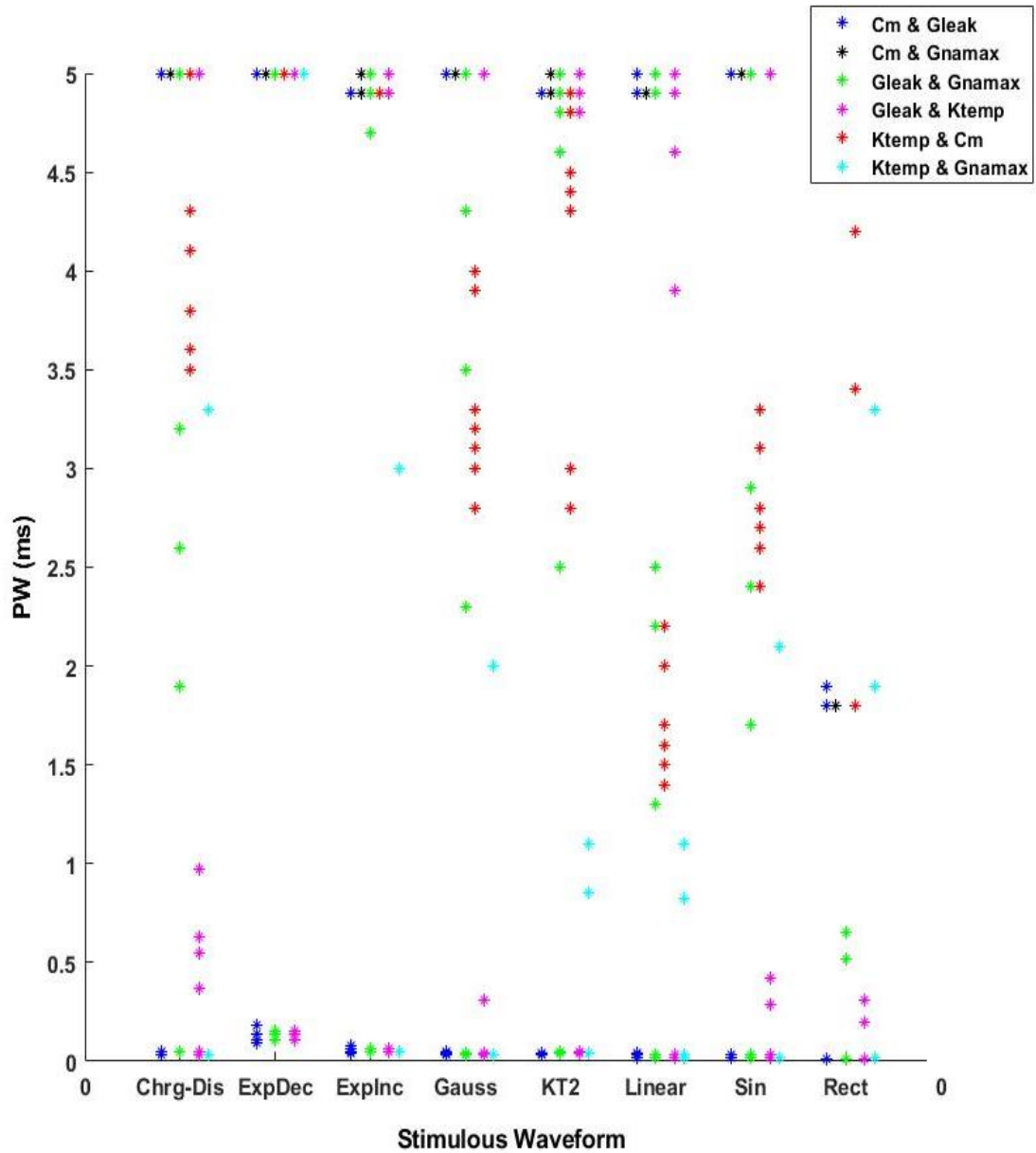
Figure 3.4 Pulse width (mSec) where the SI was selected is plotted. The graph is color coded to differentiate between different combinations as shown in the top right of the figure.
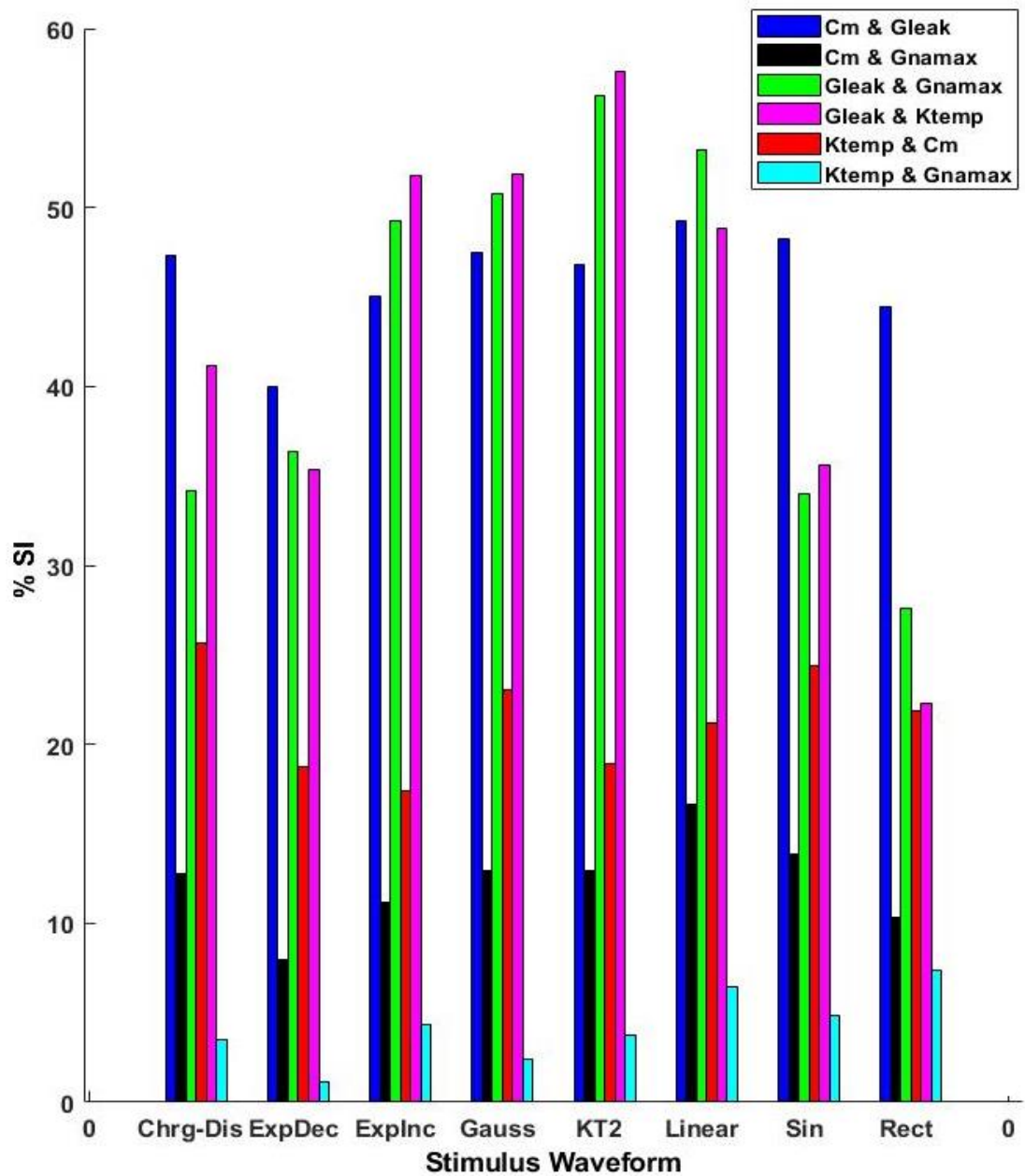
Figure 3.5A the Selectivity Index ratio is plotted in percentage (%SI). The graph is color coded to differentiate between different parameters companions as shown in the top left of the figure. Bars are grouped by stimulus Type. A) For stimulus with hyperpolarization pre-pulse.
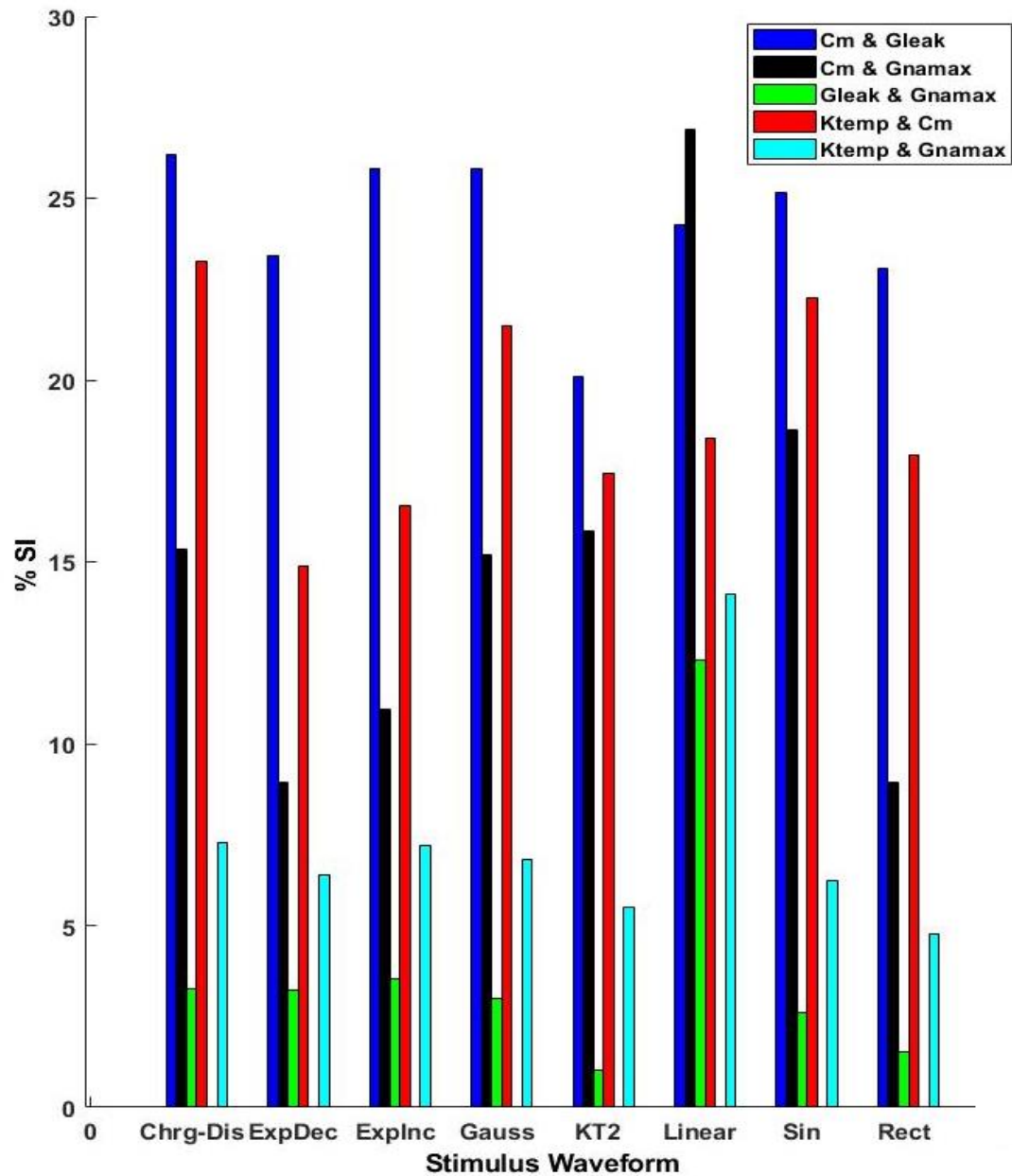
Figure 3.5B the Selectivity Index ratio is plotted in percentage (%SI). The graph is color coded to differentiate between different parameters companions as shown in the top left of the figure. Bars are grouped by stimulus Type. B) For Using Monophasic stimulus pulse.
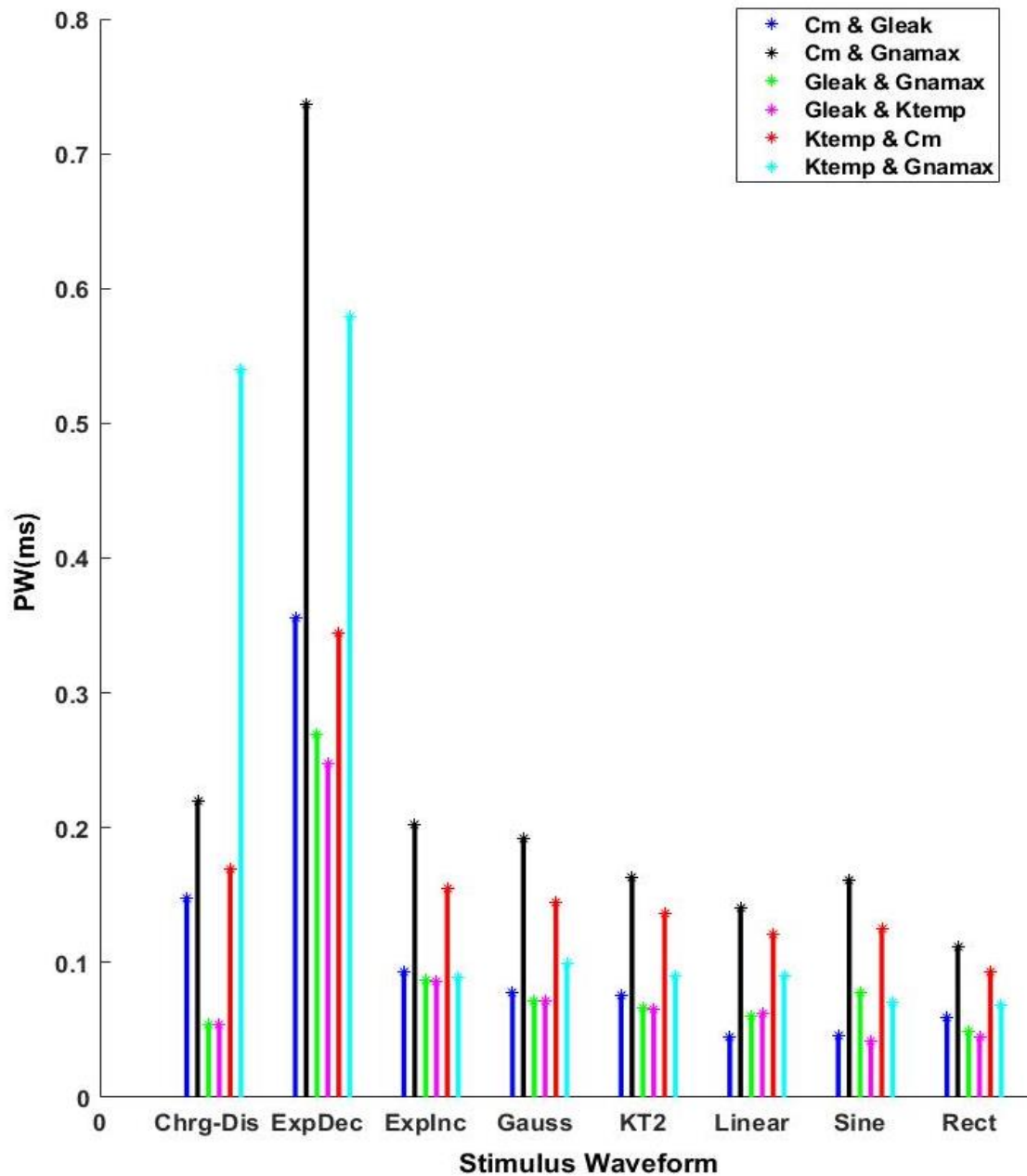
Figure 3.6 Pulse width (mSec) where the crossing occurred is plotted. The graph is color coded to differentiate between different combinations as shown in the top right of the figure.

3.4 Discussion

In the first chapter sensitivity analysis reported the effect of each parameter on the chronaxie time (Chr) and the rheobase (Rhe). We showed that variance in two or more parameters have a large effect causing higher selectivity Index (SI). Additionally, we compared between different combinations and different variation of the rectangular stimulus pulse, showing the great impact that Hyperpolarization rectangular pulse on selectivity index especially if G_{Leak} is different between two different neural cells.

This chapter further investigates the effect of non-rectangular waveform on neural selectivity by studying seven different non-rectangular waveforms. We started by running sensitivity analysis for each waveform to quantify the effect of stimulus waveform on chronaxie time (Chr) and rheobsae (Rhe). Sensitivity analysis revealed that some of the nonrect angular waveforms have higher Chr slope compared to rectangular waveform, and a lower Rhe slope specifically ExpInc, ExpDec and KT^2. The change in the sensitivity slope influence the SD curves movements introducing higher probability to cross. The nonrectangular waveform causes the SD curves to shift diagonally in the Chr and Rhe direction increasing the number of crossing between SD curves. The movements in the SD curves generated by ExpInc, ExpDec and KT^2 stimulus waveform is large enough to allow more crossing between SD curves compared to rectangular waveform and other nonrectangular waveforms, hence it gives higher SI% values.

Non-rectangular waveforms do not lead to selective activation of neurons per se unless the membrane parameters are allowed to vary from cell to cell. That

is, the SD curve moves in the same direction in different neurons when the electrophysiological parameters change together and do not cause the SD curves cross. Once we assume diversity of membrane parameters, however, the non-rectangular waveforms tested here seem to produce higher levels of selectivity compared to the traditional rectangular current waveforms.

Moreover, results revealed that crossing points occur at different PWs for different waveforms because the chronaxie time is different for each waveform fig (7). Therefore, designing an ideal stimulus needs to take in consideration both stimulus waveform and the neural properties of neural cells. To illustrate the importance of matching the stimulus with neural properties, one can investigate figure (7A) where rectangular stimulus waveform scored the lowest SI value percent for neural properties combination of G_{Leak} & Ktemp (purple) and G_{Leak} & Gnamax (green). Moreover, KT2 scored the highest SI index percentage followed by Linear, Gaussain ExpInc and ExpDec. With the assumption that two groups or neural cells diverse in G_{Leak} & Ktemp or G_{Leak} & Gnamax we suggest using a Kt2 stimulus to achieve higher selectivity between neural cells.

CHAPTER 4

COMPARTMENTAL AXON MODEL

4.1 Background and Significance

Nerve cell Is a major role player in transferring signal and information from the brain to all parts of the human body. It forms the electrical path that the brain uses to send signals efficiently to other locations in the human body. Nerve cells are categorized based on functionality three different groups: motor neurons, sensory neurons, and interneurons. Motor neurons are neuronal cells located in the central nervous system (CNS), they connect the brain or spinal cord to muscles and glands. MNs are categorized to two groups: Cranial and spinal subsets. they carry signal from the brain and the sensory system to control voluntary and involuntary movements. spinal MNs (SPMNs) form an irreplaceable component of the neuronal circuity they convey the commands from the CNS to the effector muscles and their axons extending through several meters in mammals. Sensory neurons are part of the nervous system and they are activated by sensory inputs from the surrounding environment. Touch, smell, and taste all are managed by different sensory neurons. Some sensory neurons can response to external stimuli and activate motor neurons to achieve involuntary movements, for instance involuntary motor reflex and involuntary pain avoidance. Finally, the interneurons which are divided into two subgroups, local and relay. Local interneurons have short axons and connects with nearby neurons to form a local circuitry. Relay interneurons have long axons and form neuro circuitry between different brain regions.

Axons usually are wrapped with insulating layers called myelin. Myelin forming neurons are specialized cells transmits information between nerve cells, muscles, and gland cells. The basic structure of neuron is like other cells, it has a cell body which is called soma and it is where the nucleus of the neuron is found. Extended from the cell body short branching processes called dendrites and longer ones which is called axon, Figure 4.1. The dendrites are where the incoming excitatory or inhibitory signals gets received and processed. The sum of all signals collected at the dendrites influence the excitation of the neurons. Then, when a

Node of Ranvier

Nucleus   **Internodal**
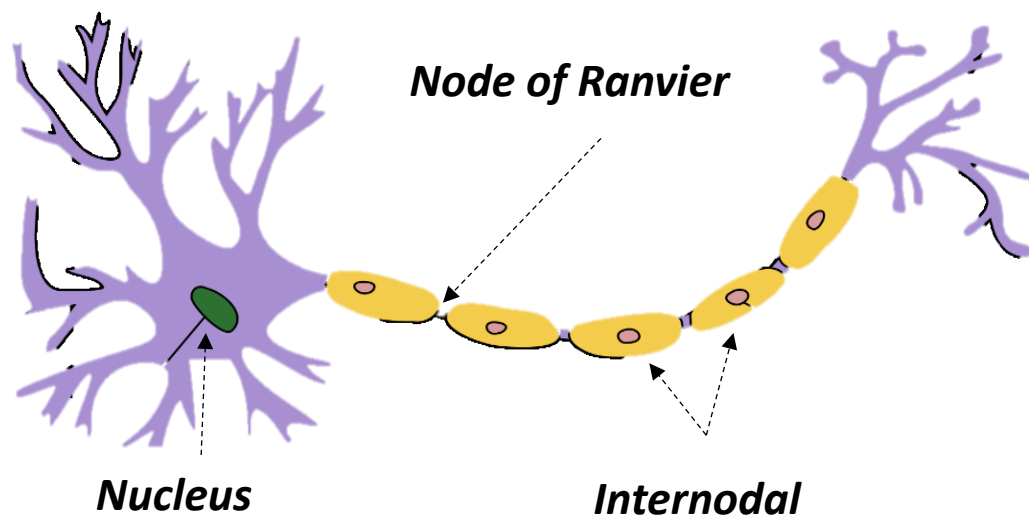
Figure 4.1 Anatomy of the neuron, the yellow parts is called Myelin (internodal). Node o Ranvier falls between two intermodals.

neuron fires it sends an action potential along the axon to the receiving end. Axon travels for long distance allowing an efficient propagation of the action potential.

Axons arise from the cell body at the hillock and they travel for longer distance with the same diameter for most of the length. They are enclosed inside an insulating material called myelin. Between each two-myelin located node of

Ranvier, where action potential jumps from node to the next across the axon. Axons usually have multi-node of Ranvier depending on the axon length and node size, Figure 4.1.

Node of Ranvier contains a neural cell that allows the propagation of the action potential along the axon length. One of the well know neural cell model is H-H which we discussed in section 1.5. The H-H model is based on experimental data that was collected on a squid giant axon[27] and represented by mathematical equations to mimic the behavior of the neural cells in. Additionally, it was modeled as an electrical circuit that gives and approximation of an action potential voltage traveling along the axon, Figure 1.3. However, to confirm our findings from the previous chapters we modeled node of Ranvier as a CRRSS model, same model used in the previous two chapters.

4.2 Methods

4.2.1 Axon Model

To confirm our findings from the previous chapters we investigated selectivity in a compartmental axon model. A 10 μm myelinated axon was simulated by incorporating the CRRSS local model [2, 29, 48], at the nodes of Ranvier that had widths of 1 μm and an inter-nodal distance of 1 mm. Since, there are almost no potassium currents in mammalian nodes of Ranvier [2, 48, 49], the CRRSS model is a good fit for the purpose of this study, it contains only the voltage-gated sodium and the leakage current. A monopolar electrode was placed 1 mm away from the

axon and aligned with its central node in a homogeneous volume conductor with a specific conductivity of 1.8 S/cm Figure 4.2.

Axon with 25 nodes were found sufficiently long for accurate predictions of the stimulation thresholds since the extracellular voltage at the ends were less than 4% of the maximum voltage in the center. The extracellular voltages generated by the monopolar current source at the nodes of Ranvier were computed and the SD curves and SIs were found with the same passive and active parameter ranges tested in the local membrane model. We selected 7 data points within the same range tested previously, that yields to 49 neurons and 1176 crossing possibility. The selected data points are ±5%, ± 15%, ±25%, that range gave us the ability to investigate the effect of the range on Selectivity.
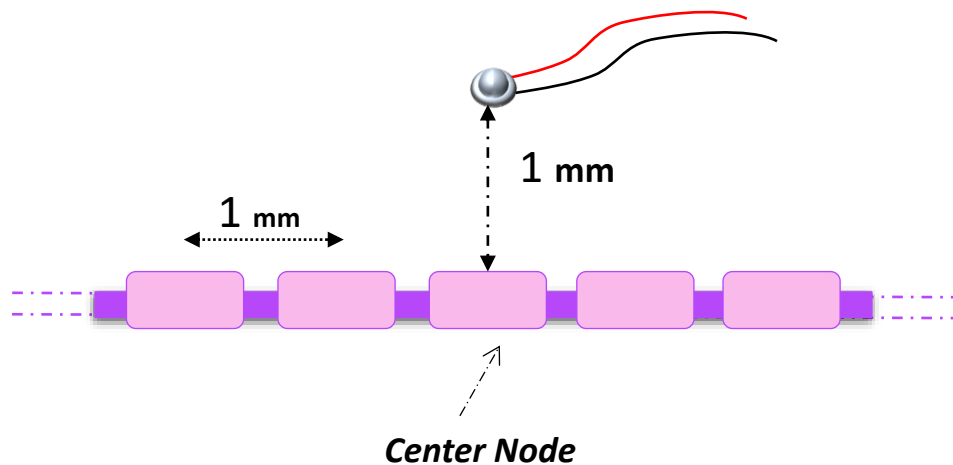
Figure 4.2 Placement of the electrode on the center node of the axon model.

4.2.2 Stimulus Waveform

The same eight stimulus waveforms used (Table 1); Charge-discharge curve (Chr-Dis), increasing and decreasing exponential (ExpInc and ExpDec) respectively, Gaussian (Gauss), KT^2, Linear (Lin), sinewave (Sine), and rectangular (Rect) as defined and tested previously for minimization of stimulation energy [15]. Results from previous simulation showed that HPP performed the best hence, all stimulus waveforms were applied as a biphasic waveform where a rectangular hyperpolarizing pre-pulse (HPP), cathodic, preceded the anodic phase (Table 3.1). The hyperpolarizing pre-pulse had the same duration as the stimulus pulse and identical area to the anodic phase to make the waveform charge-balanced.

4.2.3 Strength Duration Curve

As discussed previously the strength duration curve was calculated by sweeping over the whole range of the PW (0.01 to 5 msec) to find the stimulation threshold at each pulse width. The threshold was determined using an adaptive search algorithm to find the smallest current to activate the neural cell. An action potential was decided to occur if the m-gate variable exceeded the 0.98 threshold. Both Lapicque-Weiss [51] or Lapicque-Blair [67, 68] equations showed a poor fitting profile to the non-rectangular stimulus SD curve hence, the chronaxie time (Chr) and rheobase (Rhe) were computed using the traditional definitions. The Chr is the pulse width at which the threshold is twice the Rhe and the Rhe is the lowest intensity required to stimulate neuron within indefinite period.

4.2.4 Selectivity Index

Several selectivity measurements were proposed i.e angle measurements between Crossed SD curves and percent of number of crossings (NOC) however, the ratiometric selectivity index (rSI) used in the previous chapters showed the best representation for selectivity. All four membrane parameters, the passive (C_m and G_{leak}) and the active (G_{Namax} and K_{temp}) parameters were varied in pairs by ± 25%. Seven data points were taking in between the maximum and minimum values, as ±5%, ±15% and ±25%, the three proposed ranges were used later for investigating the effect of range on selectivity index (SI). The variation produced 49 different neurons (7X7) with 1176 possibilities of crossing. Selectivity Index ration was computed in the same way discussed in section 2.2.5.

4.3 Results

4.3.1 Selectivity - Rectangular Waveform

The feasibility of selectivity by diversity of electrophysiological parameters was confirmed in a compartmental axon model that incorporated the CRRSS local model for the nodes of Ranvier. With seven different values that each parameter was set to within the ±25% range, the combinations produced 49 different neurons with different SD curves and a maximum of 1176 possible crossings. Once more C_m & G_{leak} combination outperformed the rest with a maximum SI value of 19.2%, followed by K_{temp} & C_m, K_{temp} & G_{Namax}, and G_{leak} & K_{temp} at 18.2%, 16.11%,

15.24%, respectively (Figure 4.3). The C_m & G_{Namax} combination performed the least with 9.3 % selectivity.

One unique characteristic that the compartmental axon model revealed was that most of the crossing points occurred between 0.2 and 0.4 msec (Figure 4.4) compared to ~0.01 and ~0.1 ms in the local model (Figure 2.7 B). The PWs where the SIs were maximum also spread across the entire PW range compared to PWs less than 1ms in Figure 2.7 B.

Finally, we examined how the SI values changed as the range within which the membrane parameters were allowed to vary. This analysis showed that the selectivity increased with increasing range of diversity (Figure 4.5). The SI increased as the range of each parameter was increased individually for G_{leak} & C_m, C_m & G_{Namax} and G_{leak} & G_{Namax} combinations (Figure 4.5 - Top). However, K_{temp} dominated the SI effect regardless of the other parameter that it is paired with (Figure 4.5, bottom row). In all three combinations with Ktemp, the maximum SI depended on K_{temp} only, suggesting the importance of diversity in sodium kinetics to achieve selectivity.
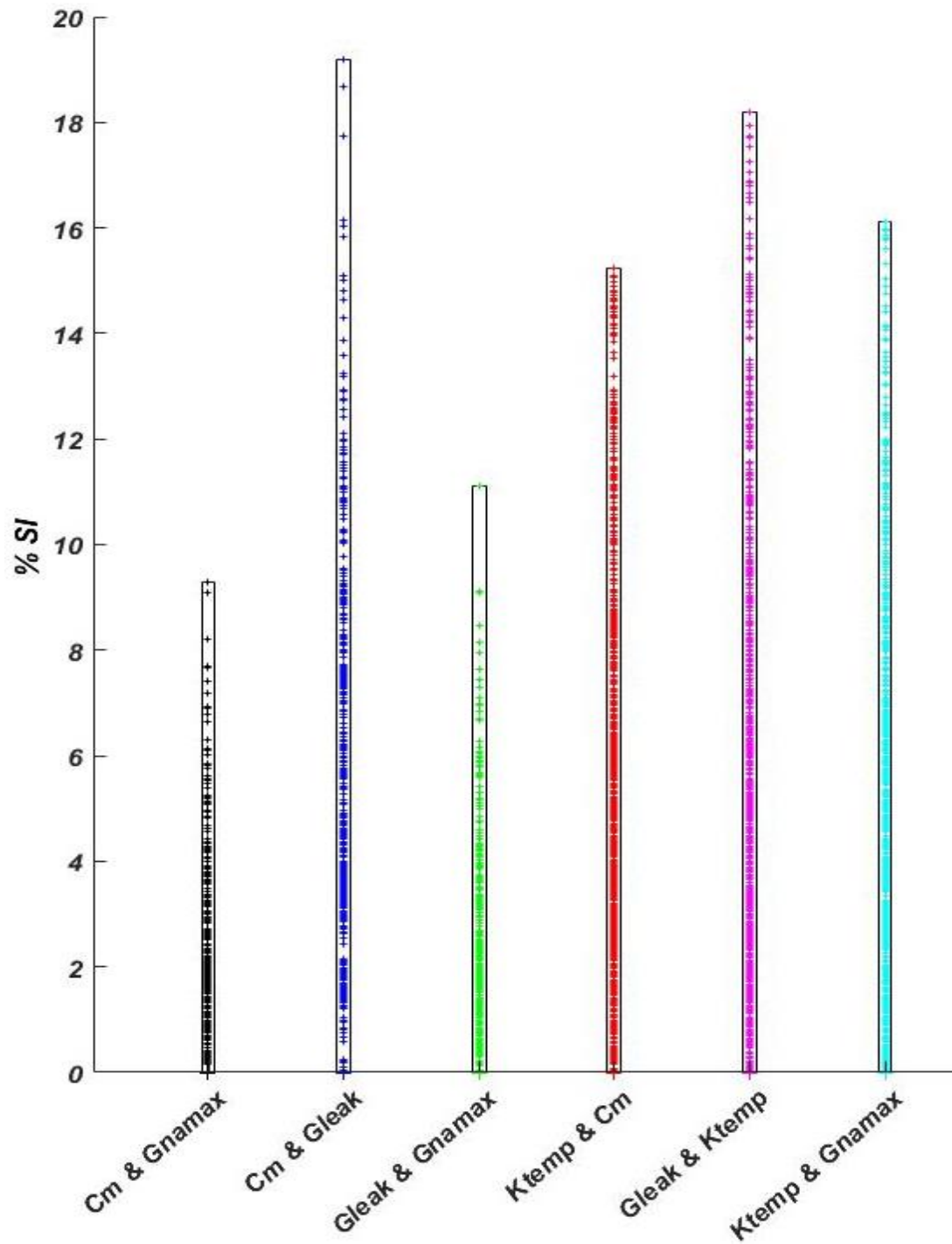
Figure 4.3 Percent selectivity index generated from crossing SD curves in the compartmental axon model. Diversity range is ±25% and the waveform is HPP. Each bar represents the combination of parameters that were diversified.
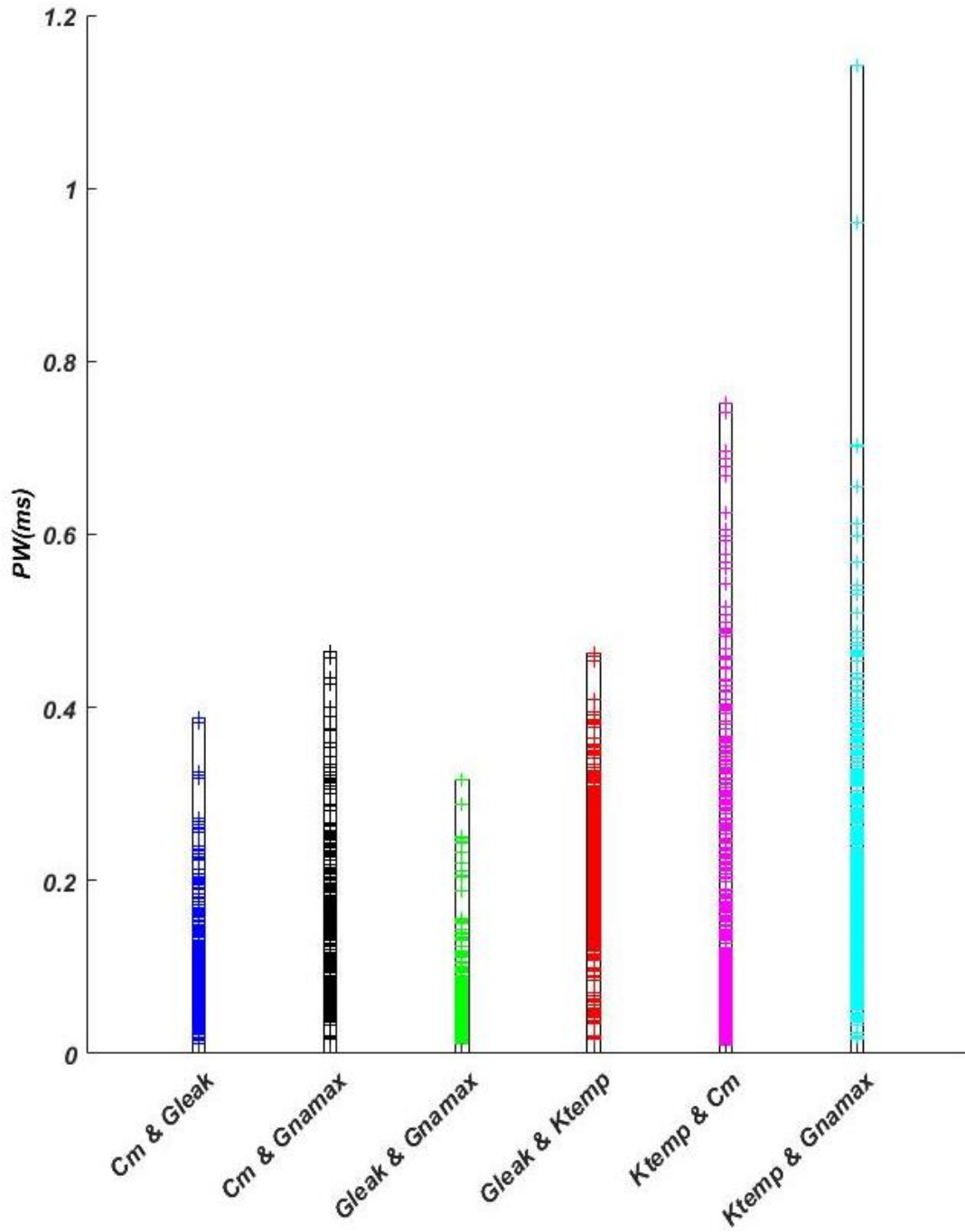
Figure 4.4 PWs at which the SDs cross are shown ("+") for the compartmental axon model. Parameter diversity is ±25% and the waveform is HPP.
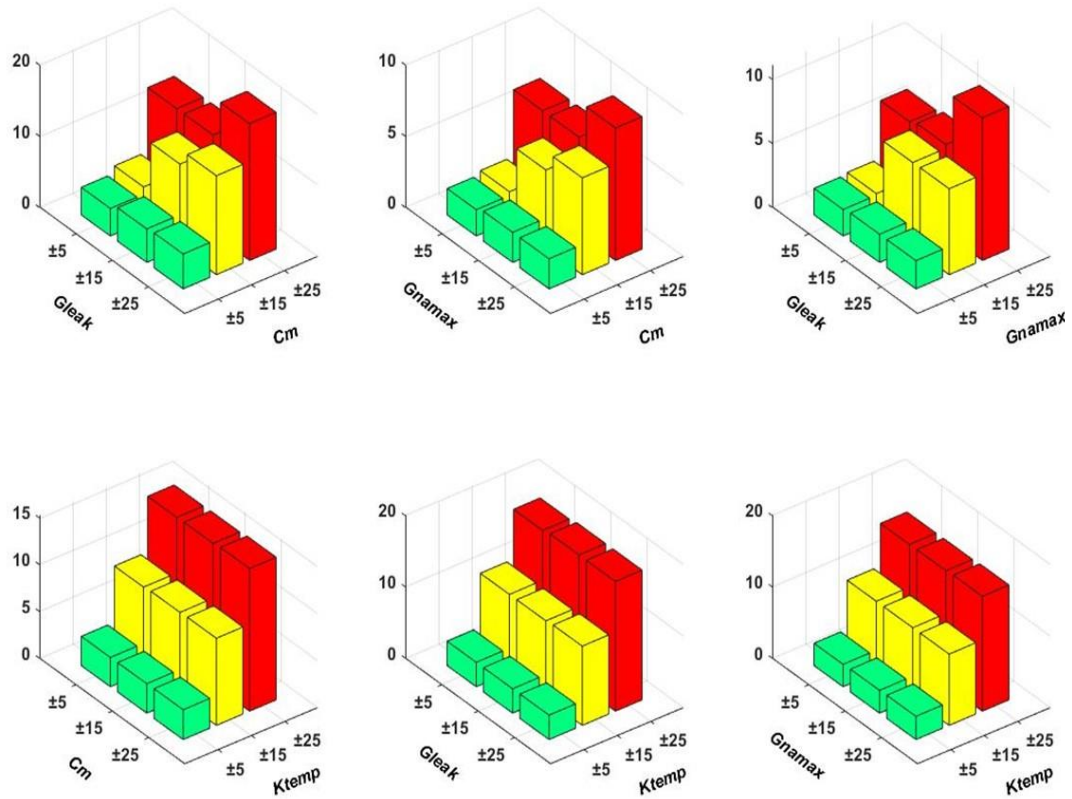
Figure 4.5 Selectivity Index plotted against the varied membrane parameters in pairs. In the top three figures, maximum SI achieved when both parameters are varied maximally (±25%). Selectivity is determined primarily by Ktemp only when it is one of the parameters tested (bottom plots).

4.3.2 Selectivity with Non-Rectangular Waveform

To be able to draw a conclusion from the results obtained from the local model, we ran a similar simulation in the compartmental axon model. Using eight stimulus waveforms, while membrane parameters were altered in pairs. Although, the results were similar yet there were few divergences. The axon model yet confirmed that KT^2 is the most selective waveform followed by Lin, Gauss when HPP is included Figure 4.6. Conversely, the axon model showed that the sine waveform more selective compared to ExpInc Figure 4.6. This could be due to the increasing contributions made to the activation threshold from the neighboring nodes in the axonal model as the PW is increasing [69]. This difference between the local and compartmental model would certainly affect the SD curve and thereby the SI values.

The axon model revealed that combinations where C_m is one of the varying parameters generated higher selectivity Index value, this is true for C_m & G_{Namax} (black), C_m & K_{temp} (red) and C_m & G_{leak} (blue) Figure 4.6. In the controversy parameters when G_{leak} is varying, then selectivity index values were reduced G_{leak} & G_{Namax} (green) and G_{leak} & K_{temp} (purple) Figure 4.6. Nevertheless, we still can draw the same conclusion from both simulation models which is, in most cases the hyperpolarization non-rectangular pulse is more selective than the rectangular one regardless to which parameters are varying.

Interestingly, when we run the simulation on the compartmental axon model, we observed that crossing PWs (the PW where crossing occurred) were more scattered over the whole range of the stimulus period (0.01 top 5 mses) except for

ExpInc Figure 4.7. which contributes to the small SI value. Comparing between the crossing PWs, we can observe that in the axon model, ExpInc has less crossing scattered compared to Sinewave Figure 4.7. Additionally, percentage of number of crossing in the Sine Waveform is higher than ExpInc supplementary Figure 4.8. Thus, translates to a higher SI values in Sinewave compared to ExpInc pulse. The contrary happened in the local axon model.
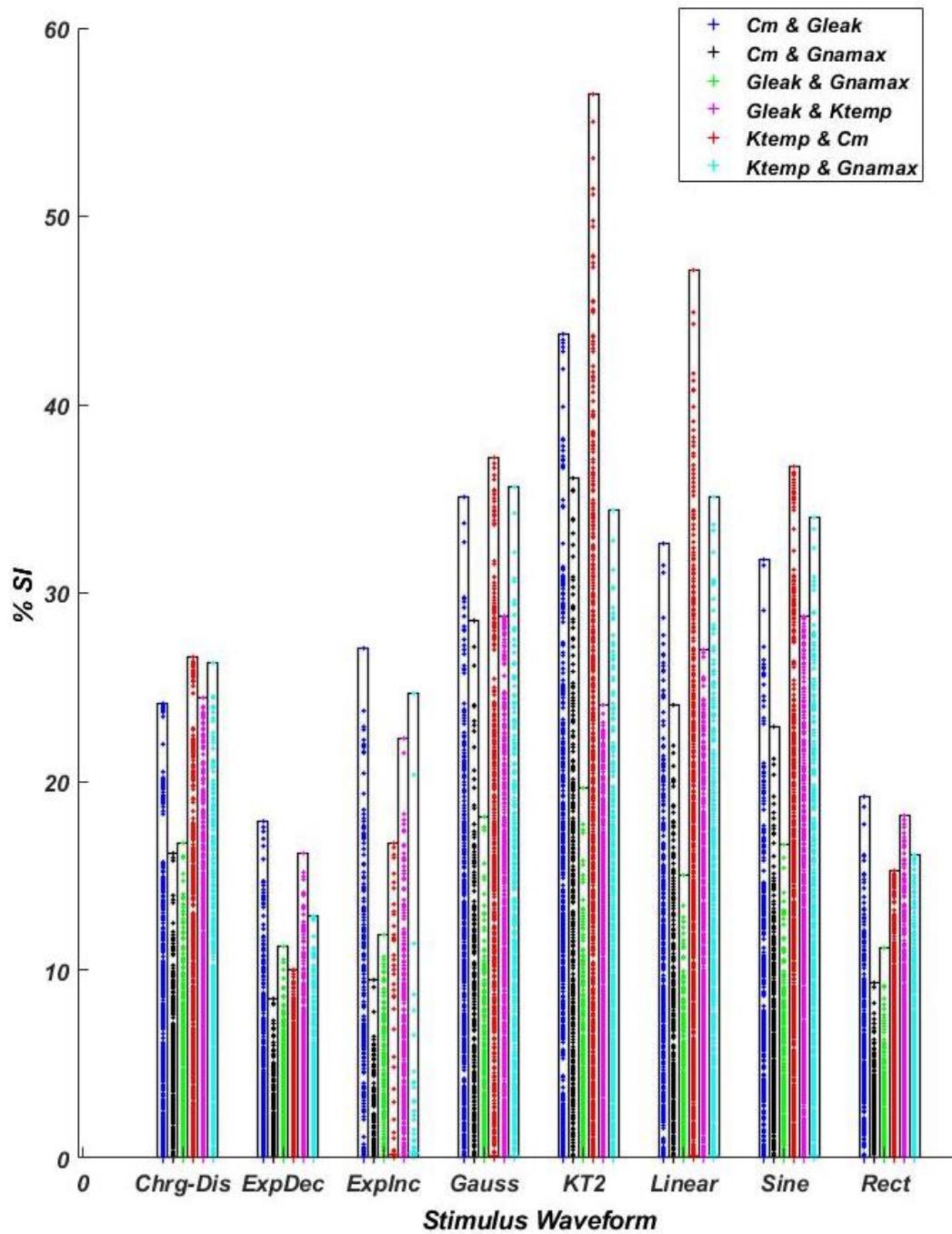
Figure 4.6 SI values for all waveforms, in the Compartmental Axon Model are represented with a "+" sign. The graph is color coded for each combination and the bars are grouped based on the waveform.
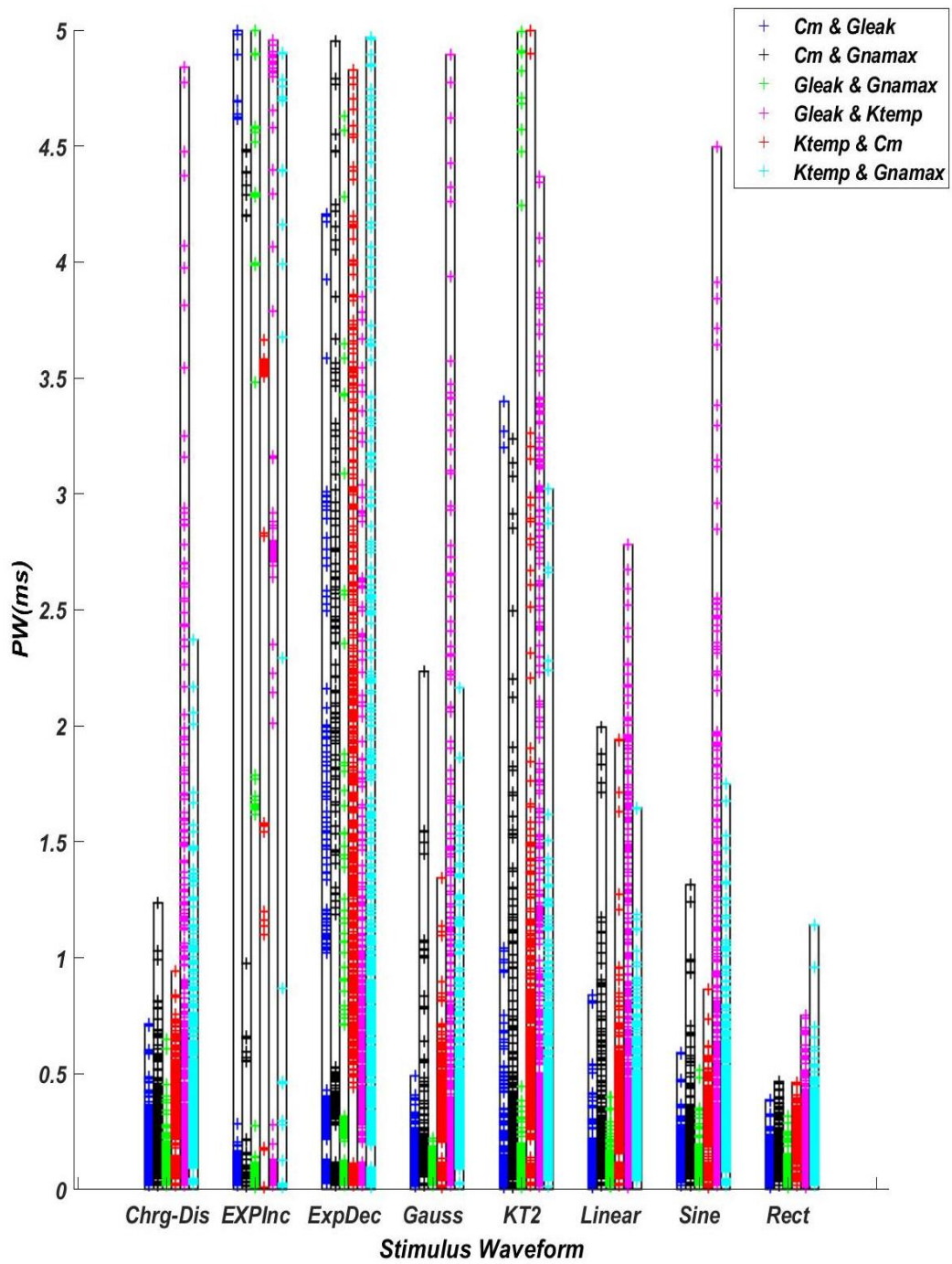
Figure 4.7 Crossing Locations (PW) in the Axon Model, are represented with a "+" sign. The graph is color coded for each combination and the bars are grouped based on the waveform.
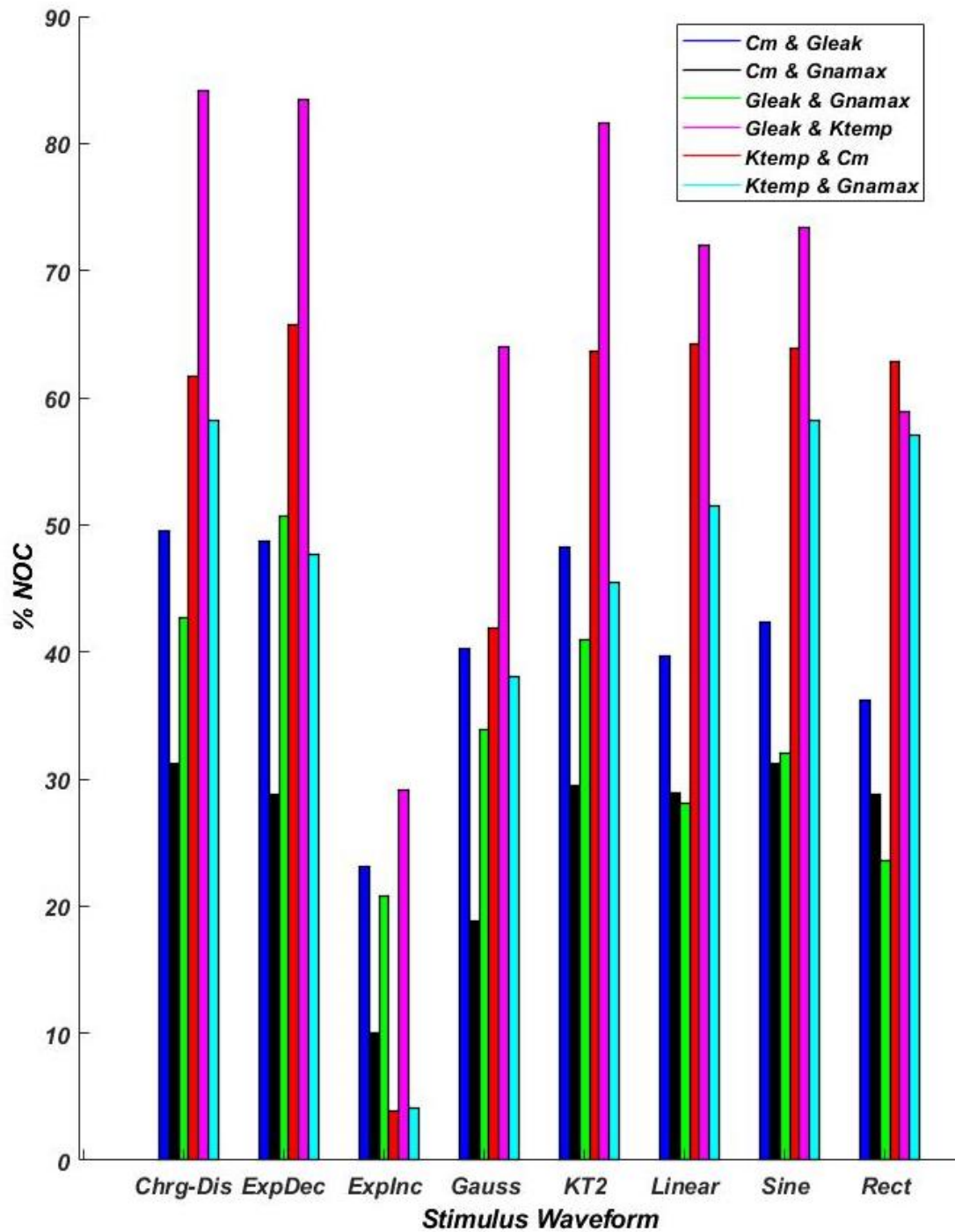
Figure 4.8 Percent of Number of crossing (NOC), in the axon model is plotted to compare between different waveforms. The graph is color coded for each combination bars are grouped based on the waveform.

4.4 Discussion

Comparing between the axon model and the local model results while using the rectangular stimulus pulse, one can notice similarity in the SI values. G_{leak} & K_{temp} combination produces SI values near 20% and the C_m & G_{Namax} combination around 10% in both models (Figure 2.7A vs. Figure 4.3). Nevertheless, the maximum SI of ~45% achieved with C_m & G_{leak} combination in the local model was limited to 19.2% in the axon model. This could be due to the increasing contributions made to the activation threshold from the neighboring nodes in the axonal model as the PW is increasing [69]. This difference between the local and compartmental model would certainly affect the SD curve and thereby the SI values.

It was crucial to run the simulation for a compartmental axon model to confirm that the same phenomena happen when introducing the nodes of Ranvier, while using non-rectangular stimulus pulse. Although, adding 25 nodes shifted the selectivity away from ExpInc and more towards Sinewave, yet it confirmed the main vital finding which is Rec is the least selective stimulus pulse. Also, it confirmed that KT^2 is the most selective waveform followed by Lin, Gauss when HPP is included Figure 4.6. Adding 25 nodes of Ranvier add a more realistic simulation to the model taking in consideration the contribution made from each node to the activation threshold which certainly affect the SD curve and thereby the SI values.

The compartmental axon model simulation results showed that no one stimulus waveform generated the absolute highest selectivity index value for all combinations, hence combinations complement stimulus waveform. In other words, we can select the stimulus waveform based on neurons properties and the variation found in a specific cluster of neurons. For instance, If one group of neurons are different in GLeak & Ktemp then using Sinewave or Gauss as the stimulus pulse achieves higher selectivity index. On the contrary, if the cluster of neurons are different in Ktemp & GNamax then Linear or Gauss stimulus pulse should be used to achieve better Selectivity. Furthermore, if the neurons are varied in Cm & GLeak then using KT2 stimulus pulse allows higher selectivity between the neurons. Yet, more work is essential to further investigate the phenomena using experimental data in addition to quantifying neurons based on their functionality and properties. Then the proposed technique can be used to select a stimulus pulse that best fit the targeted group of neurons to achieve neural selectivity.

CHAPTER 5

CONCLUSION AND FUTURE WORK

Both the local and the axon model results of this study suggest that intrinsic variations that naturally occur in the passive and dynamic membrane properties of neurons can lead to substantial levels of stimulation selectivity when the biphasic waveform is used for stimulation where the hyperpolarizing pulse precedes the depolarizing pulse. The passive membrane parameters (G_{Leak} and C_m) seem to be more influential on producing a diverse set of SD curves that can be leveraged for selectivity. The impact of diversity in dynamic parameters (K_{temp} and G_{Namax}) increase but not supersede the effect of passive parameters for smaller values of the membrane time constant. Results produced from the axon model further confirmed our main hypothesis, that the intersect variation in neuron properties combined with the non-rectangular waveform leads to high level of selectivity. The predicted levels of selectivity may lead to substantial improvemens and a paradigm shifting approach in functional neural stimulation provided that assumed electrophysiological diversity can be demonstrated between neuronal subtypes serving different functions in the CNS. We expect these results to generalize to other neuron models that include a fast voltage-gated sodium channel, which is the only kinematic variable in the basic model used in this study. It should be noted however that the diversity in other ionic channel kinematics that are not included in this study (e.g. slow sodium and potassium channels) may influence the rheobase and thereby the levels of selectivity that can be achieved.

APPEDNIX A

ELECTROPHYSIOLOGICAL DIVERSITY- SUPPLEMENTARY FIGURES
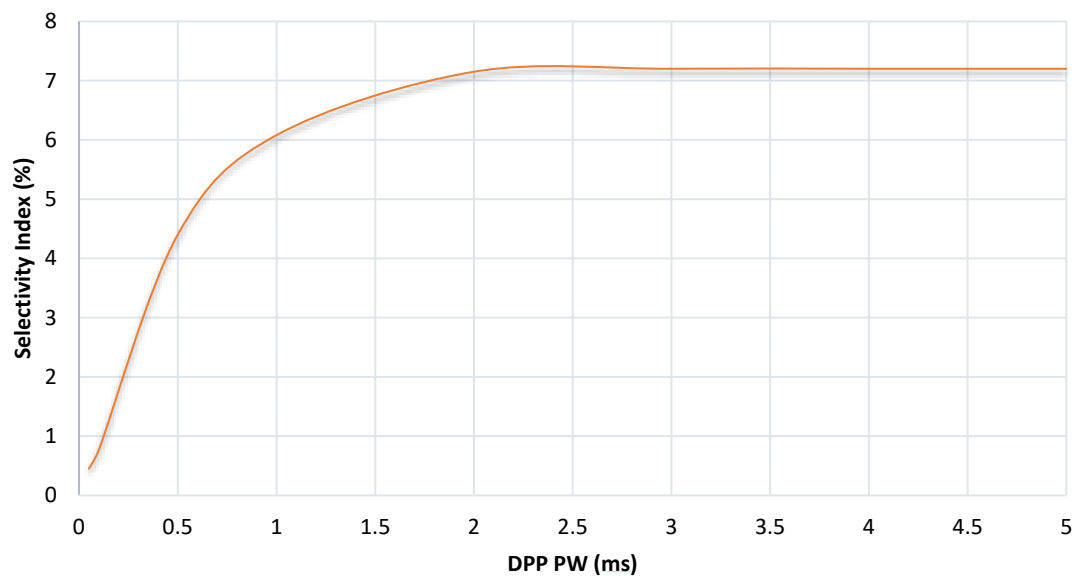
Figure A.1 Selectivity Index reaches 85% of its max at 1ms and plateaus at 2ms for increasing durations of depolarizing phase in the DPP waveform.
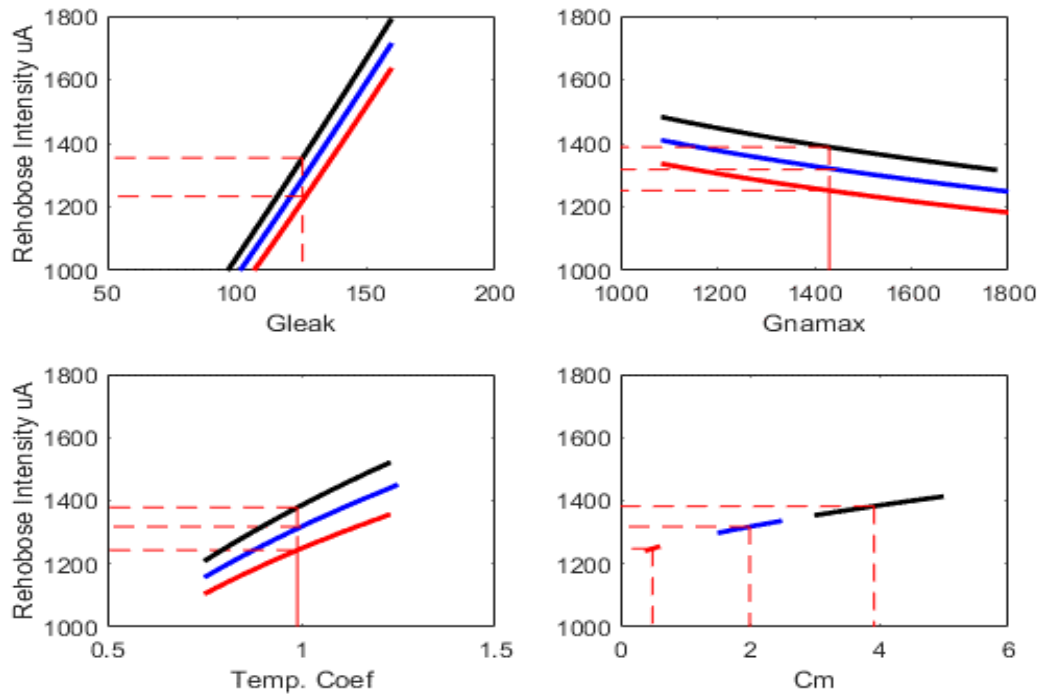
Figure A.2 Sensitivity of rheobase to the membrane parameters (G_{Leak}, G_{namax}, Temp. Coef-K_{Temp}, and Cm) as they are altered by ±25% from the nominal value and evaluated at many intermediate values. The analysis is repeated for three different default values of C_m; C_{m-def}=0.5 µF/cm² (***Red***), C_{m-def}=2 µF/cm² (***Blue***), and C_{m-def}=4 µF/cm² (***Black)*** . Dash lines show the nominal values.
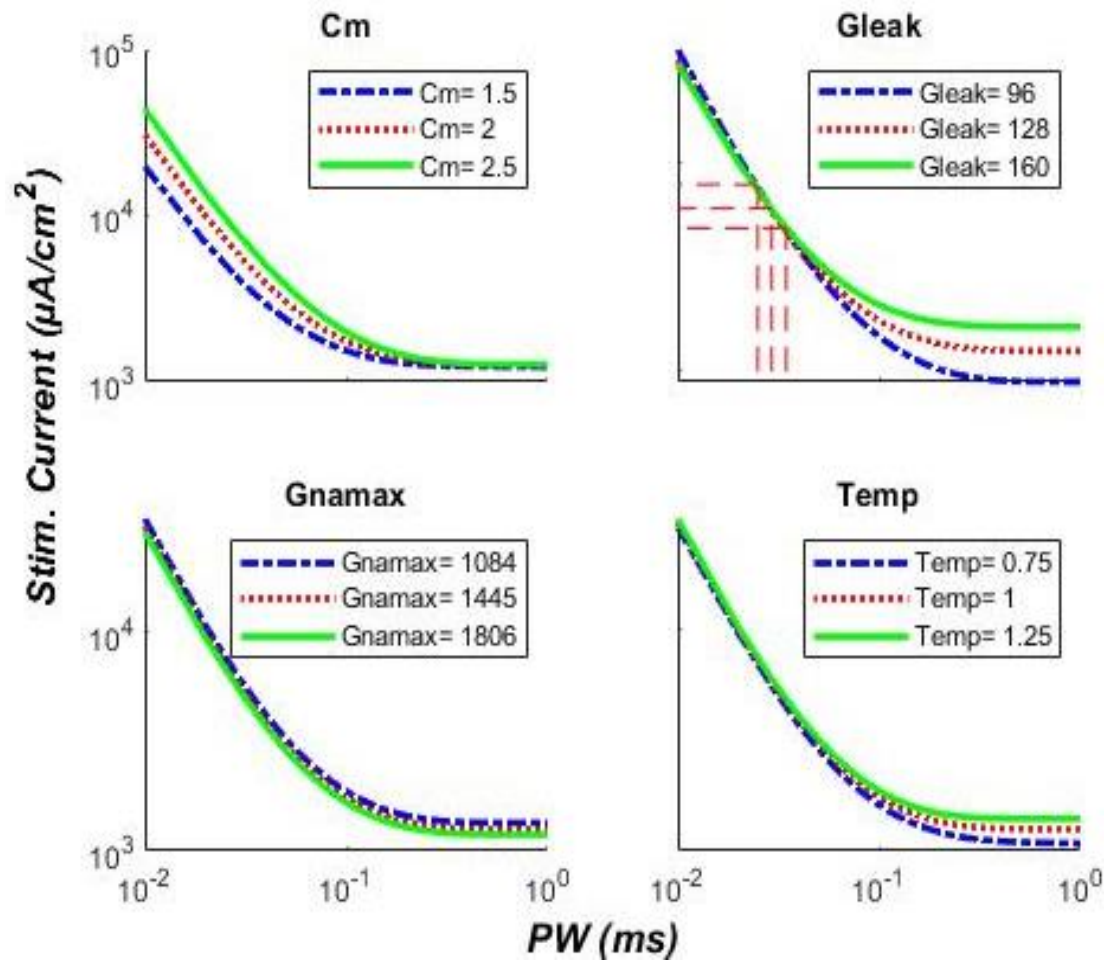
Figure A.3 Only G_{leak} variations, shown on top right panel, produce a few crossings (red dash lines) between the SD curves when using HPP stimulus waveform.
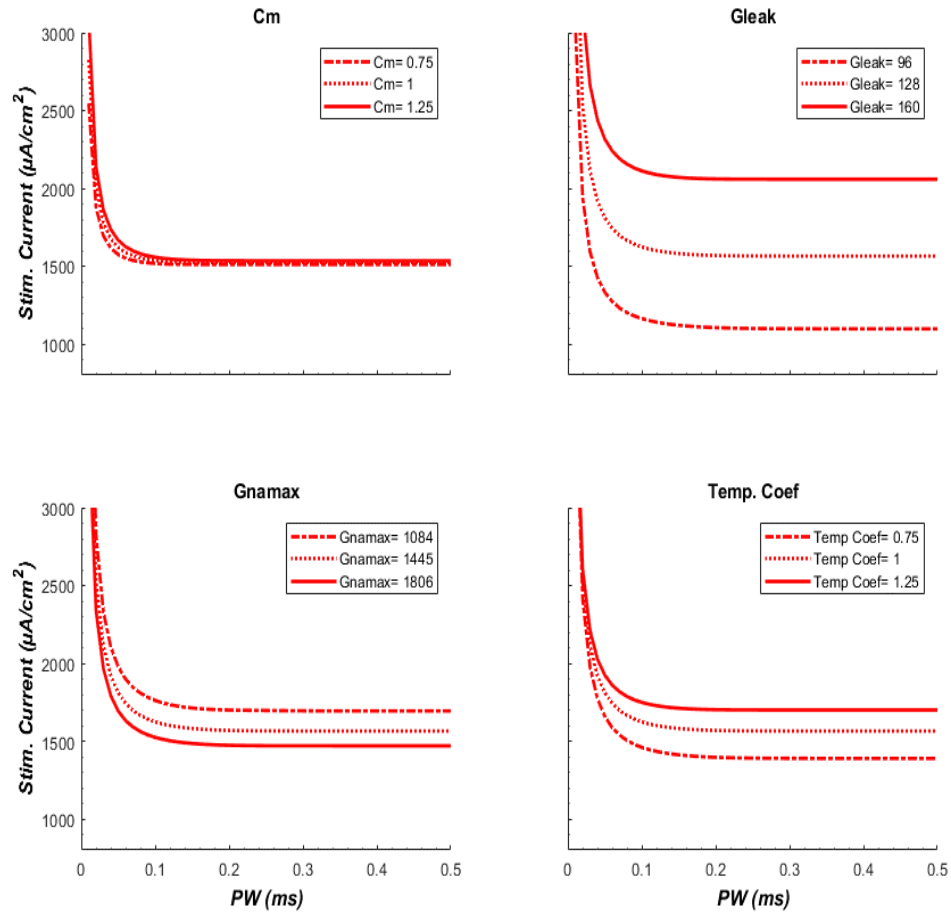
Figure A.4 The effects of the four model parameters (G_{Leak}, G_{namax}, Temp. Coef-K_{temp}, and Cm) on the strength-duration curve when DPP stimulus waveform is used. No SD crossings occur.
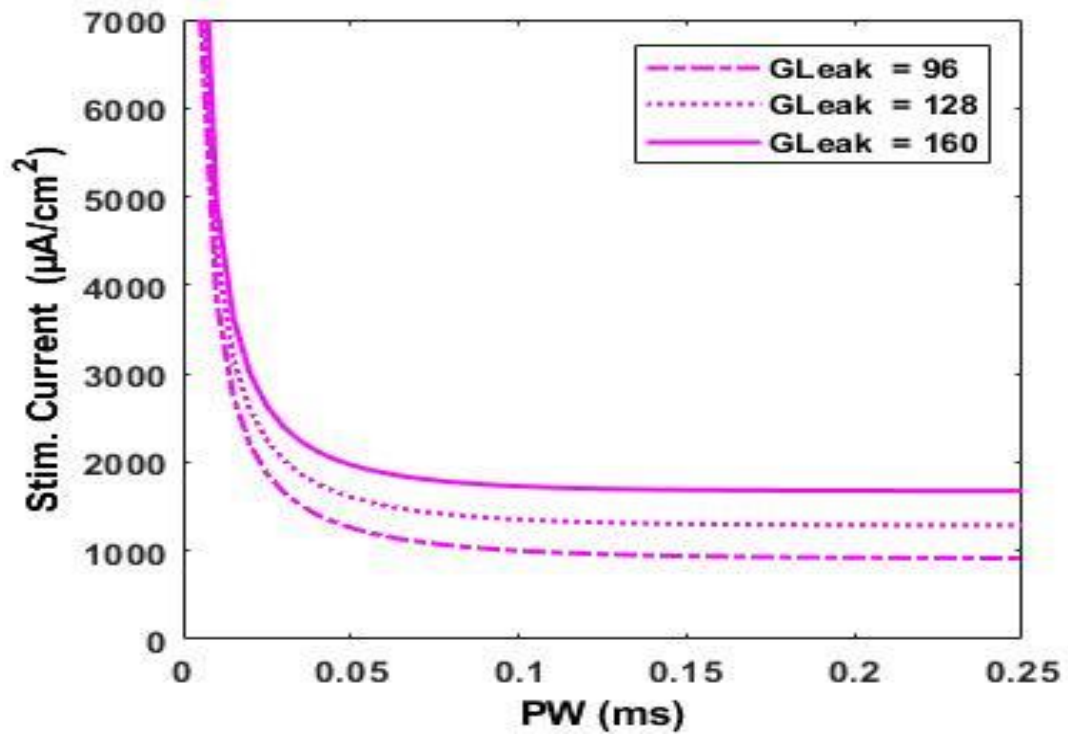
Figure A.5 Adding a 200 μs gap in the HPP waveform on the SD curve. It reverses the HPP effects for all parameter variations. Only the **G**leak results are shown here. The SD crossings seen for **G**leak diversity in Supplemental Figure A.4 are eliminated.
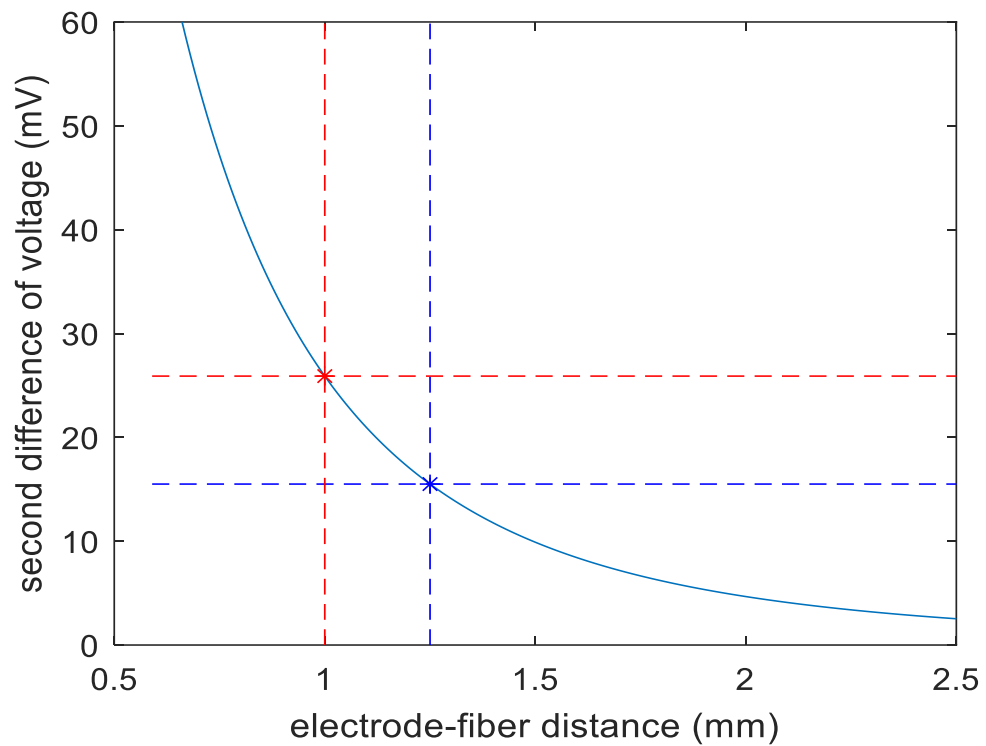
Figure A.6 The magnitude of the second spatial difference of the extracellular voltage due a monopolar electrode is plotted as a function of electrode-fiber distance for a 10µm myelinated axon assuming that intermodal distance is 100 times the fiber diameter. The differential voltage (and thus the activating function) decreases 40% when the fiber is moved from 1mm (red dash lines) to 1.25mm (blue dash). Electrode current=1mA, medium specific conductance=57 mho/m.
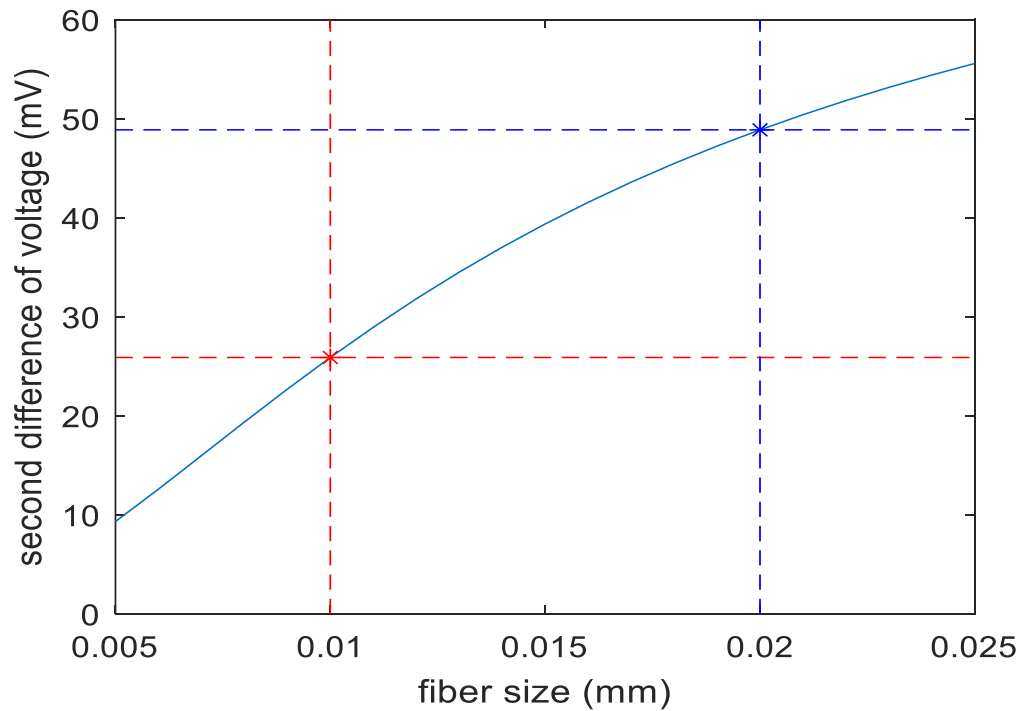
Figure A.7 The magnitude of the second spatial difference of the extracellular voltage at 1mm from a monopolar electrode as a function of axon diameter. The differential voltage (and thus the activating function) decreases 47% when a 20µm fiber (blue dash lines) is replaced by a 10µm axon (red dash). Other parameters are same as in Supplemental Figure 6.

APPENDIX B

ALTERATIVE STIMULUS WAVEFORMS-SUPPLEMENTARY FIGURES
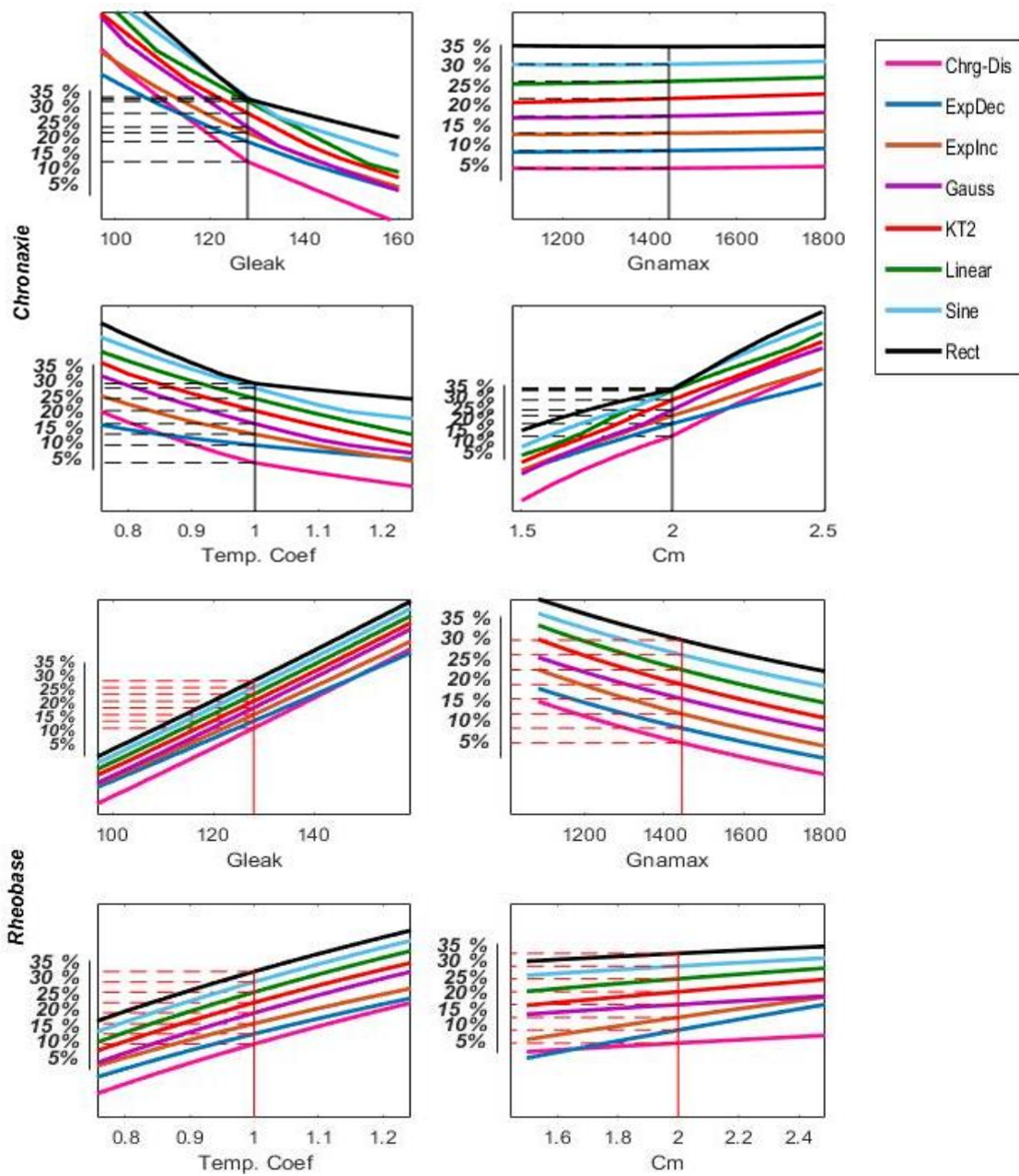
Figure B.1 Sensitivity analysis for monophasic waveforms. Both rheobase and chronaxie time slope differed small percentage from rectangular waveform slope.
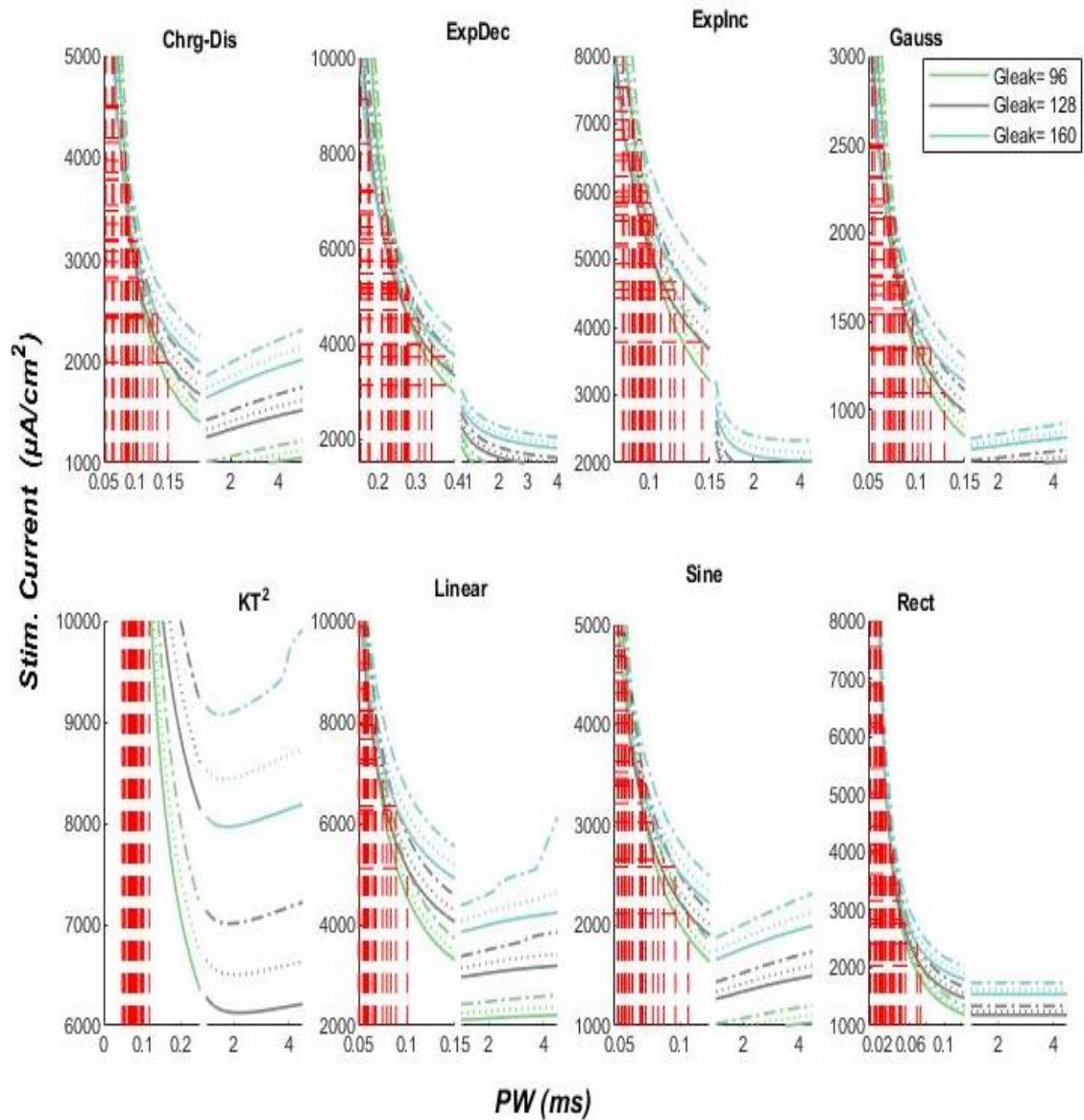
Figure B.2 GNAMAX & GLEAK are altered simultaneously in each case by the same amount, using eight different waveform. Different colors legend indicates different values for Cm parameter shown on top right of the figure. Second parameter is not color coded for clarity. The SD curves cross multiple times usually at extreme pulse widths (PW), but in mid-PWs as well in some cases. X-scale is divided for clarity, from 0 to 0.2/0.3 then from 1 to 5 mSec. The area between (0.2/0.3 to 1) ms is not shown.
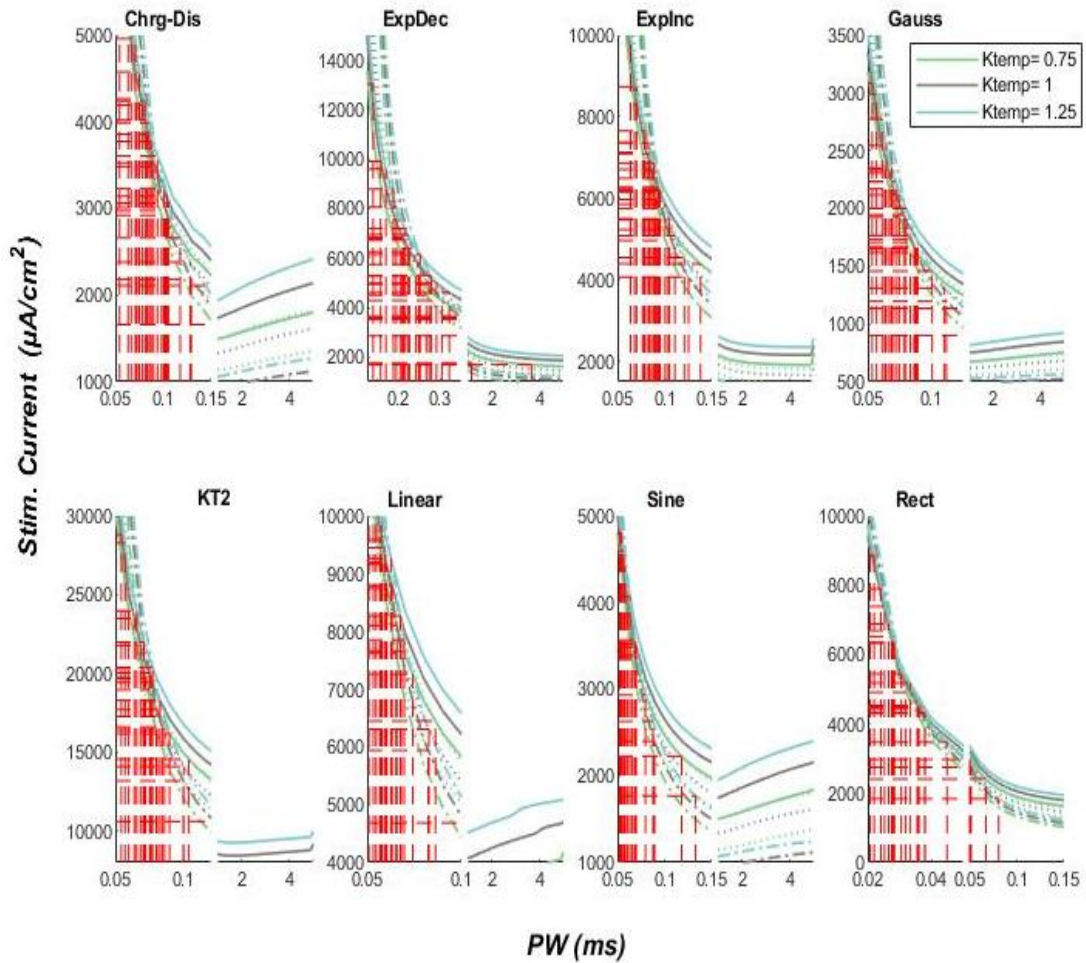
Figure B.3 KTEMP & GLEAK are altered simultaneously in each case by the same amount, using eight different waveform. Different colors legend indicates different values for Ktemp parameter shown on top right of the figure. Second parameter is not color coded for clarity. The SD curves cross multiple times usually at extreme pulse widths (PW), but in mid-PWs as well in some cases. X-scale is divided for clarity, from 0 to 0.2 then from 1 to 5 mSec. The area between (0.2 to 1) ms is not shown.
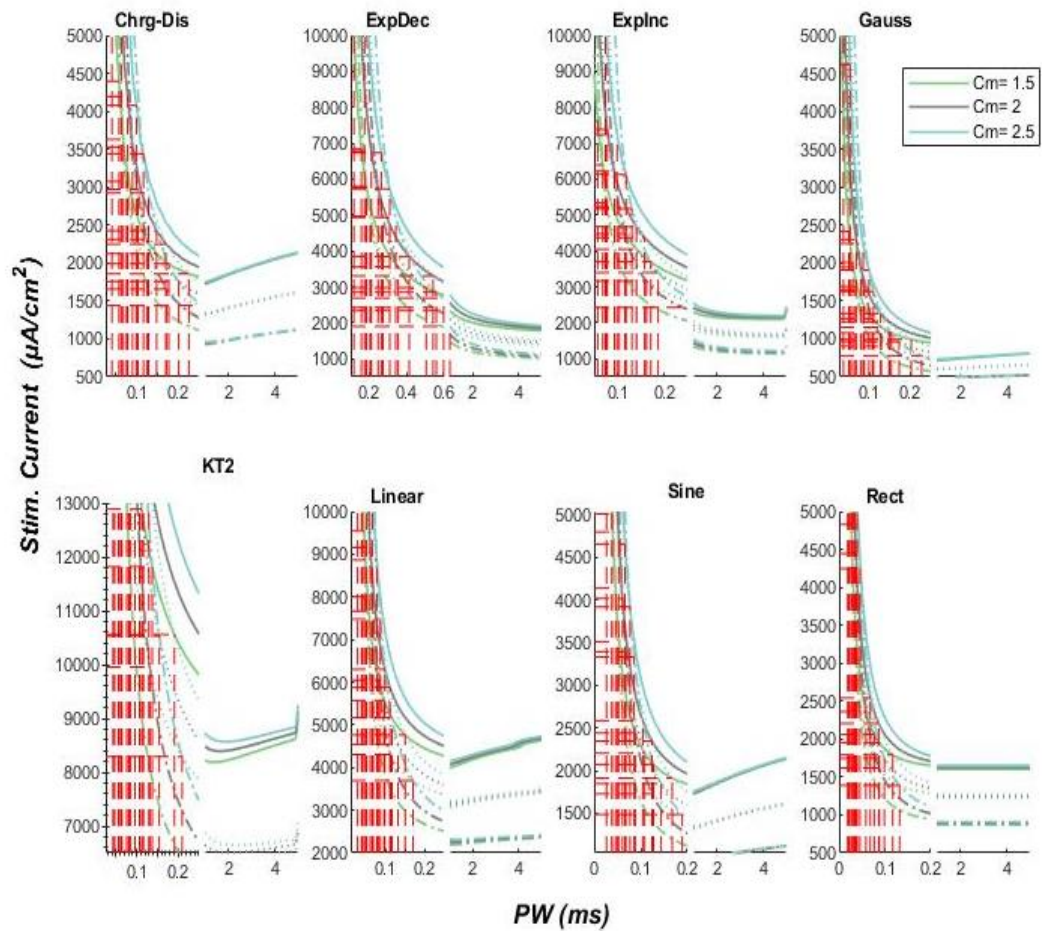
Figure B.4 GLEAK & CM are altered simultaneously in each case by the same amount, using eight different waveform. Different colors in each subplot indicate different values for Cm parameter shown on top right. Second parameter is not color coded for clarity. The SD curves cross multiple times usually at extreme pulse widths (PW), but in mid-PWs as well in some cases. X-scale is divided for clarity, from 0 to 0.2 then from 1 to 5 mSec. The area between (0.2 to 1) ms is not shown.

Table B.1. *Percent of change in Chronaxie and Rheobase slopes for mono stimulus waveforms compared to Rect waveform.*

	G_{Leak}	G_{Namax}	K_{temp}	C_m
Percent Change in Chr %				
Chrg-Dis	4.761905	0	-0.539	9.777424
ExpDec	-30.1587	0	-54.8827	-26.974
ExpInc	-19.0476	0	-13.6652	-14.8119
Gauss	4.761905	0	6.341154	6.783254
Kt^2	0	0	10.68484	1.139375
Linear	4.761905	0	11.44578	3.471118
Sine	1.587302	0	12.77743	6.465289
Rect	0	0	0	0
Percent Change in Rheobase %				
Chrg-Dis	0	0	0.134078	10.23891
ExpDec	-13.0435	0	-12.8492	261.0922
ExpInc	-7.6087	0	-14.4134	185.6655
Gauss	-1.08696	0	0.692737	21.843
Kt^2	-2.17391	0	-2.86034	74.06143
Linear	-1.08696	0	0.916201	55.9727
Sine	0	0	0.558659	15.69966
Rect	0	0	0	0

Note: . *Change in slope were calculated using the following equation $100*(S_w - S_{Rect})/S_{Rect}$). S_w is the slope for non-rectangular waveform , and S_{Rect} is the slope for rectangular waveform.*

Table B.2. Chronaxie and Rheobase slopes for HPP stimulus waveforms.

Waveform/Parameter	Gleak	Gnamax	ktemp	CM
Chronaxie time				
Chrg-Dis	-0.0069	0.0000	-0.3000	0.4357
ExpDec	-0.0037	0.0000	-0.1195	0.2366
ExpInc	-0.0042	0.0000	-0.2084	0.2702
Gauss	-0.0067	0.0000	-0.2876	0.4151
KT	-0.0056	0.0000	-0.2949	0.3503
Linear	-0.0064	0.0000	-0.3471	0.3997
Sine	-0.0069	0.0000	-0.3002	0.4253
Rect	-0.0070	0.0000	-0.3112	0.4310
Rheobase				
Chrg-Dis	0.0092	-0.0002	0.4622	0.0323
ExpDec	0.0073	-0.0002	0.3781	0.1506
ExpInc	0.0079	-0.0002	0.3447	0.1210
Gauss	0.0090	-0.0002	0.4593	0.0416
KT	0.0086	-0.0002	0.4095	0.0766
Linear	0.0090	-0.0002	0.4597	0.0509
Sine	0.0091	-0.0002	0.4684	0.0347
Rect	0.0092	-0.0002	0.5076	0.0329

Table B.3. *Chronaxie and Rheobase slopes for Mono stimulus waveforms.*

Waveform/Parameter	Gleak	Gnamax	ktemp	CM
Chronaxie time				
Chrg-Dis	-0.0066	0.0000	-0.3137	0.4143
ExpDec	-0.0044	0.0000	-0.1423	0.2756
ExpInc	-0.0051	0.0000	-0.2723	0.3215
Gauss	-0.0066	0.0000	-0.3354	0.4030
KT	-0.0063	0.0000	-0.3491	0.3817
Linear	-0.0066	0.0000	-0.3515	0.3905
Sine	-0.0064	0.0000	-0.3557	0.4018
Rect	-0.0063	0.0000	-0.3154	0.3774
Rheobase				
Chrg-Dis	0.009185	-0.000171	0.448081	0.032345
ExpDec	0.007979	-0.000164	0.390040	0.105780
ExpInc	0.008473	-0.000179	0.382965	0.083724
Gauss	0.009138	-0.000172	0.450570	0.035748
KT	0.009029	-0.000184	0.434742	0.050986
Linear	0.009103	-0.000182	0.451593	0.045664
Sine	0.009158	-0.000171	0.450015	0.033944
Rect	0.009214	-0.000170	0.447520	0.029269

APPENDIX C

MATLAB CODE AND FUNCTIONS FOR THE MODEL

```matlab
%Update  bY: B.Ghobreal          Date: 09/25/2018
% Version 12 is the last stable version release on 10/17/2017.
% Version 012 in this version
% it is going back to the original and repeating everything and replotting
% changing the K value for both of them or indvidually
%PLOTS THE Action potential
% Problem that mentioned by Dr. Sahin is fix , where the plotting was not
% correct and I fixed the plotting and the threshold porblem
% we plot the SUB threshold Vs THe PW
% I discovered an issue on the 11/11/2019 that cm is define as parm_array
% and it should of been difeind as parm_array2..
% I fixed the issue and it didn't effect the results because CM was always
% pram1 11/29/2019

close all;
clear all

current_directry = pwd;
v0=-80;%mv  Resting memebrane voltage
duration=5;%ms
KQM_alpha = 1;
KQM_Beta=1;
KQH_alpha = 1;
KQH_Beta = 1;
Temp_Cofe = 1;

Next =0 ;
signal_used = 0;
%PW=[0.02,0.04,0.06,0.08,0.1,0.2,0.3,0.5]; % Creathinga Pulsh Width Array to cycle
throught and find the best K
% PW = 0.01:.01:duration;
% PW =[ 0.01:.01:1 1.1:0.1:5 ] ;
% PW =[ 0.01:.01:1 1.1:0.5: 5 ] ;
PW =[ 0.01:.01:0.25 0.3:0.05:0.95  1:1: 5 ] ;
%PW_half=PW/2; % I divided the PW to  two halfs, each ahlf willhave  part of the signal.
for example if PW =.2 --> PW1 =.1 for the cathodic part andPW2 = .1 for the Anodic part
of the signal
Q=length(PW); % length of Puls Width array
dt=10^(-3); %10^(-3);%ms     Delta t
M=duration/dt;   % length of time change array to
IS=zeros(1,M); % the simulation current, unit: microAmpere, 0.1 msec duration.
Paramter_chng = [];
output1=zeros(1,Q);
output11=zeros(1,Q);
output12=zeros(1,Q);
output2=zeros(1,Q);
output21=zeros(1,Q);
output22=zeros(1,Q);
output3=zeros(1,Q);
output31=zeros(1,Q);
output32=zeros(1,Q);
output4=zeros(1,Q);
output41=zeros(1,Q);
output42=zeros(1,Q);
output5=zeros(1,Q);
output51=zeros(1,Q);
output52=zeros(1,Q);
output6=zeros(1,Q);
output61=zeros(1,Q);
output62=zeros(1,Q);
```

```matlab
output7=zeros(1,Q);
output71=zeros(1,Q);
output72=zeros(1,Q);
output8=zeros(1,Q);
output81=zeros(1,Q);
output82=zeros(1,Q);

gnamax=1445; % mmho/(cm*cm) [K/ ( Ohm* CM*CM)2.5
gleak=128; % mmho/(cm*cm)
%Ek=-84;%mV  ?????
Ena= 35.64; %mV
Eleak=-80.01;%mV
Cm=2;%uF/(cm*cm)
% Cm=0.25

i=1;
m=1;
n=1;
k=0;
k1=0;
AM=zeros(1,M);
BM=zeros(1,M);

AH=zeros(1,M);
BH=zeros(1,M);

HINF=zeros(1,M);

MGATE=zeros(1,M);
HGATE=zeros(1,M);

GNA=zeros(1,M);

INA=zeros(1,M);
ILEAK=zeros(1,M);
Signal_names = {' INcreasing Expotential' , ' Rectangular Waveform' ' Linear Waveform'
'KT^2 Waveform' ' Decaying Expotential' ' Charge Dis-Charge waveform ' ' Gaussian
Waveform' ' Sine Waveform',...
              ' Cathodic Puls and INcreasing Expotential' , ' Cathodic Puls and
Rectangular Waveform' ' Cathodic Puls and Linear Waveform'  'Cathodic Puls and KT^2
Waveform' ' ' ' Cathodic Puls and Decaying Expotential'    ' Cathodic Puls and Charge
Dis-Charge waveform ' ' Cathodic Puls and Gaussian Waveform' ' Cathodic Puls and Sine
Waveform' '' ''  ' Cathodic + 200uS gap + Rectangular'};

% Prectage_bar = waitbar(0, 'Precentage completead ....');
%% Choosing variable you wanna change
NumOFParameters=0;

NumOFParameters = str2num( questdlg ('How many Parameters Of Interest for this Cell ?',
'Number of Parameters Of Interest' ,'1', '2' ,'3' ));% uiwait(NumOFParameters_MSGBOX) ;
% num_of_parm = str2num(NumOFParameters);

%% Choosing variable you wanna change
Exit = 0;
Min=0;
Max=0;
step=0;
Max_P2 =0;
Min_P2=0;
step_P2=0;
Skip =5;
sensitivity=0;
DefinedPrecentage = 0;
Paramter_chng=0;
Paramter2_chng=0;
Paramter_VAl=1;
Paramter_VAl2=1;
Paramters_Of_Interest = {'Gnamax','Gleak','Alpha','Beta','Temp. Coef', 'Cm'};
switch NumOFParameters
    case 1
        while Exit <1
```

```matlab
        figure(1)
        clf
        %    scrsz = get(0,'ScreenSize');
        position_default = [650 250 600 300];
        set(gcf,'position',position_default)
        set(gcf,'ToolBar','none')
        set(gcf,'MenuBar','none')


        popup = uicontrol(gcf,'Style', 'popup','String',
{'gnamax','gleak','KQM_alpha','KQM_Beta','Tempreature Coef' ,
'Cm'},'Value',Paramter_VAl,'units','normalized','Position',[.125 .8 .35
.1],'Callback','if popup.Value == 1;Paramter_chng = gnamax ; elseif popup.Value == 2;
Paramter_chng = gleak;elseif popup.Value ==3; Paramter_chng = KQM_alpha ;elseif
popup.Value ==4;Paramter_chng = KQM_Beta; elseif popup.Value ==5;Paramter_chng =
Temp_Cofe;elseif popup.Value ==6;Paramter_chng = Cm;else; end; uiresume;');
        pbStr =
uicontrol(gcf,'Style','edit','String',Paramter_chng,'units','normalized','Position',[.60
.8 .25 .1],'Callback',' uiresume;');
        pbStr =
uicontrol(gcf,'Style','text','String','Current','units','normalized','Position',[.60 .90
.25 .05],'Callback','uiresume;');
        pbStrMIN =
uicontrol(gcf,'Style','edit','Value',Min,'units','normalized','Position',[.10 .40 .25
.15],'Callback', 'Min = str2num(pbStrMIN.String);');
        pbStr =
uicontrol(gcf,'Style','text','String','Min','units','normalized','Position',[.10 .60 .25
.05],'Callback',' ');
        pbStrMax =
uicontrol(gcf,'Style','edit','Value',Max,'units','normalized','Position',[.40 .40 .25
.15],'Callback','    Max = str2num(pbStrMax.String) ;');
        pbStr =
uicontrol(gcf,'Style','text','String','MAx','units','normalized','Position',[.40 .60 .25
.05],'Callback',' uiresume;');
        pbStrStep =
uicontrol(gcf,'Style','edit','Value',step,'units','normalized','Position',[.70 .40 .25
.15],'Callback','    step = str2num(pbStrStep.String);');
        pbStr =
uicontrol(gcf,'Style','text','String','Step','units','normalized','Position',[.70 .60 .25
.05],'Callback','uiresume;');
        pbexit =
uicontrol(gcf,'Style','pushbutton','String','Skip','units','normalized','Position',[.65
.10 .15 .15],'Callback','Skip=0;Exit = 5; uiresume;');
        pbexit =
uicontrol(gcf,'Style','pushbutton','String','Sensitivity','units','normalized','Position'
,[.45 .10 .15 .15],'Callback','sensitivity = 5; Exit = 5; uiresume;');

        pbexit =
uicontrol(gcf,'Style','pushbutton','String','Next','units','normalized','Position',[.25
.10 .15 .15],'Callback','Exit = 5; uiresume;');

        uiwait(gcf)
        Paramter VAl =  popup.Value;

    end


    if Skip >0
        if (sensitivity >0)
            switch(Paramter_VAl)
                case 1
                  Pram_Array = 1084:2*36.1:1806;
                case 2
                  Pram_Array = 96:2*3.2:160;
                case 5
                    Pram_Array = 0.75:2*0.025:1.25;
                case 6
                    Pram_Array =  1.5:2*0.05:2.5;
            end
        else
            Pram_Array=Min:step:Max;
```

```matlab
                end
        else
            Pram_Array =0;
        end
        LBL =  popup.String(Paramter_VAl);
        Pram_Array2 = [ 1445]; % Array for the second paramter (gnamax now)
        Paramter_VAl2 = 1 ;




    case 2
        while Exit <1
            figure(1)
            clf
            %    scrsz = get(0,'ScreenSize');
            position_default = [650 250 600 300];
            set(gcf,'position',position_default)
            set(gcf,'ToolBar','none')
            set(gcf,'MenuBar','none')

            % first paramter contorl panel
            Frame =
uicontrol(gcf,'Style','frame','String','','units','normalized','Position',[.65 .1 .32
.72],'Callback',' uiresume;');
            Fram_text = uicontrol(gcf,'Style','text','String','Parameter #
1','FontSize',11.0,'units','normalized','Position',[.65 .85 .25
.05],'Callback','uiresume;');
            popup = uicontrol(gcf,'Style', 'popup','String',
{'gnamax','gleak','KQM_alpha','KQM_Beta','Tempreature
Coef','Cm'},'Value',Paramter_VAl,'units','normalized','Position',[.7 .7 .25
.1],'Callback','if popup.Value == 1;Paramter_chng = gnamax; elseif popup.Value == 2;
Paramter_chng = gleak;elseif popup.Value ==3; Paramter_chng = KQM_alpha ;elseif
popup.Value ==4;Paramter_chng = KQM_Beta ; elseif popup.Value ==5;Paramter_chng =
Temp_Cofe ;elseif popup.Value ==6; Paramter_chng = Cm;else; end; uiresume;');
            pbStr =
uicontrol(gcf,'Style','edit','String',Paramter_chng,'units','normalized','Position',[.80
.6 .1 .1],'Callback',' uiresume;');
            pbStr =
uicontrol(gcf,'Style','text','String','Current','units','normalized','Position',[.70 .6
.1 .05],'Callback','uiresume;');
            pbStrMax =
uicontrol(gcf,'Style','edit','Value',Max,'units','normalized','Position',[.80 .45 .1
.1],'Callback','    Max = str2num(pbStrMax.String) ;');
            pbStr =
uicontrol(gcf,'Style','text','String','MAx','units','normalized','Position',[.70 .45 .1
.05],'Callback',' uiresume;')
            pbStrMIN =
uicontrol(gcf,'Style','edit','Value',Min,'units','normalized','Position',[.80 .3 .1
.1],'Callback', 'Min = str2num(pbStrMIN.String);');
            pbStr =
uicontrol(gcf,'Style','text','String','Min','units','normalized','Position',[.70 .3 .1
.05],'Callback',' ');
            pbStrStep =
uicontrol(gcf,'Style','edit','Value',step,'units','normalized','Position',[.80 .15 .1
.1],'Callback','    step = str2num(pbStrStep.String);');
            pbStr =
uicontrol(gcf,'Style','text','String','Step','units','normalized','Position',[.70 .15 .1
.05],'Callback','uiresume;');


            % second Parameter control panel
            Frame =
uicontrol(gcf,'Style','frame','String','','units','normalized','Position',[.05 .1 .32
.72],'Callback',' uiresume;');
            Fram_text = uicontrol(gcf,'Style','text','String','Parameter #
2','FontSize',11.0,'units','normalized','Position',[.05 .85 .25
.05],'Callback','uiresume;');
            popup_Par2 = uicontrol(gcf,'Style', 'popup','String',
{'gnamax','gleak','KQM_alpha','KQM_Beta','Tempreature
Coef','Cm'},'Value',Paramter_VAl2,'units','normalized','Position',[.1 .7 .25
```

```matlab
.1],'Callback','if popup_Par2.Value == 1;Paramter2_chng = gnamax; elseif popup_Par2.Value
== 2; Paramter2_chng = gleak;elseif popup_Par2.Value ==3; Paramter2_chng = KQM_alpha
;elseif popup_Par2.Value ==4;Paramter2_chng = KQM_Beta; elseif popup_Par2.Value
==5;Paramter2_chng = Temp_Cofe;elseif popup_Par2.Value ==6; Paramter2_chng = Cm ;else;
end; uiresume;');
            pbStr_Par2 =
uicontrol(gcf,'Style','edit','String',Paramter2_chng,'units','normalized','Position',[.2
.6 .1 .1],'Callback',' uiresume;');
            pbStr_Par2 =
uicontrol(gcf,'Style','text','String','Current','units','normalized','Position',[.1 .6 .1
.05],'Callback','uiresume;');
            pbStrMax_Par2 =
uicontrol(gcf,'Style','edit','Value',Max_P2,'units','normalized','Position',[.2 .45 .1
.1],'Callback','    Max_P2 = str2num(pbStrMax_Par2.String) ;');
            pbStr_Par2 =
uicontrol(gcf,'Style','text','String','MAx','units','normalized','Position',[.1 .45 .1
.05],'Callback',' uiresume;');
            pbStrMIN_Par2 =
uicontrol(gcf,'Style','edit','Value',Min_P2,'units','normalized','Position',[.2 .3 .1
.1],'Callback', 'Min_P2 = str2num(pbStrMIN_Par2.String);');
            pbStr_par2 =
uicontrol(gcf,'Style','text','String','Min','units','normalized','Position',[.1 .3 .1
.05],'Callback',' ');
            pbStrStep_par2 =
uicontrol(gcf,'Style','edit','Value',step_P2,'units','normalized','Position',[.2 .15 .1
.1],'Callback','    step_P2 = str2num(pbStrStep_par2.String);');
            pbStr_par2 =
uicontrol(gcf,'Style','text','String','Step','units','normalized','Position',[.1 .15 .1
.05],'Callback','uiresume;');




            pbexit =
uicontrol(gcf,'Style','pushbutton','String','Skip','units','normalized','Position',[.425
.2 .15 .15],'Callback','Skip=0;Exit = 5; uiresume;');
            pbexit =
uicontrol(gcf,'Style','pushbutton','String','Next','units','normalized','Position',[.425
.6 .15 .15],'Callback','Exit = 5; uiresume;');
             pbexit = uicontrol(gcf,'Style','pushbutton','String','Use defined Percentage
" +-25 %" ','units','normalized','Position',[.330 .84 .35
.15],'Callback','DefinedPrecentage=5;Exit = 5; uiresume;');

            uiwait(gcf)
            Paramter_VAl =  popup.Value;
            Paramter_VAl2= popup_Par2.Value;

        end

        if Skip >0
            if DefinedPrecentage > 0
                if Paramter_VAl2 == 1 %gnamax
                    Pram_Array2 = round(([-.25 -.15 -.05 0 0.05 0.15 0.25 ]
*1445+1445));% 1084:120.33333:1806;% 1084:180.5:1806 ; %1011.5:144.5:1878.5; %
1084:144.5:1878.5; %1084:361:1806
                elseif Paramter_VAl2 == 2 %gleak
                    Pram_Array2= round(([-.25 -.15 -.05 0 0.05 0.15 0.25 ] *128+128))
;%96:10.666666:160;  %96:16:160;% 89.6:12.8:166.4; %96:32:160;
                elseif Paramter_VAl2 ==3
                    Pram_Array2 = KQM_alpha *Pram_Array2;
                elseif Paramter_VAl2 ==4
                    Pram_Array2 =  KQM_Beta * Pram_Array2;
                elseif Paramter_VAl2 ==5 % Change in Tempreature chznges both K for alpha
and Beta H and M gates
                        Pram_Array2=([-.25 -.15 -.05 0 0.05 0.15 0.25 ] *1+1); %
0.75:0.08333:1.25;% 0.75:0.125:1.25 ;% 0.7:0.1:1.3;% 0.75:0.25:1.25;
                elseif Paramter_VAl2 ==6  % Change in Cm
                    Pram_Array2 =([-.25 -.15 -.05 0 0.05 0.15 0.25 ] *2+2); %
1.5:0.16666:2.5 ;%1.5:0.25:2.5;%  1.4:0.2:2.6;%1.5:0.5:2.5;
                end
```

```matlab
                if Paramter_VAl == 1 %gnamax
                    Pram_Array = round(([-.25 -.15 -.05 0 0.05 0.15 0.25 ] *1445+1445));%
1084:120.33333:1806; % 1084:180.5:1806 ;% 1084:180.5:1806 ;% 1084:120.33333:1806
;%1011.5:144.5:1878.5; %  1084:361:1806; 1084:361:1806 ;%
                elseif Paramter_VAl == 2
                    Pram_Array= round(([-.25 -.15 -.05 0 0.05 0.15 0.25 ] *128+128)) ;
%96:10.666666:160; %89.6:12.8:166.4; % 96:32:160;
                elseif Paramter_VAl ==3
                    Pram_Array = KQM_alpha * Pram_Array;
                elseif Paramter_VAl ==4
                    Pram_Array =  KQM_Beta * Pram_Array;
                elseif Paramter_VAl ==5 % Change in Tempreature chznges both K for alpha
and Beta H and M gates
                    Pram_Array=  ([-.25 -.15 -.05 0 0.05 0.15 0.25 ] *1+1);
%0.75:0.08333:1.25; %0.7:0.1:1.3;% 0.75:0.25:1.25;
                elseif Paramter_VAl ==6  % Change in Cm
                    Pram_Array =([-.25 -.15 -.05 0 0.05 0.15 0.25 ] *2+2)  ;%
1.5:0.16666:2.5 ;%1.4:0.2:2.6;% 1.5:0.5:2.5;
                end
            else
                Pram_Array=Min:step:Max;
                Pram_Array2=Min_P2:step_P2:Max_P2;
            end
        else
            Pram_Array2 = 0;
            Pram_Array = 0;
        end
        LBL =  popup.String(Paramter_VAl);
        LBL_2 =  popup_Par2.String(Paramter_VAl2);
end

%%
K_DPP=0;
Answer =  questdlg ('What type of stimulation ?','Stimulation Type!','DPP', 'Gap',
'Non','Skip' );% uiwait(NumOFParameters_MSGBOX) ;
if (strcmp(Answer,'DPP'))
     DPP_PW=1;
    M=M+DPP_PW/dt;
    PW =(PW(1)+DPP_PW):.01:(duration+DPP_PW);


elseif (strcmp(Answer,'Gap'))
    PW_Gap=200/1000;
end


%%
Exit = 0;
while Exit <1

    while Next < 1
        cd (current_directry);
        figure(2)
        clf
        scrsz = get(0,'ScreenSize');
        position_default = [0.01*scrsz(3) 0.07*scrsz(4) 0.98*scrsz(3) 0.85*scrsz(4)];
        set(gcf,'position',position_default)

        Frame =
uicontrol(gcf,'Style','frame','String','','units','normalized','Position',[.922 .14 .057
.77],'Callback',' uiresume;');
        Fram_text = uicontrol(gcf,'Style','text','String','Anodic
Signal','FontSize',11.0,'units','normalized','Position',[.9255 .85 .05
.1],'Callback','uiresume;');
        pbexit = uicontrol(gcf,'Style','pushbutton','String','Increasing
EXP','units','normalized','Position',[.925 .85 .05 .05],'Callback','signal_used = 1;
uiresume;');
        pbexit = uicontrol(gcf,'Style','pushbutton','String','rectangular
waveform','units','normalized','Position',[.925 .75 .05 .05],'Callback','signal_used = 2;
uiresume;');
```

```matlab
        pbexit = uicontrol(gcf,'Style','pushbutton','String','linear
waveform','units','normalized','Position',[.925 .65 .05 .05],'Callback','signal_used = 3;
uiresume;');
        pbexit = uicontrol(gcf,'Style','pushbutton','String','KT^2 wave
form','units','normalized','Position',[.925 .55 .05 .05],'Callback','signal_used = 4;
uiresume;');
        pbexit = uicontrol(gcf,'Style','pushbutton','String',' Decaying
exponential','units','normalized','Position',[.925 .45 .05 .05],'Callback','signal_used =
5; uiresume;');
        pbexit = uicontrol(gcf,'Style','pushbutton','String','Charge-Discharge
Curve','units','normalized','Position',[.925 .35 .05 .05],'Callback','signal_used = 6;
uiresume;');
        pbexit = uicontrol(gcf,'Style','pushbutton','String','Gaussian
Stimulus','units','normalized','Position',[.925 .25 .05 .05],'Callback','signal_used = 7;
uiresume;');
        pbexit = uicontrol(gcf,'Style','pushbutton','String','Sinusoidal
Stimulus','units','normalized','Position',[.925 .15 .05 .05],'Callback','signal_used = 8;
uiresume;');
%        pbexit = uicontrol(gcf,'Style','pushbutton','String','ALL Signals
','units','normalized','Position',[.925 .95 .05 .05],'Callback','All_Signals = 1;
uiresume;');


        Frame =
uicontrol(gcf,'Style','frame','String','','units','normalized','Position',[.122 .14 .057
.77],'Callback',' uiresume;');
        Fram_text = uicontrol(gcf,'Style','text','String','Cathodic + Anodic
Signal','FontSize',11.0,'units','normalized','Position',[.1255 .85 .05
.1],'Callback','uiresume;');
        pbexit = uicontrol(gcf,'Style','pushbutton','String','Increasing
EXP','units','normalized','Position',[.125 .85 .05 .05],'Callback','signal_used = 9;
uiresume;');
        pbexit = uicontrol(gcf,'Style','pushbutton','String','rectangular
waveform','units','normalized','Position',[.125 .75 .05 .05],'Callback','signal_used =
10; uiresume;');
        pbexit = uicontrol(gcf,'Style','pushbutton','String','linear
waveform','units','normalized','Position',[.125 .65 .05 .05],'Callback','signal_used =
11; uiresume;');
        pbexit = uicontrol(gcf,'Style','pushbutton','String','KT^2 wave
form','units','normalized','Position',[.125 .55 .05 .05],'Callback','signal_used = 12;
uiresume;');
        pbexit = uicontrol(gcf,'Style','pushbutton','String',' Decaying
exponential','units','normalized','Position',[.125 .45 .05 .05],'Callback','signal_used =
14; uiresume;');
        pbexit = uicontrol(gcf,'Style','pushbutton','String','Charge-Discharge
Curve','units','normalized','Position',[.125 .35 .05 .05],'Callback','signal_used = 15;
uiresume;');
        pbexit = uicontrol(gcf,'Style','pushbutton','String','Gaussian
Stimulus','units','normalized','Position',[.125 .25 .05 .05],'Callback','signal_used =
16; uiresume;');
        pbexit = uicontrol(gcf,'Style','pushbutton','String','Sinusoidal
Stimulus','units','normalized','Position',[.125 .15 .05 .05],'Callback','signal_used =
17; uiresume;');


    % adding the Gap between the cathodic and anodic
    pbexit = uicontrol(gcf,'Style','pushbutton','String','200uS +
Rec','units','normalized','Position',[.180 .75 .06 .05],'Callback','signal_used = 20;
uiresume;');




        pbexit =
uicontrol(gcf,'Style','pushbutton','String','Next','units','normalized','Position',[.925
.05 .05 .05],'Callback','Next = 5; uiresume;');
        uiwait(gcf)

    end
```

```matlab
%%

for Pram2 = 1:length(Pram_Array2)

    if Paramter_VАl2 == 1
        gnamax=Pram_Array2(Pram2);
    elseif Paramter_VАl2 == 2
        gleak=Pram_Array2(Pram2);
    elseif Paramter_VАl2 ==3
        KQM_alpha = Pram_Array2(Pram2);
        KQH_alpha = Pram_Array2(Pram2);
    elseif Paramter_VАl2 ==4
        KQM_Beta = Pram_Array2(Pram2);
        KQH_Beta = Pram_Array2(Pram2);
    elseif Paramter_VАl2 ==5 % Change in Tempreature chznges both K for alpha and Beta
H and M gates
        KQM_alpha = Pram_Array2(Pram2);
        KQH_alpha = Pram_Array2(Pram2);
        KQM_Beta = Pram_Array2(Pram2);
        KQH_Beta = Pram_Array2(Pram2);
    elseif Paramter_VАl2 ==6  % Change in Cm
        Cm = Pram_Array2(Pram2);
    end


    for P=1:length(Pram_Array)


        clear HGATE_Array_at_eah_K GNA_array_at_each_K  Minfinite_array_at_each_K
Tm_array_at_each_K Hinfinite_array_at_each_K Th_array_at_each_K AM_array_At_each_K
BM_Array_At_each_K AH_array_At_each_K BH_Array_At_each_K    V_Action_potential
MGATE_Array_at_each_K
        clear K  mgate   V2   MGATE  MGATE_AP   HGATE  HGATE_AP    GNA  GNA_AP
Minfinite  Minfinite_AP     Tm Tm_AP   Hinfinite  Hinfinite_AP Th  Th_AP AM  AM_AP BM
BM_AP  AH  AH_AP  BH  BH_AP  Is1_AP
        clear am   bm bh ah m0 h0 minfinite tm hinfinite th mgate hgate gna Slope
deltav V V_plotting V2 T_plotting Current deltav_array slope_Array
        clear AM BM AH BH HINF Hinfinite Th  Minfinite tm MGATE HGATE GNA INA ILEAK

        if Paramter_VАl == 1
            gnamax=Pram_Array(P);
        elseif Paramter_VАl == 2
            gleak=Pram_Array(P);
        elseif Paramter_VАl ==3
            KQM_alpha = Pram_Array(P);
            KQH_alpha = Pram_Array(P);
        elseif Paramter_VАl ==4
            KQM_Beta = Pram_Array(P);
            KQH_Beta = Pram_Array(P);
        elseif Paramter_VАl ==5 % Change in Tempreature chznges both K for alpha and
Beta H and M gates
            KQM_alpha = Pram_Array(P);
            KQH_alpha = Pram_Array(P);
            KQM_Beta = Pram_Array(P);
            KQH_Beta = Pram_Array(P);
        elseif Paramter_VАl ==6  % Change in Cm
            Cm = Pram_Array(P);
        end

        % increasing exponential waveform
        IS=zeros(1,M);
        T_plotting=zeros(1,M);
        i=1;
        m=1;
        n=1;
        klow = 0;
        khigh = 8.8897e+007;%uA/cm^2
        Kstart=khigh;
        K_AP = 0;
        AP = 1;
```

```matlab
            for n=1:Q, % changing the PW for The current it is clear when changing T and
calculaes a new Is (stimulation current) every cycle based on PW
                if (PW(n) ==5 && P == 2 && Pram2==3)
                    Pram_Array2(3)
                    Pram_Array(P)
                    PW(n)

                end
                n;
                T1=dt:dt:PW(n);
                klow = 0;
                khigh = 8.8897e+007;
                K_AP = 0;
                V_AP=0;
                if strcmp(Answer,'Non')
                    [ K_AP  V_AP]  =
FIndIdealThreshold(v0,M,T1,PW,n,dt,signal_used,KQM_alpha,KQM_Beta,KQH_Beta,KQH_alpha,gnam
ax,gleak,Ena,Eleak,Cm);

                elseif (strcmp(Answer,'DPP'))
                    [ K_AP  V_AP]  =
FIndIdealThreshold(v0,M,T1,DPP_PW,1,dt,signal_used,KQM_alpha,KQM_Beta,KQH_Beta,KQH_alpha,
gnamax,gleak,Ena,Eleak,Cm);
                    K_DPP = 0.95* K_AP ;
                    % construct the DPP  Waveform
                    [ K_AP  V_AP]  =
FIndIdealThreshold(v0,M,T1,PW,n,dt,signal_used,KQM_alpha,KQM_Beta,KQH_Beta,KQH_alpha,gnam
ax,gleak,Ena,Eleak,Cm,Answer,DPP_PW,K_DPP);
                elseif (strcmp(Answer,'Gap'))
                    [ K_AP  V_AP]  =
FIndIdealThreshold(v0,M,T1,PW,n,dt,signal_used,KQM_alpha,KQM_Beta,KQH_Beta,KQH_alpha,gnam
ax,gleak,Ena,Eleak,Cm,Answer,PW_Gap);
                end

%%%%%%%%%%%%%%%%%%%%%%%%%%%%%%%%%%%%%%%%%%%%%%%%%%%%%%%%%%%%%%%%%%%%%%%%%%

                if (length(V_AP)> 1)
                    V2=0;
                    K=0;
                    k=K_AP ;
                    V2= V_AP ;
%               elseif(~exist('V_AP'))
%                   break;
%               end
%               klow = 0;
%               khigh = 2*k;
                a(n)=k;
%                                   figure(900);plot(V_AP,'r');

                %%%%  this loop is to generrate the full action potential at the selected
K ,
                %%%%  IT usese the selected K values and
                %%%%  recalcualte the current at this value and
                %%%%  recalcualte the Full cycle of the AP and all
                %%%%  other variables
                %%% in order to replot V as a full scale we have to
                %%% recalcualte all Other varaibles,  this will
                %%% save the variables at the selected K only
                if (strcmp(Answer,'Non'))
                    IS(1:round(PW(n)/dt))=SimulationCurrent( k,T1,PW , n , dt , signal_used
);   % Current at selected k
                 elseif (strcmp(Answer,'DPP'))
                    IS(1:round(PW(n)/dt))=ReconstructDPP( k,T1,PW , n , dt ,
signal_used,K_DPP,DPP_PW );
                elseif (strcmp(Answer,'Gap'))
%                   IS(1:round(PW(n)/dt)+2000)=SimulationCurrent( k,T1,PW , n , dt ,
signal_used );    % Current at selected k
                    IS(1:round(PW(n)/dt) + round(PW_Gap/dt))=SimulationCurrent( k,T1,PW , n
, dt , signal_used ,Answer, K_DPP,PW_Gap);
                        if length(IS)>M
                            IS(M+1:end)=[];
```

111

```matlab
        end
    end
V=-80;
am= KQM_alpha * ((126+0.363*V)/(1+exp(-(49+V)/53)));
bm= KQM_Beta * (am/(exp((V+56.2)/4.17)));

bh= KQH_Beta * (15.6/(1+exp(-(V+56)/10)));
ah=KQH_alpha *  (bh/(exp((V+74.5)/5)));
%
mgate=am/(am+bm);
hgate=ah/(ah+bh);

Current=[];
deltav_array=[];
slope_Array=[];
V2=[];
T_plotting =[];
V2(1)  = v0;

for i=1:M
    i;
    am= KQM_alpha * ((126+0.363*V)/(1+exp(-(49+V)/53)));
    bm= KQM_Beta * (am/(exp((V+56.2)/4.17)));
    bh= KQH_Beta *(15.6/(1+exp(-(V+56)/10)));
    ah= KQH_alpha * (bh/(exp((V+74.5)/5)));
    m0=mgate;
    h0=hgate;
    minfinite=am/(am+bm);
    tm=1/(am+bm);
    hinfinite=ah/(ah+bh);
    th=1/(ah+bh);
    mgate=m0-(m0-minfinite)*(1-exp(-dt/tm)) ;
    hgate=h0-(h0-hinfinite)*(1-exp(-dt/th)) ;
    gna=gnamax*(mgate^2)*hgate;

    slope=(IS(i)-gna*(V-Ena)-gleak*(V-Eleak))/Cm;
    deltav=slope*dt;
    V=deltav+V;
    V_plotting(i) = V;
    V2(i)=V;
    T_plotting(i)= i*dt; %(ms)  (Micro Seconds )
    Current(i) = IS(i);
    deltav_array (i) = deltav;
    slope_Array (i) =slope;
    AM(i)=am;
    BM(i)=bm;
    AH(i)=ah;
    BH(i)=bh;
    HINF(i)=hinfinite;
    Hinfinite (i) = hinfinite;
    Th(i) =th;
    Minfinite(i) = minfinite;
    Tm(i) = tm;
    MGATE(i)=mgate;
    HGATE(i)=hgate;
    GNA(i)=gna;
    INA(i)=gna*(V-Ena);
    ILEAK(i)=gleak*(V-Eleak);

end

%%%%%%%%%%%%%%%%%%%%%%%%%%%%%%%%%%%%%%%%%%%%%%%%%%%%%%%%%%%


% IS(1:round(PW(n)/dt))=[ -k*100*ones(1,round(PW_half(n)/dt))
k*(exp(5*T1/PW_half(n))-1)]; % the simulation current array in time
%                         IS(1:round(PW(n)/dt))=k*(exp(5*T1/PW(n))-1);
% WE only save data at the fitted/ selected K value
% at each Is(n)  which is generated at PW(n)
% K is printed on the screen as well. All the
```

112

```matlab
            % following array represents what happens at PW(n)
            % all is saved in terms of (n) so if size of PW is
            % 50 then all the below array should be size of 50
            % as well,
            %                       output1=zeros(1,Q);
            if (signal_used ==1)
                output1(n)=k*(exp(5)-1);

            elseif (signal_used == 2)
                output1(n)=k;

            elseif (signal_used == 3 )

                output1(n)= k*PW(n);

            elseif (signal_used==4)

                output1(n)=k*PW(n)^2;

            elseif (signal_used==5)

                output1(n)=k;
            elseif (signal_used==6)
                A=5;
                output1(n)=k*(1-exp(-A));

            elseif (signal_used== 7)
                A=5;
                output1(n)=k*normpdf(PW(n)/2,PW(n)/2,PW(n)/A);

            elseif (signal_used== 8)
                output1(n)=k;
            elseif (signal_used== 9 )
                output1(n)=k*(exp(5)-1);

            elseif (signal_used == 10)
                output1(n)=k;

            elseif (signal_used == 11 )

                output1(n)= k*PW(n);

            elseif (signal_used== 12 )

                output1(n)=k*PW(n)^2;
            elseif(signal_used== 13 )

            elseif (signal_used== 14)

                output1(n)=k;
            elseif (signal_used==15)
                A=5;
                output1(n)=k*(1-exp(-A));

            elseif (signal_used== 16)
                A=5;
                output1(n)=k*normpdf(PW(n)/2,PW(n)/2,PW(n)/A);

            elseif (signal_used== 17)

                output1(n)=k;
            elseif (signal_used== 20)

                output1(n)=k;

            end

            V_Action_potential(n) = {V2};
            PW_Action_potential(n) = PW(n) ; % the same as PW
            K_Action_potentail(n) = k; % actuaal K values  the same as  K_Array_INCEXP
    when K = output 1
```

```matlab
            c(n) = output1(n);% the plotted k values K_Array_INCEXP
            V_Action_potential_plotting{n} ={V_plotting};
            MGATE_Array_at_each_K(n) = {MGATE};
            HGATE_Array_at_eah_K(n) = {HGATE};
            GNA_array_at_each_K (n) = {GNA};
            Minfinite_array_at_each_K(n) = { Minfinite};
            Tm_array_at_each_K(n)= {Tm };
            Hinfinite_array_at_each_K(n)= {Hinfinite};
            Th_array_at_each_K(n)= {Th};
            AM_array_At_each_K(n)= {AM};
            BM_Array_At_each_K(n)= {BM};
            AH_array_At_each_K(n)= {AH};
            BH_Array_At_each_K(n)= {BH};


            k

            for m=1:M,
                output11(n)=output11(n)+IS(m)^2*dt;
                output12(n)=output12(n)+IS(m)*dt;
            end

            figure(121)
            clf
            scrsz = get(0,'ScreenSize');
            position_default = [0.01*scrsz(3) 0.07*scrsz(4) 0.98*scrsz(3)
0.85*scrsz(4)];
            set(gcf,'position',position_default)

            subplot(331)
            plot(T_plotting , V2)
            xlabel ('Time (ms) ')
            title('Action Potential ')
            subplot(332)
            plot(T_plotting,MGATE)
            xlabel ('Time (ms) ')
            title('Mgate')
            subplot(333)
            plot(T_plotting,HGATE)
            xlabel ('Time (ms) ')
            title('Hgate')
            subplot(334)
            plot(T_plotting,GNA)
            xlabel ('Time (ms) ')
            title('GNA')
            subplot(335)
            %                              plot(Tm,Minfinite)
            plot(T_plotting,Minfinite)
            xlabel ('Time (ms) ')
            ylabel ('Minfinitea (am/(am+bm)) ');
            %                              xlabel ('Tm (1/am+bm)')
            subplot(336)
            %                              plot(Th,Hinfinite)
            plot(T_plotting,Hinfinite)
            xlabel ('Time (ms) ')
            ylabel('Hinifinite   (ah/(ah+bh))')
            %                              xlabel ('Th (1/ah+bh)')
            subplot(337)
            plot(T_plotting,AM)
            hold on
            plot(T_plotting,BM,'r')
            xlabel('AM  && BM')
            legend ('AM','BM')
            subplot(338)
            plot(T_plotting,AH)
            hold on
            plot(T_plotting,BH,'r')
            xlabel('AH && BH')
            legend ('AH','BH')
            subplot(339)
            plot(T_plotting,IS)
%           hold on
```

114

```matlab
%               plot(T_plotting,Current,'r')
                xlabel ('Time (ms) ')
                pause(0)
                annotation('textbox',[ 0.4 0.9 0.50 .10 ],'LineStyle','none','String',['PW
= ' num2str(PW(n))  Paramters_Of_Interest{Paramter_VAl} ' = ' num2str(Pram_Array(P)) ' &
' Paramters_Of_Interest{Paramter_VAl2} ' = '
num2str(Pram_Array2(Pram2))],'FitBoxToText','on','FontSize',12,'FontWeight','bold','FontN
ame','Times New Roman','FontAngle','italic','Color','r');



%               elseif(~exist('V_AP'))
%                   break;

%               end
                PW(n)
                else
%               The reason I added the nan is that sometimes at a specific PW we can't
generate an AP
%               So I but a nan instead as a markler that at this pulse wedith no action
potential was generate
                output11(n) = NaN;
                output1(n) = NaN;

            end
            end
            [Val,Index] = min(output11);
            figure(2)
            subplot(221)
            plot(PW,output1);
            hold on ;
            plot(PW(Index),output1(Index),'r*');hold off;
            title('Exponential');
            set(gcf,'color',[1,1,1]);
            subplot(222)
            plot(PW,output11,'r')
            hold on;
            plot(PW(Index),output11(Index),'k*');hold off;
            title('Energy: red-exponential - Outpit 1')
            subplot(223)
            plot(PW,output12,'r')
            hold on
            plot(PW(Index),output12(Index),'r*');hold off;
            title('Charge: red-exponential - output 2')
            subplot(224)
            plot(IS)
            title('Simulation signal')


%           if(exist('V_AP'))
            % Saving Data
            IdeaL_K_Array_INCEXP(Pram2,P) =  output1(Index); % THis is the mimum K at each
gnamax or gleak.Minmum K represnts the best values to consume power
            IdeaL_Energey_Array_INCEXP(Pram2,P) = output11(Index); % Energy value at the
K_min for each gnamax or gleak
            IdeaL_Charge_Array_INCEXP (Pram2,P)= output12(Index); % Charge required at
k_min for each gnamax or gleak
            Ideal_PW_Array_INCEXP(Pram2,P) = PW(Index);    %% the Pw at K_min
            %           Energy_array_INCEXP(P,1:length(PW))= output11;
            %           Energy_array_INCEXP(P,1:length(PW))= output11;
            Energy_array_INCEXP(Pram2,P)= {output11};
            %           K_Array_INCEXP(P,1:length(PW)) =  output1;
            %           K_Array_INCEXP(Pram2,P,1:length(PW)) =  output1;
            K_Array_INCEXP(Pram2,P) =  {output1};
            %           Stimulation_Amplitude_INCEXP(P,1:length(IS)) = IS;
            %           Stimulation_Amplitude_INCEXP(Pram2,P,1:length(IS)) = IS;
            Stimulation_Current(Pram2,P) = {IS};

            Ideal_V_Action_potential(Pram2,P)  = V_Action_potential(Index);
            Ideal_MGATE_Array(Pram2,P)  = MGATE_Array_at_each_K(Index);
            Ideal_HGATE_Array(Pram2,P)  = HGATE_Array_at_eah_K(Index);
```

```matlab
            Ideal_GNA_array (Pram2,P)  = GNA_array_at_each_K(Index);
            Ideal_Minfinite_array(Pram2,P)  =  Minfinite_array_at_each_K(Index);
            Ideal_Tm_array (Pram2,P)  = Tm_array_at_each_K(Index);
            Ideal_Hinfinite(Pram2,P) =Hinfinite_array_at_each_K(Index);
            Ideal_Th_array (Pram2,P) = Th_array_at_each_K(Index);
            Ideal_AM_array (Pram2,P) = AM_array_At_each_K(Index);
            Ideal_BM_Array(Pram2,P) = BM_Array_At_each_K(Index);
            Ideal_AH_array(Pram2,P) = AH_array_At_each_K(Index);
            Ideal_BH_Array(Pram2,P) = BH_Array_At_each_K(Index);
            All__V_Action_potential{Pram2,P} = V_Action_potential;
%            end



            P
            pause(.001);
        end
    end



    %% plotting when more than variable is changing

    gcf1 = figure(8);
    fig_num = 1;
    Prameter1_array_L = length(Pram_Array) ;
    Prameter2_array_L = length(Pram_Array2) ;

    for Parm2 = 1 :length(Pram_Array2)
        if length(Pram_Array2)>1
            subplot(round(Prameter2_array_L/2),2,Parm2)
        end
        for P = 1 : length(Pram_Array)

            plot(PW, K_Array_INCEXP {Parm2,P})
            hold on
            xlabel ('PW')
            ylabel (' K-Array' )
            if length(Pram_Array2)>1
                legendinfo{P} = [ num2str(Paramters_Of_Interest{Paramter_VAl2}) '= '
num2str(Pram_Array2(Parm2)) ' '  num2str(Paramters_Of_Interest{Paramter_VAl}) '= '
num2str(Pram_Array(P))];
                title(['Waveform is '  cell2mat(Signal_names(signal_used))  ':'
num2str(Paramters_Of_Interest{Paramter_VAl2})  ' = '  num2str(Pram_Array2(Parm2)) ]);
            else
                legendinfo{P} = [   num2str(Paramters_Of_Interest{Paramter_VAl}) '= '
num2str(Pram_Array(P))];
                title(['Waveform is '  cell2mat(Signal_names(signal_used)) ':'
num2str(Paramters_Of_Interest{Paramter_VAl})])

            end


            %legendinfo{P} = [     'gnamax = '   num2str(Pram_Array(P))];

        end
        legend(legendinfo)


    end
%%
for Pram2 = 1:length(Pram_Array2)


    for P = 1:length(Pram_Array)

        if length(Pram_Array2)>1
            title_fig = (['Waveform is '  cell2mat(Signal_names(signal_used)) ': @ PW = '
num2str(PW(1)) ' '   num2str(Paramters_Of_Interest{Paramter_VAl2})  ' ='
num2str(Pram_Array2(Pram2))      num2str(Paramters_Of_Interest{Paramter_VAl}) ' = '
num2str(Pram_Array(P))  '( a-> alpha  & b-> beta)']) ;
```

116

```matlab
        else
            title_fig = (['Waveform is  '    cell2mat(Signal_names(signal_used)) ':'
num2str(Paramters_Of_Interest{Paramter_VAl}) ' = '  num2str(Pram_Array(P))   '( a-> alpha
& B-> beta)']) ;

        end
        figure(fig_num+ 100)

        suptitle(title_fig)
        subplot(331)
        plot(T_plotting,Ideal_V_Action_potential{Pram2,P})
        ylabel('Action Potential ')
        subplot(332)
        plot( T_plotting,Ideal_MGATE_Array{Pram2,P})
        ylabel('Mgate')
        subplot(333)
        plot( T_plotting,Ideal_HGATE_Array{Pram2,P})
        ylabel('Hgate')
        subplot(334)
        plot( T_plotting, Ideal_GNA_array {Pram2,P})
        ylabel('GNA')
        subplot(335)
        %                                      plot(Ideal_Tm_array {Pram2,P},
Ideal_Minfinite_array{Pram2,P})
        plot(T_plotting,Ideal_Minfinite_array{Pram2,P})
        ylabel ('Minfinitea (am/(am+bm)) ');
        %                                      xlabel ('Tm (1/am+bm)')
        subplot(336)
        %plot(Ideal_Th_array {Pram2,P}, Ideal_Hinfinite{Pram2,P})
        plot(T_plotting, Ideal_Hinfinite{Pram2,P})
        ylabel('Hinifinite   (ah/(ah+bh))')
        %xlabel ('Th (1/ah+bh)')
        subplot(337)
        plot(T_plotting, Ideal_AM_array {Pram2,P})
        hold on
         plot(T_plotting,Ideal_BM_Array{Pram2,P})
        ylabel('Alpha M & Beta M')
        subplot(338)
        %plot(T_plotting,Ideal_Tm_array{Pram2,P})
      plot(T_plotting,Stimulation_Current{Pram2,P})
        ylabel('Stimulation Current')
        ylim([0 nanmax(Stimulation_Current{Pram2,P})])
        subplot(339)
        plot(T_plotting,Ideal_AH_array{Pram2,P})
        hold on
        plot(T_plotting,Ideal_BH_Array{Pram2,P},'r')
        ylabel('Alpha H && Beta H')
        legend ('AH','BH')
        pause(0)
        POI_Value_plotted (Pram2,P ) = fig_num ;

        fig_num = fig_num+1;



    end

end

%% Automatically Count number of corssing Between ALl neurons update 9/25/2018
{Selectivity Index based on angle between STD curves)
%%This is the most updated way to calculate number fo crossing, it doesn't allow
%%curve to be crossed with its self, and it doesn't allow duplicated crossing
% AUtomatically find number of crossings usign the interscection function
 % When adding the Catrhodic part I noticed that all the signals crossed @
 % specific PW and a specific Threshold  seems like they all starting from
 % the same point so to count the correct number of crossing I search for
 % the crossing after that point
 figure(18);
%   subplot(224)
```

```matlab
LG=1;
Start =1;
  for Parm2 = 1 :length(Pram_Array2)
      if length(Pram_Array2)>1
%             subplot(round(Prameter2_array_L/2),2,Parm2)

      end
      for P = 1 : length(Pram_Array)
          Neuron_SD_curve =K_Array_INCEXP {Parm2,P} ;
          plot(PW(Start:end), Neuron_SD_curve(Start:end))
          hold on
          xlabel ('PW')
          ylabel (' K-Array' )
          if length(Pram_Array2)>1
              ALLlegendinfo{LG} = [ num2str(Paramters_Of_Interest{Paramter_VAl2}) '= '
num2str(Pram_Array2(Parm2)) ' '  num2str(Paramters_Of_Interest{Paramter_VAl}) '= '
num2str(Pram_Array(P))];
                  title(['Waveform is '   cell2mat(Signal_names(signal_used))  ':'
num2str(Paramters_Of_Interest{Paramter_VAl2})  ' = '   num2str(Pram_Array2(1)) ':'
num2str(Pram_Array2(end)) ]);
          else
              ALLlegendinfo{LG} = [   num2str(Paramters_Of_Interest{Paramter_VAl}) '= '
num2str(Pram_Array(P))];
                  title(['Waveform is '  cell2mat(Signal_names(signal_used)) ':'
num2str(Paramters_Of_Interest{Paramter_VAl})])
          end
          LG=LG+1;
      end
      legend(ALLlegendinfo)


  end
% AUtomatically find number of crossings usign the interscection function

NOC = 0;
count=1;
c=1;
UC=1;
used_crossing=zeros(0,1);
N2_Ind_array=zeros(0,1);
for I = 1 :Parm2
    for L= 1 :P
        SD_Curve_Neuron1 = K_Array_INCEXP {I,L};
        for ISearch = 1:Parm2
            for LSearch =L :P
                SD_Curve_Neuron2 = K_Array_INCEXP{ISearch,LSearch} ;
%                to make usre crossing counts only once number of
%                crossing = n!/r!-(n-r)! --r=2 (pairs)
                N1_IND =  I*10+L;
                N2_Ind = ISearch*10+LSearch;
                comb1 =N1_IND*100+N2_Ind;
                Comb2 = N2_Ind*100+N1_IND;

              if(SD_Curve_Neuron1~=SD_Curve_Neuron2)
              if (isempty(find (ismember(used_crossing,comb1 )==1) ) && isempty(find
(ismember(used_crossing,Comb2 )==1) ))

                  crossing{c} = [ I L ; ISearch LSearch];
                  c=c+1;
                  used_crossing (UC) = comb1;
                  used_crossing(UC+1) = Comb2;
                  UC=UC+2;
              if ~isempty(
intersections(PW(Start:end),SD_Curve_Neuron1(Start:end),PW(Start:end),SD_Curve_Neuron2(St
art:end),0))
                  [x0,y0,iout,jout] =
intersections(PW(Start:end),SD_Curve_Neuron1(Start:end),PW(Start:end),SD_Curve_Neuron2(St
art:end),0);

                  if(~isempty(x0) && (~isempty(y0)))
                      NOC = NOC+1;
```

```matlab
 figure(18);
hold on;
for NumX =1:length(x0)
    x =x0(NumX);y=y0(NumX);
    plot([0 x],[y y],'r--')
    plot([x x],[0 y],'r--')
end
%%%%%%%%%%%%%%%%%%%%%%%%%%%%%%%%%%%%%%%%%%%%%%%%
% Angle ANalysis
[Great_array_rows Great_array]= find(PW> x);   P1 =
(Great_array(1));

[Less_array_rows Less_array]  = find(PW< x);  P2=Less_array(end);
Slope_Neuron1 = (SD_Curve_Neuron1(P2)-
SD_Curve_Neuron1(P1))/((PW(P2)-PW(P1)));
Slope_Neuron2 = (SD_Curve_Neuron2(P2)-
SD_Curve_Neuron2(P1))/((PW(P2)-PW(P1)));

Inclination_angle_neuron1 = atand(Slope_Neuron1);
Inclination_angle_neuron2 = atand(Slope_Neuron2);
Inclination_angle_Difference = abs( Inclination_angle_neuron2 -
Inclination_angle_neuron1);

% %%%%%%%%%%%%%%%%%%%%%%%%%%%%%%%%%%%%%%%%%%%%%%%
% ratiometric Analysis

 A1 = abs( SD_Curve_Neuron2-SD_Curve_Neuron1);
if ( nanmean(SD_Curve_Neuron2(1:P2))
<nanmean(SD_Curve_Neuron1(1:P2)))
        B1 =  SD_Curve_Neuron2(1:P2);
elseif ( nanmean(SD_Curve_Neuron1(1:P2))
<nanmean(SD_Curve_Neuron2(1:P2)))
        B1 =  SD_Curve_Neuron1(1:P2);
end
if ( nanmean(SD_Curve_Neuron2(P1:end))
<nanmean(SD_Curve_Neuron1(P1:end)))
        B2 =  SD_Curve_Neuron2(P1:end);
elseif ( nanmean(SD_Curve_Neuron1(P1:end))
<nanmean(SD_Curve_Neuron2(P1:end)))
        B2 =  SD_Curve_Neuron1(P1:end);
end
Ratio1 = A1(1:length(B1))./(A1(1:length(B1))+B1);
Ratio2 = (A1(end-length(B2)+1:end))./(A1(end-
length(B2)+1:end)+B2);
[Value1 Indx1 ] = max(Ratio1);
[Value2 Indx2 ] = max(Ratio2);
Actual_Indx2 = Indx2 + length(B1);

PW_max_ratio1 = PW(Indx1);
PW_max_ratio_2 = PW(Actual_Indx2);

plot(PW(Indx1),SD_Curve_Neuron1(Indx1),'rh')
plot(PW(Indx1),SD_Curve_Neuron2(Indx1),'rh')

plot(PW(Actual_Indx2),SD_Curve_Neuron1(Actual_Indx2),'rh')
plot(PW(Actual_Indx2),SD_Curve_Neuron2(Actual_Indx2),'rh')


%%%%%%%%%%%%%%%%%%%%%%%%%%%%%%%%%%%%%%%%%%%%%%



Slope_Neuron1_array(count) = Slope_Neuron1 ;
Slope_Neuron2_array (count) = Slope_Neuron2 ;
Inclination_angle_neuron1_array (count)
=Inclination_angle_neuron1;
Inclination_angle_neuron2_array (count)  =
Inclination_angle_neuron2;
Inclination_angle_Difference_array(count)
=Inclination_angle_Difference;
Ratio_array(count)= min(Value1 ,Value2);
```

```matlab
                                    count =count +1;


                            end
                        end
                      end
                    end
                end
            end


        end
end
Total_Number_of_Crossing = NOC
if(NOC~=0)
Avrage_Angle = nanmean(Inclination_angle_Difference_array)
Avrage_Std = nanstd(Inclination_angle_Difference_array)
Total_Number_of_Neurons = length(Pram_Array) *length(Pram_Array2)
Avrage_Ratio = nanmean(Ratio_array)
STD_Ratio = nanstd(Ratio_array)

Total_Number_of_possibilities = factorial(Total_Number_of_Neurons) /(factorial(2)*
factorial(Total_Number_of_Neurons-2))
Crossing_Percentage= ((Total_Number_of_Crossing*100)/Total_Number_of_possibilities) %
Precentage Analysis

if length(Pram_Array2)>1
    title(['Waveform is '   cell2mat(Signal_names(signal_used))  '; POI :- '
num2str(Paramters_Of_Interest{Paramter_VAl})   ' & '
num2str(Paramters_Of_Interest{Paramter_VAl2})  ' ; Avrage Angle = ' num2str(
nanmean(Inclination_angle_Difference_array))  ' ^o ; STD Angle = '
num2str(nanstd(Inclination_angle_Difference_array)) ' ; NOC = ' num2str(NOC) ' ;
%Crossing  = ' num2str((Total_Number_of_Crossing*100)/Total_Number_of_possibilities) '%'
, ' ; Avrage Ratio = ' num2str(Avrage_Ratio ) ' ; STD_Ratio = ' num2str(STD_Ratio)]);
else
    title(['Waveform is '  cell2mat(Signal_names(signal_used)) ':'
num2str(Paramters_Of_Interest{Paramter_VAl})    ' ; Avrage Angle = ' num2str(
mean(Inclination_angle_Difference_array)) ' ^o ; STD Angle = '
num2str(std(Inclination_angle_Difference_array)) ' ; Crossing % = '
num2str((Total_Number_of_Crossing*100)/Total_Number_of_possibilities) '%',' ; Avrage
Ratio = ' num2str(Avrage_Ratio ) ' ; STD Ratio = ' num2str(STD_Ratio)]);
end

end


%%
if length(Pram_Array2)>1
folder_name = ['Waveform' cell2mat( Signal_names(signal_used)) '  POI '
Paramters_Of_Interest{Paramter_VAl2} ' && ' Paramters_Of_Interest{Paramter_VAl}];
else
folder_name = ['Waveform' cell2mat( Signal_names(signal_used)) '  POI '
Paramters_Of_Interest{Paramter_VAl}];
end
New_folder = [current directry  '\' folder_name];
mkdir(New_folder)
cd (New_folder );
%%

n =Min:step:Max ;
FigArray= 101:1:100+fig_num;
 for FigIdx = 1:fig_num-1
    [ Rparm2 , CP] = find(POI_Value_plotted == FigIdx);
    if length(Pram_Array2)>1
     Figname =[ 'Parameters plotted when ' Paramters_Of_Interest{Paramter_VAl} '='
num2str(Pram_Array(CP)) ' & ' Paramters_Of_Interest{Paramter_VAl2} '='
num2str(Pram_Array2(Rparm2)) '.fig'] ;
    else
     Figname =[ 'Parameters plotted when ' Paramters_Of_Interest{Paramter_VAl} '='
num2str(Pram_Array(CP)) '.fig'] ;
    end
     saveas(figure(FigArray(FigIdx)),Figname)
```

```matlab
    end
%%
if  length(Pram_Array2)>1
    Figname  = ['SD_Curve ' 'POI_' Paramters_Of_Interest{Paramter_VAl2} '_'
Paramters_Of_Interest{Paramter_VAl} ' Wavefrom_' cell2mat(Signal_names(signal_used)) '
Min_' num2str(Min) '_MAX_' num2str(Max) '_Step=' num2str(step)];
    Crossing_Figname  = ['Crossing_for_SD_Curve ' 'POI_'
Paramters_Of_Interest{Paramter_VAl2} '_' Paramters_Of_Interest{Paramter_VAl} ' Wavefrom_'
cell2mat(Signal_names(signal_used)) ' Min_' num2str(Min) '_MAX_' num2str(Max) '_Step='
num2str(step)];

else
    Figname  = ['SD_Curve ' 'POI_'  '_' Paramters_Of_Interest{Paramter_VAl} ' Wavefrom_'
cell2mat(Signal_names(signal_used)) ' Min_' num2str(Min) '_MAX_' num2str(Max) '_Step='
num2str(step)];
    Crossing_Figname  = ['Crossing_For_SD_Curve ' 'POI_'  '_'
Paramters_Of_Interest{Paramter_VAl} ' Wavefrom_' cell2mat(Signal_names(signal_used)) '
Min_' num2str(Min) '_MAX_' num2str(Max) '_Step=' num2str(step)];

end
saveas(figure(8),[Figname '.fig'])
 saveas(figure(18),[Crossing_Figname '.fig'])

Mfilename = [Figname '.mat' ];

save(Mfilename);

SAvingMSGBOX = msgbox ('please select a nother waveform or exit ?', 'End Of Saving' );
uiwait(SAvingMSGBOX) ;
%MSfilename =  cell2mat(Signal_names(signal_used)) ;
   %save(MSfilename,'K_Array_INCEXP','PW','Pram2','Pram_Array2','Pram_Array');

        gcf = figure(2);
    pbexit =
uicontrol(gcf,'Style','pushbutton','String','Exit','units','normalized','Position',[.225
.05 .05 .05],'Callback','Exit = 5; uiresume;');
    uiwait(gcf)

end


%% End OF MAIN CODE
```

REFERENCES

1. Warren, M.G., J. Thomas Mortimer, *<Stimulus waveforms for selective neural stimulation>.* IEEE Engineering in Medicine and biology 1995. **0739-5175/96**.
2. Chiu, S.Y., et al., *A quantitative description of membrane currents in rabbit myelinated nerve.* J Physiol, 1979. **292**: p. 149-66.
3. Grill, W.M. and J.T. Mortimer, *Inversion of the current-distance relationship by transient depolarization.* IEEE Trans Biomed Eng, 1997. **44**(1): p. 1-9.
4. *Nearly 1 in 6 of world's population suffer from neurological disorders – UN report*, in *UN News Center*. 2007, United Nations: Online p. 1.
5. *Brain Disorders: By the Numbers*. 2014, Brain Research at MIT

McGovern Institute for Brain Research at MIT. p. 1.
6. Espay, A.J., et al., *Technology in Parkinson's disease: Challenges and opportunities.* Mov Disord, 2016. **31**(9): p. 1272-82.
7. Johnson, M.D., et al., *Neuromodulation for brain disorders: challenges and opportunities.* IEEE Trans Biomed Eng, 2013. **60**(3): p. 610-24.
8. Lehto, L.J., et al., *Orientation selective deep brain stimulation.* J Neural Eng, 2017. **14**(1): p. 016016.
9. Rush, A.J., et al., *Vagus nerve stimulation (VNS) for treatment-resistant depressions: a multicenter study.* Biol Psychiatry, 2000. **47**(4): p. 276-86.
10. Grill, W.M., *Model-based analysis and design of waveforms for efficient neural stimulation.* Prog Brain Res, 2015. **222**: p. 147-62.
11. Fang, Z.P. and J.T. Mortimer, *Selective activation of small motor axons by quasi-trapezoidal current pulses.* IEEE Trans Biomed Eng, 1991. **38**(2): p. 168-74.
12. McNeal, D.R., *Analysis of a model for excitation of myelinated nerve.* IEEE Trans Biomed Eng, 1976. **23**(4): p. 329-37.
13. Deurloo, K.E., J. Holsheimer, and P. Bergveld, *The effect of subthreshold prepulses on the recruitment order in a nerve trunk analyzed in a simple and a realistic volume conductor model.* Biol Cybern, 2001. **85**(4): p. 281-91.
14. Qing, K.Y., M.P. Ward, and P.P. Irazoqui, *Burst-Modulated Waveforms Optimize Electrical Stimuli for Charge Efficiency and Fiber Selectivity.* IEEE Trans Neural Syst Rehabil Eng, 2015. **23**(6): p. 936-45.
15. Sahin, M. and Y. Tie, *Non-rectangular waveforms for neural stimulation with practical electrodes.* J Neural Eng, 2007. **4**(3): p. 227-33.
16. Rijkhoff, N.J., et al., *Modelling selective activation of small myelinated nerve fibres using a monopolar point electrode.* Med Biol Eng Comput, 1995. **33**(6): p. 762-8.
17. Stieglitz, T., *Diameter-dependent excitation of peripheral nerve fibers by multipolar electrodes during electrical stimulation.* Expert Rev Med Devices, 2005. **2**(2): p. 149-52.
18. Grill, W.M., Jr. and J.T. Mortimer, *The effect of stimulus pulse duration on selectivity of neural stimulation.* IEEE Trans Biomed Eng, 1996. **43**(2): p. 161-6.
19. Foutz, T.J. and C.C. McIntyre, *Evaluation of novel stimulus waveforms for deep brain stimulation.* J Neural Eng, 2010. **7**(6): p. 066008.
20. Jezernik, S. and M. Morari, *Energy-optimal electrical excitation of nerve fibers.* (0018-9294 (Print)).

21.   Wongsarnpigoon, A. and W. Grill, *Energy-efficient waveform shapes for neural stimulation revealed with genetic algorithm.* Journal of neural engineering, 2010. **7**: p. 046009.

22.   Maciejasz, P., et al., *Delaying discharge after the stimulus significantly decreases muscle activation thresholds with small impact on the selectivity: an in vivo study using TIME.* Medical & biological engineering & computing, 2015. **53**(4): p. 371-379.

23.   van den Honert, C. and J.T. Mortimer, *The response of the myelinated nerve fiber to short duration biphasic stimulating currents.* Ann Biomed Eng, 1979. **7**(2): p. 117-25.

24.   Kilgore, K.L., et al., *Electrode characterization for functional application to upper extremity FNS.* IEEE Trans Biomed Eng, 1990. **37**(1): p. 12-21.

25.   Rattay, F., *Analysis of models for extracellular fiber stimulation.* IEEE Trans Biomed Eng, 1989. **36**(7): p. 676-82.

26.   Dali, M., O. Rossel, and D. Guiraud, *Numerical simulation of multipolar configuration and prepulse technique to obtain spatially reverse recruitment order.* Annu Int Conf IEEE Eng Med Biol Soc, 2016. **2016**: p. 5461-5464.

27.   Hodgkin, A.L. and A.F. Huxley, *A quantitative description of membrane current and its application to conduction and excitation in nerve.* J Physiol, 1952. **117**(4): p. 500-44.

28.   Rattay, F. and M. Aberham, *Modeling axon membranes for functional electrical stimulation.* IEEE Transactions on Biomedical Engineering, 1993. **40**(12): p. 1201-1209.

29.   Sweeney, J.D., J.T. Mortimer, and D. Durand. *Modeling of mammalian myelinated nerve for functional neuromuscular stimulation* 1987. IEEE.

30.   De Zeeuw, C.I., et al., *Microcircuitry and function of the inferior olive.* Trends Neurosci, 1998. **21**(9): p. 391-400.

31.   Torben-Nielsen, B., I. Segev, and Y. Yarom, *The generation of phase differences and frequency changes in a network model of inferior olive subthreshold oscillations.* PLoS Comput Biol, 2012. **8**(7): p. e1002580.

32.   Zhang, Y., et al., *Effects of maximal sodium and potassium conductance on the stability of Hodgkin-Huxley model.* Comput Math Methods Med, 2014. **2014**: p. 761907.

33.   Gentet, L.J., G.J. Stuart, and J.D. Clements, *Direct measurement of specific membrane capacitance in neurons.* Biophys J, 2000. **79**(1): p. 314-20.

34.   Rall, W., *Theory of physiological properties of dendrites.* Ann N Y Acad Sci, 1962. **96**: p. 1071-92.

35.   Kuykendal, M., et al., *Targeted Stimulation Using Differences in Activation Probability across the Strength–Duration Space.* Processes, 2017. **5**(2): p. 14.

36.   McKay, C.M. and H.J. McDermott, *Loudness perception with pulsatile electrical stimulation: the effect of interpulse intervals.* J Acoust Soc Am, 1998. **104**(2 Pt 1): p. 1061-74.

37.   Gorman, P.H. and J.T. Mortimer, *The effect of stimulus parameters on the recruitment characteristics of direct nerve stimulation.* IEEE Trans Biomed Eng, 1983. **30**(7): p. 407-14.

38.   Grill, W.M. and J.T. Mortimer, *Stimulus waveforms for selective neural stimulation.* IEEE Engineering in Medicine and Biology Magazine, 1995. **14**(4): p. 375-385.

39.   McIntyre, C.C. and W.M. Grill, *Selective microstimulation of central nervous system neurons.* Ann Biomed Eng, 2000. **28**(3): p. 219-33.

40.   van Aerde, K.I. and D. Feldmeyer, *Morphological and physiological characterization of pyramidal neuron subtypes in rat medial prefrontal cortex.* Cereb Cortex, 2015. **25**(3): p. 788-805.

41.	Cho, R.H., et al., *Intracellularly labeled pyramidal neurons in the cortical areas projecting to the spinal cord. I. Electrophysiological properties of pyramidal neurons.* Neurosci Res, 2004. **50**(4): p. 381-94.

42.	Dasen, J.S., et al., *A Hox regulatory network establishes motor neuron pool identity and target-muscle connectivity.* Cell, 2005. **123**(3): p. 477-91.

43.	Gao, B.X. and L. Ziskind-Conhaim, *Development of ionic currents underlying changes in action potential waveforms in rat spinal motoneurons.* J Neurophysiol, 1998. **80**(6): p. 3047-61.

44.	Stifani, N., *Motor neurons and the generation of spinal motor neuron diversity.* Front Cell Neurosci, 2014. **8**: p. 293.

45.	De Schutter, E. and J.M. Bower, *An active membrane model of the cerebellar Purkinje cell II. Simulation of synaptic responses.* J Neurophysiol, 1994. **71**(1): p. 401-19.

46.	De Schutter, E. and J.M. Bower, *An active membrane model of the cerebellar Purkinje cell. I. Simulation of current clamps in slice.* J Neurophysiol, 1994. **71**(1): p. 375-400.

47.	Jaeger, D. and J.M. Bower, *Synaptic control of spiking in cerebellar Purkinje cells: dynamic current clamp based on model conductances.* J Neurosci, 1999. **19**(14): p. 6090-101.

48.	Schwarz, J.R. and G. Eikhof, *Na currents and action potentials in rat myelinated nerve fibres at 20 and 37 degrees C.* Pflugers Arch, 1987. **409**(6): p. 569-77.

49.	Schwarz, J.R., G. Reid, and H. Bostock, *Action potentials and membrane currents in the human node of Ranvier.* Pflugers Arch, 1995. **430**(2): p. 283-92.

50.	Cho, R.H., et al., *Intracellularly labeled pyramidal neurons in the cortical areas projecting to the spinal cord. II. Intra- and juxta-columnar projection of pyramidal neurons to corticospinal neurons.* Neurosci Res, 2004. **50**(4): p. 395-410.

51.	Lapicque , L., *Recherches Quantitatives sur l'Excitation Electrique des Nerfs Traitée comme une Polarization.* Journal de Physiologie et Pathologie General, 1907. **9**: p. 620--635.

52.	Rattay, F., *Modelling of the excitation and the propagation of nerve impulses by natural and artificial stimulations.* Mathematics and Computers in Simulation, 1995. **39**(5): p. 589-595.

53.	Kiernan, M.C., K. Cikurel, and H. Bostock, *Effects of temperature on the excitability properties of human motor axons.* Brain, 2001. **124**(Pt 4): p. 816-25.

54.	Smit, J.E., T. Hanekom, and J.J. Hanekom, *Modelled temperature-dependent excitability behaviour of a generalised human peripheral sensory nerve fibre.* Biol Cybern, 2009. **101**(2): p. 115-30.

55.	Motz, H. and F. Rattay, *A study of the application of the Hodgkin-Huxley and the Frankenhaeuser-Huxley model for electrostimulation of the acoustic nerve.* Neuroscience, 1986. **18**(3): p. 699-712.

56.	Goldman, L. and J.S. Albus, *Computation of impulse conduction in myelinated fibers; theoretical basis of the velocity-diameter relation.* Biophysical journal, 1968. **8**(5): p. 596-607.

57.	Bostock, H., *The strength-duration relationship for excitation of myelinated nerve: computed dependence on membrane parameters.* J Physiol, 1983. **341**: p. 59-74.

58.	Cohen, I., D. Attwell, and G. Strichartz, *The dependence of the maximum rate of rise of the action potential upstroke on membrane properties.* Proc R Soc Lond B Biol Sci, 1981. **214**(1194): p. 85-98.

59.	Walton, M. and H.A. Fozzard, *The relation of Vmax to INa, GNa, and h infinity in a model of the cardiac Purkinje fiber.* Biophys J, 1979. **25**(3): p. 407-20.

60. Carp, J.S., *Physiological properties of primate lumbar motoneurons.* J Neurophysiol, 1992. **68**(4): p. 1121-32.
61. Mitra, P. and R.M. Brownstone, *An in vitro spinal cord slice preparation for recording from lumbar motoneurons of the adult mouse.* J Neurophysiol, 2012. **107**(2): p. 728-41.
62. Eccles, J.C., R.M. Eccles, and A. Lundberg, *The action potentials of the alpha motoneurones supplying fast and slow muscles.* J Physiol, 1958. **142**(2): p. 275-91.
63. Rattay, F., *Analysis of models for external stimulation of axons.* IEEE Trans Biomed Eng, 1986. **33**(10): p. 974-7.
64. Offner, F., *Stimulation with minimum power.* (0022-3077 (Print)).
65. Kajimoto, H., N. Kawakami, and S. Tachi, *Optimal design method for selective nerve stimulation.* Electronics and Communications in Japan (Part III: Fundamental Electronic Science), 2004. **87**(9): p. 62-72.
66. Fishler, M.G., *Theoretical predictions of the optimal monophasic and biphasic defibrillation waveshapes.* (0018-9294 (Print)).
67. Blair, H.A., *On the Intensity-Time Relations for Stimulation by Electric Currents. Ii.* J Gen Physiol, 1932. **15**(6): p. 731-55.
68. Blair, H.A., *On the Intensity-Time Relations for Stimulation by Electric Currents. I.* J Gen Physiol, 1932. **15**(6): p. 709-29.
69. Warman, E.N., W.M. Grill, and D. Durand, *Modeling the effects of electric fields on nerve fibers: Determination of excitation thresholds.* IEEE Transactions on Biomedical Engineering, 1992. **39**(12): p. 1244-1254.